

ULTIMATE LOAD CAPACITY OF STEEL BEAMS WITH WEB OPENINGS
BY THE FINITE ELEMENT METHOD

by

Aslam G. Porbandarwala

B. Tech., Indian Institute of Technology, Bombay, 1974

A MASTER'S THESIS

submitted in partial fulfillment of the

requirements for the degree

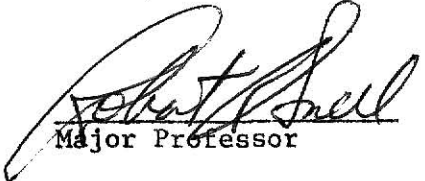
MASTER OF SCIENCE

Department of Civil Engineering

KANSAS STATE UNIVERSITY
Manhattan, Kansas

1975

Approved by:


Major Professor

LD
2668
T4
1975
P67
C-2
Document

TABLE OF CONTENTS

	Page
Introduction	1
Literature Review	2
The Finite Element Method	7
The Finite Element Program	9
Introduction	9
Element Properties	9
Elastic-Plastic Analysis	10
Laboratory Experiments	14
Preparation for Computer Analysis	16
Idealization	16
Discretization	17
Solid Beams	18
Presentation of Results	19
Discussion	22
Ultimate Loads	22
Yield Patterns and Modes of Failure	23
Conclusions	26
Acknowledgements	27
Appendix I	28
Details of the Computer Program	28
Example Problem	52
Appendix II - References	56
Appendix III - Notations	59
Tables	61
Figures	67

LIST OF TABLES

	Page
Table 1. Test Variables	61
Table 2. Static Yield Stresses	62
Table 3. Idealized Properties of Beams	63
Table 4. Idealized Properties of Solid Beams	64
Table 5. Loading Details for Beams with Opening and Solid Beams	65
Table 6. Ultimate Loads	66

LIST OF FIGURES

	Page
Figure 1. Bar and Plate Element	67
Figure 2. Test Setup and Reinforcement Details	68
Figure 3. Actual and Idealized Beam Sections	69
Figure 4. Discretization of a Deep Beam	70
Figure 5. Yield Pattern for Solid Beam 1 at Ultimate Load (144 ^k)	71
Figure 6. Yield Pattern in Vicinity of Opening for Beam 1 at 80 ^k	72
Figure 7. Yield Pattern in Vicinity of Opening for Beam 1 at 96 ^k	73
Figure 8. Yield Pattern in Vicinity of Opening for Beam 1 at 112 ^k	74
Figure 9. Yield Pattern for Beam 1 at Ultimate Load (144 ^k)	75
Figure 10. Yield Pattern in Vicinity of Opening for Beam 1 at Ultimate Load (144 ^k)	76
Figure 11. Yield Pattern for Solid Beam 2 at Ultimate Load (168 ^k)	77
Figure 12. Yield Pattern in Vicinity of Opening for Beam 2 at 96 ^k	78
Figure 13. Yield Pattern for Beam 2 at 144 ^k	79
Figure 14. Yield Pattern in Vicinity of Opening for Beam 2 at 144 ^k	80
Figure 15. Yield Pattern for Beam 2 at Ultimate Load (152 ^k)	81
Figure 16. Yield Pattern in Vicinity of Opening for Beam 2 at Ultimate Load (152 ^k)	82
Figure 17. Yield Pattern for Solid Beam 5 at Ultimate Load (144 ^k)	83

LIST OF FIGURES (Continued)

	Page
Figure 18. Yield Pattern for Beam 5 at Ultimate Load (128^k)	84
Figure 19. Yield Pattern in Vicinity of Opening for Beam 5 at Ultimate Load (128^k)	85
Figure 20. Yield Pattern for Solid Beam 6 and 7 at Ultimate Load (112^k)	86
Figure 21. Yield Pattern in Vicinity of Opening for Beam 6 at 54^k	87
Figure 22. Yield Pattern in Vicinity of Opening for Beam 6 at 72^k	88
Figure 23. Yield Pattern for Beam 6 at Ultimate Load (84^k)	89
Figure 24. Yield Pattern in Vicinity of Opening for Beam 6 at Ultimate Load (84^k)	90
Figure 25. Yield Pattern for Beam 7 at Ultimate Load (96^k)	91
Figure 26. Yield Pattern in Vicinity of Opening for Beam 7 at Ultimate Load (96^k)	92
Figure 27. Secondary Moments	93
Figure 28. Four Hinged Mechanism at the Opening	94

INTRODUCTION

In the past few years, openings in the webs of steel beams for access to or passing of utility components have been a much discussed subject.

In the construction of multistoried steel buildings, openings through the webs of wide flange beams are frequently necessary to accommodate the passage of ductwork for heating, ventilation and air-conditioning. This helps in reducing the height of each story and thus significant savings are realized through the reduction of the materials used.

When a portion of the web is removed, the beam may be weakened in the vicinity of the opening and often it becomes essential to reinforce the hole. A considerable amount of analytical and experimental work has been done on this topic yielding several theoretical solutions which have been verified.

The purpose of this study was to use the finite element method of analysis to observe the behavior of steel beams with reinforced eccentric web openings under ultimate load conditions, using a computer program developed at the Illinois Institute of Technology (1). The objective was to obtain the ultimate load data, the yield patterns and the modes of failure and to compare them with the results of an experimental program carried out at Kansas State University (2).

Five W-shape steel beams with eccentric rectangular web openings were tested, all but one being reinforced at the opening. In all cases, the moment to shear ratio was 30 inches and the eccentricity was 2 inches. The variables in the analysis were the reinforcing area, the opening length and the opening height.

LITERATURE REVIEW

In 1932, Muskhelishvili (3) introduced the application of the conformal mapping technique and complex integration to plane problems of the theory of elasticity and in particular to the problem of the stress distribution in a plane or thin plate which is weakened by any type of hole.

In 1950, Joseph and Brock (4) used this complex variable method to obtain an exact solution for the stress concentrations around small openings of several shapes subjected to pure bending. The problem of stress concentration due to such openings has been much studied and many papers concerning this problem have been published (5,6,7).

Using the same method of complex variables Heller, Brock and Bart (8), in 1958, presented a solution for the stress around a rectangular opening with rounded corners in a uniformly loaded plate. In 1962 (9), they modified the procedure and obtained stress distributions due to bending with shear.

Snell (10), in 1962, used the finite element method to study the effects of various reinforcing configurations for rectangular openings in plates subjected to uniaxial tension. His work was published in 1965.

In 1963, McCutcheon, So and Gersovitz (11) submitted a report describing the test program carried out at McGill University. Tests were performed on beams with unreinforced circular openings and theoretical versus measured strains were indicated.

Segner (12,13) conducted tests on six A36 steel WF beams having rectangular openings of various sizes. The openings were all centered on the neutral axis of the beams and many different reinforcing schemes were investigated. His theoretical approach was based on the theory that a member having such openings centered on the neutral axis acts as a

Vierendeel truss and thus has a point of contraflexure at mid-length of each opening above and below the opening in the tee-section.

An analytical method for calculating stresses around elliptical holes in a wide-flange beam under a uniform load was presented by Bower (14,15) in 1966. The applicability of the analysis depends on the hole size and on the magnitude of the M/V ratio at the hole. Later in the same year, he conducted tests on simply supported wide-flange beams with and without cantilever action having circular or rectangular web openings loaded by concentrated loads.

A comparison of the stresses from the elasticity solution to the experimental tangential stress measurements, for cases of pure bending and bending with shear, was conducted by Redwood (16), in 1967. There seemed to be a good agreement for cases of pure bending but the stresses were underestimated when shear was present.

In the same year the ultimate moment capacity of a beam was investigated by Redwood and McCutcheon (17) using several test specimens. The parameters investigated were shape, number of openings, and the ratio of moment to shear at the opening. The results showed that large reductions in ultimate capacity occur and that the size of those reductions increases with the amount of shear present. Openings that were circular seemed to perform better than rectangular openings and the presence of a second opening nearby seemed to further reduce the strength of the beam.

In 1968, Redwood and McCutcheon (18) reported on tests to failure of wide-flanged steel beams containing one or two unreinforced openings. Different shear to moment ratios were investigated. The openings were of various shapes but all had the same height which was 57% of the beam depth. The experimental results indicated that under pure bending the moment capacity

of the beams with one or two openings could be calculated based on the plastic modulus of the net section through the opening. The presence of shear reduced the moment capacity of the beam at the opening below that for pure bending. The reduction was a function of the opening shape, dimension, the spacing of openings and the shear to moment ratio. When a single rectangular opening was present, the moment capacity of the beam was reduced to approximately 40% of M_p , but when an identical opening was added at a spacing equal to the opening depth, only a small additional reduction resulted. At an M/V ratio of 0.425, the moment capacity reduced to 64% to 72% for both simple and double circular openings.

Also in 1968, Bower (19) suggested criteria for elastic, plastic and buckling design. He concluded that, for elastic design, beams with web holes should be designed using the same basic factors of safety against yielding as in the AISC specifications, except that the maximum allowable bending and shear stresses should be computed using the actual stresses causing yielding at the hole rather than nominal beam stresses. For plastic design, beams with web holes should be designed using the AISC load factor of 1.70, except that the maximum allowable loads should be computed using the actual ultimate strength of the beam at the hole rather than the strength of the gross beam. For large spacings of holes, the effects of each hole should be computed individually. For more than two adjacent holes, the Vierendeel frame analysis should be used while for geometrically dissimilar adjacent holes a frame analysis may be used. With regards to buckling, the same type of buckling analysis should be used as in case of beams without web holes, so long as the edge of the hole is at least four inches from the edge of bearing. When a hole is located in a region of pure bending, the possibility of vertical flange buckling could be checked by assuming that the compression T-section at the hole acts as a column.

In the same year Redwood (20) presented a method of deriving an interaction curve relating moments and shears, as well as a simplified, slightly conservative solution to obtain an approximation to the interaction curve. Bower (21) provided the information on the plastic behavior of beams with web openings along with equations predicting their ultimate strength. As the load on the beam increases, the first yielding in the vicinity of the hole occurs at the corners because of the stress concentration at that location.

In 1969, Cheng (22) experimentally analyzed the stresses around a rectangular web opening in a W shape beam using the photostress method and electrical resistance strain gage technique.

Several papers (23,24,25,26) have been published concerning the plastic behavior and ultimate strength of beams with web openings.

In 1970, Congdon and Redwood (27) conducted an investigation concerning the plastic analysis of reinforced openings through beam webs based on the assumptions of perfectly plastic material behavior. A series of tests were carried out to determine the effects of M/V ratio, reinforced area, hole aspect ratio, ratio of hole depth to beam depth, and location of reinforcement on the beam behavior. The experimental results confirmed the assumption of simple stress distribution at failure. An equation for obtaining the area of reinforcement to take up the maximum shear capacity was also provided. The effects due to one-sided reinforcement for the web opening were not much different from those obtained from reinforcements on both sides of the web at critical points.

An analytical method of determining the moment carrying capacity of beams with eccentric rectangular web holes was given by Richard (28) in 1971.

The effects of varying the opening eccentricity, opening length and opening height were investigated. By increasing the opening eccentricity, the moment carrying capacity for high shear values increased. As the opening length and opening height increased, the moment carrying capacity decreased. When the opening height became larger than the opening length, the moment carrying capacity of the beam increased. It was also found that the shear forces were unequally distributed across unequal web areas.

In 1972, Cooper and Snell (29) performed tests on beams with reinforced web openings and confirmed the validity of the Vierendeel Analysis for the estimation of the normal stresses in the vicinity of the hole. Ultimate load tests were run on three beams and the results were consistent with the predictions obtained from the ultimate strength theory for reinforced web openings presented in Ref. (26).

Frost (30), 1973, conducted an experimental investigation on eight beams to determine their ultimate strength. The web openings were tested with an eccentricity of 1 in. and 2 in. and with the moment to shear ratio at the hole at values of 0 in. and 40 in. The Vierendeel Method was used for the theoretical analysis and several different formulas for determining the shear force distribution were presented and compared.

THE FINITE ELEMENT METHOD

The concept of the finite element method was originally introduced by Turner, et al. in 1956 (31). The method has proved to be quite convenient from an automation point of view, for the solution of problems in continuum mechanics. The first applications were in plane stress problems (32). O. C. Zienkiewicz and Y. K. Cheng (33) also presented the theory necessary for the analysis of a plane elastic continua. The finite element method has since then been extended to axi-symmetric stress analysis, flat plate bending, three-dimensional stress analysis and shell analysis.

The basic concept of the finite element method is that every structure may be considered to be an assemblage of individual structural components or elements. A plane continuum is divided into elements interconnected at a finite number of nodes. Certain approximations have been introduced into the formulation of this discretization of the original continuum and the evaluation of element properties. Judgement is required in making the proper subdivisions, such as element shape and degree of freedom, so that the substitute structure can simulate the actual structure. It is also important to choose a suitable displacement function which can satisfy the requirements of displacement continuity between adjacent elements. All of these factors will determine whether the substitute structure is stiffer or more flexible than the real structure and to what degree the approximation simulates the behavior of the actual structure.

In brief, the finite element analysis of an elastic continuum has the following characteristics:

- (1) Structural discretization
- (2) The necessity for choosing an appropriate displacement function.

- (3) The evaluation of element properties
- (4) The assemblage of finite elements and the following of standard displacement method procedures.

In applying this method, the following requirements must be satisfied simultaneously.

- (1) Force equilibrium in each element
- (2) Displacement compatibility at nodal points between adjacent elements
- (3) The internal forces and deformations are related through the geometric and material property characteristics.

Various shapes of finite elements were employed in these analyses. In general, applicable rectangular elements give a little better approximation of stresses and deflections for a given nodal pattern than triangular elements, because they employ a closer deformation approximation. However, the use of quadrilateral elements could entail arithmetical difficulty and consequently a disproportionate increase of computing time in deriving the element characteristics. Because of the greater adaptability of the triangular shape in fitting arbitrary boundary geometries, triangular elements have been used more widely in the development of general purpose analysis programs.

THE FINITE ELEMENT PROGRAM

Introduction

The computer program used (1) in this project is for the stress analysis of plane structures in the elastic-plastic range by the finite element method. It was developed jointly by the Illinois Institute of Technology Research Institute and the Air Force Flight Dynamics Laboratory. The program can handle bar and triangular plate elements so that it is applicable to trusses and to the analysis of in-plane stresses in reinforced plates. The material behavior is assumed to be isotropic and the user has a choice of three types of stress-strain laws namely Ramberg-Osgood, Goldberg-Richard and the Bilinear laws. In this project the Bilinear law has been used. The program is developed to handle up to ten different materials.

A numerical step by step procedure for obtaining solutions which satisfy the requirements of the incremental theory of plasticity for materials which obey the Mises yield condition and the associated flow rule is used in the program. At each step in the solution, an iterative procedure is used to find the correct values of the strain increments. Changes in plastic strain are accounted for by the addition of fictitious plastic forces to the actual loading on the structure in such a way that the deflections of the structure under the modified loading with assumed elastic behavior are equal to the actual deflections.

Element Properties

The two types of elements used in the analysis (the bar and the triangular plate) are shown in Fig. (1). The coordinates of the end points of the bar and the vertices of the triangle are referred to a fixed coordinate system in a plane. The nodes of each element are numbered in the anti-clockwise

direction as shown in the figure. The geometry of the structure is determined by specifying the x and y coordinates of each node, with respect to a fixed set of coordinate axes and by specifying the thickness of the triangular element or the cross-sectional area in the case of a bar element. The cartesian components of the nodal displacements for each of these elements comprise the element displacement vector \bar{X} . The total element strain designated by the vector ϵ can be expressed in terms of the nodal displacement by an equation of the form

$$\epsilon = B\bar{X}$$

The stresses are related to the elastic strains by Hooke's Law

$$\sigma = C\epsilon$$

The nodal forces, F , corresponding to given displacement, \bar{X} , are found by the principle of virtual work.

Elastic-Plastic Analysis:

In the elastic range of material behavior the equilibrium equations for a structure composed of plate and bar elements of the type considered can be written as

$$F = K\bar{X} \quad (1)$$

where the force and displacement vectors now have as their components, the cartesian components of force and displacement at all the nodes and K is the assembled stiffness matrix for the whole structure. The solution of Eq. (1) for the unknown displacement is given symbolically by $\bar{X} = K^{-1} F$.

The displacements known, the element strain and stresses can be obtained. However, when the stresses reach the intensity required to cause plastic flow, it becomes necessary to determine the increments of plastic strain caused by the load increment. The material is assumed to obey the Mises yield condition and the associated flow rule. For plane stress the following equations apply:

$$\bar{\sigma} = (\sigma_x^2 - \sigma_x \sigma_y + \sigma_y^2 + 3\tau_{xy}^2)^{1/2} = H(\bar{\epsilon}^p) \quad (2)$$

$$\Delta \bar{\epsilon}^p = \frac{2}{\sqrt{3}} (\Delta \epsilon_x^p{}^2 + \Delta \epsilon_x^p \Delta \epsilon_y^p + \Delta \epsilon_y^p{}^2 + \frac{1}{4} \gamma_{xy}^p{}^2) \quad (3)$$

$$\left. \begin{aligned} \Delta \epsilon_x^p &= \frac{\Delta \bar{\epsilon}^p}{2\bar{\sigma}} (2\sigma_x - \sigma_y) \\ \Delta \epsilon_y^p &= \frac{\Delta \bar{\epsilon}^p}{2\bar{\sigma}} (2\sigma_y - \sigma_x) \\ \Delta \gamma_{xy}^p &= 3 \frac{\Delta \bar{\epsilon}^p}{\bar{\sigma}} \tau_{xy} \end{aligned} \right\} \quad (4)$$

where $\bar{\sigma}$ and $\bar{\epsilon}^p$ are the effective stress and the effective plastic strain, respectively, and where $H(\bar{\epsilon}^p)$ is the stress-plastic strain relation for uniaxial stress.

If it is assumed that the response of the structure to the removal of a load increment will be completely elastic then Equation (1) can be modified to account for plastic flow as follows

$$K\bar{X} = F + F^p \quad (5)$$

where X and F are the displacement and load after the application of the increment and F^p is the vector of plastic forces corresponding to the plastic strains. The plastic strain increments caused by the increment of load must satisfy Equations (4) and for an element undergoing plastic flow the stresses must satisfy the yield condition (Equation (2)).

In general, the following steps give the iterative method used to obtain solution. For the details refer to the program in Appendix I:

1. An increment is given to the applied loads.
2. New values of displacement are found from Equation (5) using the current values of the plastic forces (these will be zero for the first step).

3. The displacements are used to compute total strains, elastic strains, stresses, and the effective stress.
4. If the new value of the effective stress is greater than the largest previous value, the element is plastic and the effective stress is used to determine a new value of the effective strain.
5. Plastic strain increments computed from Equations (4) are added to the current values of the plastic strain and new values of the plastic forces are calculated.
6. If the increment in effective plastic strain is sufficiently small the iteration is complete and a return to step 1 is made, if not a return is made to step 2 and a new cycle begun.

This procedure is applied to each of the elements and the decision to start a new step (apply a load increment) is based on the largest plastic strain increment found among all the elements.

An important feature of the method is the way in which the effective plastic strain is computed from the new value of the effective stress at each iteration. If the inverse of Equation (2) is used to give $\bar{\epsilon}^P$ as a function of $\bar{\sigma}$ the solution may become unstable. This becomes obvious when one considers the case of the elastic, perfectly plastic material for which the inverse of the function $H(\bar{\epsilon}^P)$ does not exist. To avoid this difficulty, the total strain ϵ_t is taken equal to the sum of the value of $\bar{\epsilon}^P$ computed in the previous iteration and $\bar{\sigma}/E$.

The stress-strain law can be written in the form

$$\epsilon_t = \frac{\bar{\sigma}}{E} + \bar{\epsilon}^P$$

or

$$\epsilon_t = \frac{H(\bar{\epsilon}^P)}{E} + \bar{\epsilon}^P \quad (6)$$

The new value of $\bar{\epsilon}^P$ can be found from Equation (6) without difficulty.

The criterion used in Step 6 of the iterative procedure given above, to decide whether the plastic strains have been determined with sufficient accuracy, is the size of the ratio of the increment in effective plastic strain to $\bar{\sigma}/E$. This ratio is a measure of the difference between the ordinates to the theoretical stress-strain curve and the curve that is actually being used at that step in the calculations.

LABORATORY EXPERIMENTS

Ultimate load tests were conducted on five A36 steel beams, two of which were W16 x 45 shapes and three were W16 x 40 shapes. Though the length of the beam was not the same in all the cases, the moment-to-shear ratio, M/V , at the centerline of the opening was kept constant at 30 inches. The test set up, as depicted in Fig. 2a, consisted of simple supports at the ends and a concentrated load applied at midspan. A variable, X , describes the variation of the span length as illustrated in the figure and tabulated in Table 1 for the various test specimens. Beams 3 and 4 are not listed in Table 1 since they were subjected to elastic tests only.

The size of an opening, one of the experimental variables, is given by half its length, a , half its depth, h , and the corner radius, r . Table 1 gives these values for each of the test specimens. However the eccentricity of the opening, that is the distance between the mid-depth of the beam and the centerline of the opening was 2 inches for all the beams. The eccentricity was towards the compression flange in Beams 1, 2 and 5. In Beams 6 and 7, it was towards the tension flange.

Except for Beam 1, all Beams were reinforced at the opening with two bars, one above and one below the opening and at a distance $1/4$ inch from the edge of the opening. Beam 5 was reinforced on both sides of the web and the others on one side only. Figure 2b shows the general layout of the reinforcement used. The reinforcement was comprised of bars $2 \times 1/4$ inches which were considered as the practical minimum size in accordance with the AISC Specifications (34). In all cases the reinforcement was extended 3 inches beyond the edges of the opening. This 3 inches was calculated to be sufficient to develop the strength of the bar using a $3/16$ inch fillet weld.

Bars of 3 x 1/2 inches, welded to the web and the flanges with a 3/16 inch fillet weld served as bearing stiffeners in all the beams. All except Beam 1 were provided with bearing stiffeners at the supports and at the load point. Beam 1 was provided with bearing stiffeners only at the load point.

In Beams 2 and 5, cover plates were attached with 1/4" fillet welds to both the flanges at the centerline of the beam. The function of these cover plates was to strengthen the beam at the center and force the failure to occur at the opening. Table 1 gives the dimensions of the cover plates. In Beams 1, 6 and 7 no cover plates were used because the opening sizes and the spans used were such that failure occurred at the opening before a plastic hinge could form at mid-span.

The actual static yield stresses were determined from tensile tests on coupons which were cut from the web and flanges. Similar tests were also conducted to obtain the static yield stresses of the reinforcing bars. The average static yield stresses and the maximum deviation from the average are listed in Table 2.

Load was applied in increments with a Tinius-Olsen screw type machine until specified deflections were reached, and the load then allowed to drop off to the static level. A detailed description of the experimental work can be found in Ref. (2). The experimental ultimate loads were measured and the load-deflection curves plotted. The ultimate loads were corrected for strain hardening and the corrected values are given in Table 6.

PREPARATION FOR COMPUTER ANALYSIS

Idealization

In order to apply a plane stress finite element method to a three-dimensional structure, certain modifications must be made. The procedure followed was to substitute equivalent bar members pin-connected to the appropriate nodes of the plate elements for the flanges and reinforcing bars. These bar members do not have an associated thickness but have one dimensional material properties which can transfer only axial forces.

To find the equivalent flange element, therefore, there is a conflict between maintaining the area of the flange and maintaining the moment of inertia of the beam. Since retaining the actual strength of the beam is more important compared to maintaining the actual area, the equivalent flanges were determined in such a way that the moment of inertia was kept a constant, Fig. 3.

The moment of inertia, I , of the beam is given as:

$$I = \frac{t_w}{12} (d - 2t_f)^3 + 2 \left\{ b_f \frac{t_f^3}{12} + b_f t_f \left(\frac{d}{2} - \frac{t_f}{2} \right)^2 \right\}$$

and the moment of inertia, I_{eq} , of the equivalent idealized beam is given as:

$$I_{eq} = \frac{t_w d^3}{12} + 2 \left\{ A_{eff} \left(\frac{d}{2} \right)^2 \right\}$$

If $I_{eq} = I$, then the effective flange area, A_{eff} , of the idealized beam is given as

$$A_{eff} = \frac{2I}{d^2} - \frac{t_w d}{6}$$

where t_w is the web thickness of the actual and idealized beam sections, d is the total depth of the beam, t_f is the thickness of the flange and b_f is the width of the flange. The idealized properties of the beams are listed in Table 3.

The bar elements representing the flanges had to be increased in the corresponding length of the beam to account for the cover plates. The actual modified moment of inertia of the beam at that section is

$$I_{\text{mod}} = I + I_{\text{cp}}$$

where $I_{\text{cp}} = 2A_{\text{cp}} \left(\frac{d}{2} - \frac{d'}{2} \right)^2$; being the moment of inertia of the cover plates about the x-axis of the beam,

d' = thickness of the cover plate.

The equivalent modified moment of inertia is given as $I_{\text{eq.mod.}} = \frac{t_w d^3}{12} + 2\{A_{\text{mod}} (d/2)^2\}$. If $I_{\text{eq.mod.}} = I_{\text{mod}}$ then the modified area for the flange elements to account for cover plates is given by

$$A_{\text{mod}} = \frac{2I}{d^2} - \frac{t_w d}{6} + A_{\text{cp}} \left(1 - \frac{d'}{d} \right)^2$$

The idealization using a plane stress procedure to simulate the beam behavior was similar for one and two sided reinforcement. This is based on the conclusions of other investigators (27,29), that one sided reinforcement has no significant effects different from those of two sided reinforcement. Therefore, the results of the study can represent both types of reinforcement with the same total cross-sectional area. The equivalent reinforcing elements were obtained by replacing the reinforcement by bars which have the same location and cross-sectional area as the reinforcement and shown in Fig. 3b.

Discretization

Though no general rule can be stated as how to best discretize a given structure, it is obvious that the accuracy improves as the size of the mesh decreases. Good results are frequently obtained with rather coarse

subdivisions Ref. (35). Consider a case of a deep rectangular beam subjected to pure bending. Two types of rectangular discretizations are shown in Fig. 4. Now, the assumptions of the beam theory states that plane cross-sections remain plane in bending though the axial fibers of the beam become curved. Thus in order to best approximate the straight transverse sections and the curved axial sections that occur during deformation, the discretization (b) in Fig. 4 is preferred over the discretization (a).

From the results of the examples considered in Ref. (35), it is found that if triangular elements are well formed, i.e. essentially equilateral, better results are expected. The poorest overall displacement patterns are produced with the discretization which contains many weak triangles.

Keeping the above mentioned points in mind, the test beams were divided into a mesh of triangular and bar elements as given in Table 3. Smaller triangular elements were used near the opening in order to get a better picture of the yield pattern near the opening. The rounded corners of the hole were approximated by the best suited triangular elements. The element configuration for the fillets at the corners of the opening were slightly different in beams 6 and 7. This change made no significant difference in terms of the yield pattern or the ultimate load.

Solid Beams

A regular beam without any opening was called a solid beam. Every beam with an opening had a corresponding solid beam. Test runs, by the finite element method only, were made on each of the solid beams in order to aid in comprehending the effects of the openings. The details of the idealization of the solid beams are given in Table 4.

PRESENTATION OF RESULTS

The solid beams were tested first, in order to get an idea of the ultimate capacity of the beams without an opening. Table 5 gives the loading details of the beams with the opening and the solid beams.

The actual experimental ultimate loads, the ultimate loads corrected for strain hardening and the ultimate loads obtained from the finite element analysis are given in Table 6.

From the computer output, the yielded elements were determined and were then plotted in order to show the yield patterns. A triangular element having any effective strain was considered yielded. With an error tolerance of 0.03 in the effective strain the effective stresses of the yielded elements were not exactly equal to the yield stress of the material but rather close to it. For a bar element to yield, its stress value must reach the yield point, however, due to the error tolerance used, it was decided to consider a bar element yielded whenever its stress was within 0.15 kip/in^2 of the yield stress.

The usual sign convention is used in the program, namely tensile stresses are positive and compressive stresses are negative. If the stresses in both the directions, that is x and y, are positive then the element is considered to have been yielded in tension and likewise, in compression if both are negative. But if the stress in one direction is positive and in the other direction is negative, the element is considered to be yielded in a combination of tensile and compressive stresses. Compressive yielding is shown by horizontal lines while tensile yielding is shown by verticle lines. A combination type of yielding is shown by solid shading.

Since the elements near the opening are very small, the figures showing the yield pattern have been divided into two types. One showing the enlarged

view in the vicinity of the opening and the other showing the remaining portion of the beam. None of the stiffeners in any of the beams were close to yielding. Hence they have been omitted in order to simplify the figures.

The yield pattern for the ultimate load is shown for all the beams. Additional plots for intermediate loads are also shown for beams 1, 2 and 6. The details of the figures are given below:

- Figure 5: Yield pattern for Solid Beam 1 at ultimate load of 144 kips.
- Figure 6: Yield pattern in the vicinity of its opening for Beam 1 at a load of 80 kips. No other elements in the Beam have yielded at this load.
- Figure 7: Yield pattern in the vicinity of its opening for Beam 1 at a load of 96 kips. No other elements being yielded in the Beam.
- Figure 8: Yield pattern in the vicinity of its opening for Beam 1 at a load of 112 kips. No other elements being yielded in the Beam.
- Figure 9: Full view of Beam 1 showing yield pattern at ultimate load of 144 kips.
- Figure 10: Yield pattern in the vicinity of its opening for Beam 1 at ultimate load of 144 kips.
- Figure 11: Yield pattern for Solid Beam 2 at ultimate load of 168 kips. There are cover plates at midspan and stiffeners at the supports. This being the only difference between Solid Beam 2 and Solid Beam 1.
- Figure 12: Yield pattern in the vicinity of its opening for Beam 2 at a load of 96 kips. No other elements being yielded in the Beam.
- Figure 13: Full view of Beam 2 showing yield pattern at a load of 144 kips.
- Figure 14: Yield pattern in the vicinity of its opening for Beam 2 at a load of 144 kips.
- Figure 15: Full view of Beam 2 showing yield pattern at ultimate load of 152 kips.
- Figure 16: Yield pattern in the vicinity of its opening for Beam 2 at ultimate load of 152 kips.
- Figure 17: Yield pattern for Solid Beam 5 at ultimate load of 144 kips.

- Figure 18: Full view of Beam 5 showing yield pattern at ultimate load of 128 kips.
- Figure 19: Yield pattern in the vicinity of its opening for Beam 5 at ultimate load of 128 kips.
- Figure 20: Yield pattern for Solid Beams 6 and 7 at ultimate load of 112 kips. Since the only difference between Beams 6 and 7 is in the size of the opening, there is no difference between the Solid Beams 6 and 7.
- Figure 21: Yield pattern in the vicinity of its opening for Beam 6 at a load of 54 kips, no other elements being yielded in the Beam.
- Figure 22: Yield pattern in the vicinity of its opening for Beam 6 at a load of 72 kips. No other elements in the Beam have yielded at this load.
- Figure 23: Full view of Beam 6 showing yield pattern at ultimate load of 84 kips. None of the flange elements have yielded. Since a 100 iterations per step have been reached with an error tolerance of 0.03, the Beam is considered to have been yielded in a practical sense.
- Figure 24: Yield pattern in the vicinity of its opening for Beam 6 at ultimate load of 84 kips.
- Figure 25: Full view of Beam 7 showing yield pattern at ultimate load of 96 kips. Here again none of the flange elements have yielded. For the same reason as in Beam 6, the Beam is considered to have been yielded in a practical sense.
- Figure 26: Yield pattern in the vicinity of its opening for Beam 7 at ultimate load of 96 kips.

DISCUSSION

Ultimate Loads

The ultimate loads obtained from the finite element results are given in Table 6. The accuracy of these ultimate loads depends on the size of the load increments used in the analysis. The smaller the increment size the better the accuracy, but the cost of running the computer program increases as the increment size is decreased. The ultimate load predicted by the finite element method is an upper bound value. Theoretically it should satisfy the inequality:

$$P_u^{\text{true}} \leq P_u^{\text{FE}} < (P_u^{\text{true}} + i)$$

where i = increment size.

The experimental ultimate loads corrected for the effects of strain hardening (2), along with their ratios to those obtained from the finite element method are also listed in Table 6. These ratios indicate that the values predicted by the finite element method are within 6% of those obtained experimentally in all cases.

A further comparison of the finite element results is made with those obtained from an ultimate strength analysis (2). These theoretical ultimate loads were found through the use of interaction diagrams which were obtained from a computer program developed by Wang (36). Once again the ratios of the theoretical and the finite element ultimate loads show a good correlation. Thus it can be concluded that the finite element method predicts the ultimate loads with reasonably good accuracy.

The ultimate loads of the solid beams and their ratios to the ultimate loads of the beams with the openings are also given in Table 6. These ratios show the reductions in the load carrying capacities of the beams due to the web openings. The value of this ratio for Beam 1 is 1.00, thus indicating that

the opening has very little or no effect on the ultimate load of the beam under the existing conditions. This is consistent with the experimental findings (2).

Yield Patterns and Modes of Failure

To begin with, a brief discussion of the effects of secondary moments will aid in a better understanding of the yield patterns.

Consider a section of a loaded beam at the opening. See Fig. 27a. The high moment edge of the opening is at the right, and hence primary moment $M_2 > M_1$. Equilibrium requires that $2aV = M_2 - M_1$. The shear forces V_t and V_b are distributed to the top and bottom of the opening, Fig. 27b. To maintain equilibrium, secondary moments M_T^S and M_B^S are generated,

$$\text{where} \quad 2M_T^S = 2aV_T$$

$$\text{and} \quad 2M_B^S = 2aV_B$$

Thus the individual sections, above and below the opening, behave as fixed ended beams. Due to the secondary moments there exists compressive normal stresses in the regions near b, d, f and h and tension in the region near a, c, e and g. Due to the primary moment effects only, the entire section above the opening is in compression while the entire section below the opening is in tension. Therefore the corners of the opening at the low moment edge, namely d and e, yield first due to the additive effect of the primary and secondary moments. At the corners c and f the effect of the primary and secondary moments is in the opposite sense and hence the yielding is not so pronounced.

Figures 7 and 12 show the plots of the yielded elements of Beams 1 and 2 at a load of 96 kips. The number of elements yielded in the reinforced case,

that is beam 2, is nearly half that of the unreinforced case, that is, Beam 1. The effect of the reinforcement is such that the yielding is limited to the area in the web between the reinforcement and the edge of the opening. In both cases there is greater yielding at the low moment edge because of the secondary moment effect. Yield patterns for the same beams at a load of 144 kips are shown in Figs. 10 and 14. While this is the ultimate load for the unreinforced case, the reinforced case is 8 kips below its ultimate load. In general there exists a greater amount of yielding in the unreinforced case with a substantial amount of yielding in the flanges, though, there is very little flange yielding at this stage in the reinforced case. This is attributed to the cover plates. The flange yielding in Beam 2 is only on the tension side, between the opening and the end of the cover plate. A closer look at Fig. 10 reveals the existence of a compression element in the tension region. This is due to the secondary moment effect. There are no stiffeners at the supports in Beam 1 and hence the elements at the supports have yielded. This is not so in the Solid Beam 1 because of larger elements used in the discretization of the Solid Beam. Solid Beam 2, Fig. 11, has a greater moment carrying capacity because of the cover plates at mid-span. The ultimate load for solid Beam 2 being higher, the number of elements yielded in Solid Beam 2 is substantially greater than in Solid Beam 1.

Figures 17 through 19 are for Beam 5 and reveal a reduction of 16 kips in the ultimate load due to the opening. Once again in this case the cover plates prevent flange element yielding at mid-span. The quantity of reinforcement used being large, there is no yielding in the reinforcement.

Looking at the yield patterns of Beams 6 and 7, Figs. 23 through 26, a great deal of similarity is observed. There is very little yielding at midspan and the failure in both cases is essentially at the opening.

In all the solid beams it can be observed that the yielding is more extensive towards one side of the centerline even though the loading and support conditions are symmetrical, see Figs. 5, 11, 17 and 20. This is due to the asymmetric element configuration. If the elements were symmetric about the centerline, then the yielding also would be symmetrical. The failure is a typical one hinged mechanism, with the plastic hinge developing at midspan under the load.

In all the beams the first sign of yielding is observed in the web adjacent to the corners of the opening. These yielded zones enlarge as the load increases. At the ultimate load the yielding takes up a pattern which can schematically be shown as in Fig. 28. This type of a pattern generally confirms that a four hinged mechanism develops at failure as assumed in the theoretical analysis (36).

CONCLUSIONS

From the comparison of the results obtained by the finite element method with the experimental and theoretical values, the conclusions reached were:

- 1) The ultimate loads obtained from the finite element analysis are in reasonably good agreement with those obtained from the experiments and also with those obtained theoretically from an ultimate strength analysis.
- 2) The yield patterns at various loads agree closely with those obtained in the experiments.
- 3) The failure at the opening is a four hinged mechanism as assumed in the theory, with a plastic hinge at each corner of the opening.

ACKNOWLEDGEMENTS

The author is indeed grateful to Dr. Robert R. Snell, Head of the Civil Engineering Department, for his invaluable advice and assistance offered during the preparation of this paper.

Special appreciation is due to Professor Peter B. Cooper for the keen interest he took and the able guidance he offered.

A debt of gratitude is due to Professor Stuart E. Swartz, the author's Academic Advisor and member of the Advisory Committee.

A word of thanks is extended to Professor Teddy O. Hodges, Associate Dean, College of Engineering, for serving as a member of the Advisory Committee.

Support for the research described in this paper was provided by the National Science Foundation Grant GK-35762 and the Department of Civil Engineering at Kansas State University. This support is sincerely acknowledged.

APPENDIX I

Details of the Computer Program

A brief description of the Fortran IV program for the elastic-plastic analysis of plane structures composed of bar and triangular plate elements is given here.

Table AI-I. Input Data Format

Card 1	TITLE CARD (72H)		
Col	1-72	Any alphanumeric information	
Card 2	PROPERTIES CARD (14I5)		
Col	1-5	NNODE -	number of nodes (maximum 450)
	6-10	NELEM -	number of elements (maximum 800)
	11-15	ILAW -	1 Ramberg-Osgood Law
		-	2 Goldberg-Richard Law
		-	3 Bilinear Law
	16-20	IUNLD -	1 Unloading following loading
		-	0 Loading only
	21-25	MAT -	number of materials used (maximum 10)
	26-30	MAXBND-	maximum bandwidth, MAXBND = 60
			for this program
	31-35	NBC -	number of boundary conditions with prescribed displacement. The maximum number is 30 in this program.
Card 3	MATERIAL PROPERTIES CARDS (E15.8, 3F10.5)		
Col	1-15	EE -	modulus of elasticity
	16-25	EE1 -	secant yield stress, ultimate stress, yield stress
	26-35	PRR -	Poisson's ratio
	36-45	EE2 -	shape parameter, plastic modulus
Card 4	CONTROL CARD (6I5, F10.0)		
Col	1-5	NDIV -	number of load increments
	6-10	NIT -	maximum number of iterations per step
	11-15	NPRINT-	print output for each NPRINT increment.
			(e.g., if NPRINT = 3, for increments 3, 6, 9 etc.)
	16-20	KSTART-	number of increments at which solution is to start
	21-25	KSTOP -	number of increments at which solution is to stop
	26-30	NLOAD -	number of nodes at which loads are specified
	31-40	TOL -	error tolerance

Table AI-I (Continued)

Card 5	NODE CARDS (4I5, 5F10.0)	
Col	1-5	Node number
	6-10	IBCX = 1, if displacement in x-direction is specified
	11-15	IBCY = 1, if displacement in y-direction is specified
	16-20	IBCS = 1, if slope is specified
	21-30	XCORD - x coordinate of the node
	31-40	YCORD - y coordinate of this node
	41-50	BC1 - specified displacement in x-direction
	51-60	BC2 - specified displacement in y-direction
	61-70	BC3 - specified slope at the node
Card 6	ELEMENT CARDS (5I5, F10.0)	
Col	1-5	Element number
	6-10	I1 - nodes defining the element
	11-15	I2 - nodes defining the element
	16-20	I3 - nodes defining the element
	21-25	NTYPE - material type
	26-35	Z - element thickness or cross-section area
Card 7	LOAD CARDS (I5, 2F10.0)	
Col	1-5	Node number
	6-15	x-component of force
	16-25	y-component of force

The program uses a subroutine for the solution of simultaneous equations in band form written by Professor E. L. Wilson of the University of California. Great economies in storage requirements and in time required for solution are achieved in this way.

Three types of stress-strain laws are available for use in the computer program. Each of them is a three parameter law and is given below:

1. Ramberg-Osgood Law

$$\epsilon_t = \frac{\sigma}{E} + \frac{3\sigma_1}{7E} \left(\frac{\sigma}{\sigma_1} \right)^n$$

in which

E - Young's modulus

σ_1 - secant yield stress (stress at which the secant modulus = $0.7E$)

n - shape factor

2. Goldberg-Richard Law

$$\sigma = E\epsilon_t \left\{ 1 + \left| \frac{E\epsilon_t}{\sigma_u} \right|^{n-1/n} \right\}$$

in which

E - Young's modulus

σ_u - maximum stress

n - shape factor

3. Bilinear Law

$$\sigma = E\epsilon_t \quad \text{for } \sigma < \sigma_y$$

$$\sigma = \sigma_y + E_1 \left(\epsilon_t - \frac{\sigma_y}{E} \right) \quad \text{for } \sigma \geq \sigma_y$$

in which

E - Young's Modulus

σ_y - yield stress

E_1 - slope of the plastic portion of the stress-strain curve.

The correspondence between the program variables and the stress-strain law parameters for each of three laws is given in Table AI-II.

Table AI-II

Stress Strain Law	Program Variables				
	ILAW	E	EE1	EE2	PRR
Ramberg-Osgood	1	E	σ_1	n	v
Goldberg-Richard	2	E	σ_u	n	v
Bilinear	3	E	σ_y	E_1	v

Correspondence Between Program Variables and Stress
Strain Law Parameters.

The displacement component in the x and y direction can be specified at any node or a node can be required to move along a line with a specified slope.

The x and y components of load can be specified at any node. Distributed loads must be treated as concentrated at the nodes.

The number of equal increments into which the applied loads and specified displacements are to be divided is specified as input. It is also necessary to specify the number of the increment at which the solution is to start. For example, if a number of increments $NDIV = 20$ is specified and a value of the starting increment $KSTART = 5$ is used, one quarter of the load (displacement) will be applied in the first step, the rest in 15 equal increments. If it is desired to stop the solution at an intermediate step a value of $KSTOP$ may be specified. If the unloading solution is desired the value $LUNLD = 1$ is used.

An error tolerance must be specified as input. After each cycle of iteration the maximum error among all the elements is compared with the specified tolerance. If the tolerance is met the next load increment is applied, if not, the iteration is continued. If the tolerance on error is

is not met when the allowable number of iterations is reached the solution is stopped.

The nodal forces and displacements, the maximum error and the number of the element in which it occurs are printed out at the end of each increment. The cartesian components, principal values, and direction of stress and strain are printed out at the user's option by specifying a value of NPRNT as input. For example, a value of NPRNT = 3 will cause the stresses and strains to be printed out for increment numbers divisible by three. The directions of the principal axes of stress are defined by

$$\phi = -\frac{1}{2} \tan^{-1} \frac{2\tau}{\sigma_x - \sigma_y} , \quad \frac{\pi}{2} < \phi < \frac{\pi}{2}$$

The value of ϕ in degrees is printed out. In the case of strain the principal directions are defined by

$$\phi = -\frac{1}{2} \tan^{-1} \frac{\gamma}{\epsilon_x - \epsilon_y} , \quad -\frac{\pi}{2} < \phi < \frac{\pi}{2}$$

This value is also printed out since in general the principal axes of stress and total strain do not coincide when plastic flow has taken place.

The effective stress and the effective plastic strain are also given as output for each element.

An example problem of a cantilever beam has been worked out to illustrate the use of the finite element program.

The Fortran IV source program is listed along with the input data and the output of the example problem.

ILLEGIBLE DOCUMENT

**THE FOLLOWING
DOCUMENT(S) IS OF
POOR LEGIBILITY IN
THE ORIGINAL**

**THIS IS THE BEST
COPY AVAILABLE**

```

C      ELASTIC PLASTIC FINITE ELEMENT PROGRAM                                VER70001
C      WITH THREE STRESS STRAIN LAW OPTIONS                                  VER70002
COMMON/ADD/  FE(10),EE1(10),EE2(10),PRR(10)                                VER70003
COMMON  E,CC,G1,F2,PR,FPR,X21,Y21,X31,Y31,X32,Y32,XERR,                    VER70004
1      N2,NELEM,KEL,ILAW,MAT,NBC,                                          VER70005
2      R(900,60),BC(30,3),TAB(101,20),IFIX(2),
3      X(900),XCORD(450),Y(450),ICORD(450),
4      FP(900),F(900),
5      I1(800),I2(800),I3(800),NTYPE(800),Z(800),I4(800),
6      SFF(800),SET(800),FEP(800),EXPL(800),EYP(800),EXYP(800),
7      NNODE,MRAND                                                         VER70011
      DIMENSION JX(800,3),FE(900)
      EQUIVALENCE (JX,I1)
      EQUIVALENCE (IFIX(1),IRCX),(IFIX(2),IRCY)                                VER70014
C
C      **** READ AND PRINT DATA ****                                     VER70015
C                                                                 VER70016
C                                                                 VER70017
10 READ (5,20,FND=700)
   IONE=1
20 FORMAT(72H      RCD INFORMATION
1      )
   WRITE (6,30)
30 FORMAT(1H1)
   WRITE (6,20)
   READ(5,40) NNODE,NELEM,ILAW,IUNLD,MAT,MAXRND,NBC
40 FORMAT(14I5)
   READ(5,50) (FE(I),EE1(I),PRR(I),EE2(I),I=1,MAT)
50 FORMAT(E15.8,3F10.5)
   READ(5,60)NDIV,NIT,NPRNT,KSTART,KSTOP,NLOAD,TOL
60 FORMAT(6I5,F10.0)
   IF(KSTOP.EQ.0) KSTOP=NDIV
   GO TO(70,90,110),ILAW
70 WRITE(6,80) (I,EE(I),FE1(I),FE2(I),PRR(I),TOL,I=1,MAT)
80 FORMAT(1H014X18HRAHMBERG OSGOOD LAW/
115X,30HMATERIAL----- 13/
215X30HMODULUS OF ELASTICITY----- E12.4/
315X30HSECANT YIELD STRESS----- E12.4/
415X30HSHAPE PARAMETER----- E12.4/
515X30HPOISSON'S RATIO----- F8.4/
615X30HERROR TOLERANCE----- F8.4)
   GO TO 130
90 WRITE(6,100) (I,EE(I),FE1(I),FE2(I),PRR(I),TOL,I=1,MAT)
100 FORMAT(1H014X20HGOULDBERG RICHARD LAW/
115X,30HMATERIAL----- 13/
215X30HMODULUS OF ELASTICITY----- E12.4/
315X30HSECANT YIELD STRESS----- E12.4/
415X30HSHAPE PARAMETER----- E12.4/
515X30HPOISSON'S RATIO----- F8.4/
615X30HERROR TOLERANCE----- F8.4)
   GO TO 130
110 WRITE(6,120) (I,FE(I),EE1(I),EE2(I),PRR(I),TOL,I=1,MAT)
120 FORMAT(1H014X12HBILINEAR LAW/
115X,30HMATERIAL----- 13/
215X30HMODULUS OF ELASTICITY----- E12.4/
315X30HSECANT YIELD STRESS----- E12.4/
415X30HSHAPE PARAMETER----- E12.4/
515X30HPOISSON'S RATIO----- F8.4/
615X30HERROR TOLERANCE----- F8.4)
130 WRITE (6,140)NNODE,NELEM,NDIV,NIT
140 FORMAT(1H014X30HNO. OF NODES
      NNODE =14/15X30HNO. OF ELEMFVER70060

```

```

1FNTS          NELEM =14/15X30HND. OF STEPS          NDIV =14/15X30VER70061
2HND. OF ITERATIONS/STEP  NIT =14)                  VER70062
  DO 150 I=1,NRC                                     VER70063
    DO 150 J=1,3                                       VER70064
150  BC(I,J)=0                                         VER70065
    IC=1                                               VER70066
    WRITE(6,160)                                       VER70067
160  FORMAT(25HBOUNDARY CONDITION ARRAY/10H0 NODAL PT15X1HX23X1HY VER70068
    120X7HSLIDING/1H 14X4HCODE7X5HVALUE9X4HCODE7X5HVALUE9X4HCODE VER70069
    27X5HVALUE)                                       VER70070
C                                                     VER70071
C  **** NODE COORDINATES AND BOUNDARY CONDITIONS **** VER70072
C                                                     VER70073
    DO 200 J=1,NNODE                                  VER70074
      READ(5,170) K,IBCX,IBCY,IBCS,XCORD(K),Y(K),BC1,BC2,BC3 VER70075
170  FORMAT(4I5,5F10.0)                               VER70076
      IF (IBCX+IBCY+IBCS.NE.0) WRITE(6,180)K,IBCX,BC1,IBCY,BC2,IBCS,BC3 VER70077
180  FORMAT(17,3X,3(18,1PE17.7))                     VER70078
      ICODE(K)=IBCS+10*IBCY+100*IBCX                 VER70079
      IF (BC1+BC2+BC3.EQ.0.) GO TO 200                VER70080
      ICODE(K)=ICODE(K)+IC*1000                      VER70081
      BC(IC,1)=BC1                                    VER70082
      BC(IC,2)=BC2                                    VER70083
      BC(IC,3)=BC3                                    VER70084
      IC=IC+1                                          VER70085
      IF (IC.LE.NRC)GO TO 200                         VER70086
      WRITE(6,190)                                     VER70087
190  FORMAT(54H0 MORE THAN 29 NODES HAVE NON ZERO BOUNDARY CONDITIONS) VER70088
      GO TO 620                                       VER70089
200  CONTINUE                                         VER70090
C                                                     VER70091
C  **** ELEMENT PROPERTIES ****                     VER70092
C                                                     VER70093
      READ(5,210)(K,I1(K),I2(K),I3(K),NTYPE(K),Z(K),J=1,NELEM) VER70094
210  FORMAT(5I5,F10.0)                               VER70095
C                                                     VER70096
C  **** LOADS ****                                  VER70097
C                                                     VER70098
      N2=2*NNODE                                       VER70099
      DO 220 K=1,N2                                   VER70100
220  F(K)=0                                           VER70101
      IF (NLOAD.EQ.0) GO TO 250                       VER70102
      DO 230 K=1,NLOAD                                 VER70103
230  READ(5,240)J,F(2*J-1),F(2*J)                   VER70104
240  FORMAT(1I5,2F10.0)                             VER70105
250  CONTINUE                                         VER70106
      WRITE(6,260)(K,XCORD(K),F(2*K-1), Y(K),F(2*K),ICODE(K),K=1,NNODE) VER70107
260  FORMAT(10H0 NODAL PT8X7HX-COORD8X7HX-FORCE8X7HY-COORD8X7HY-FORCE VER70108
    111X4HCODE//(4X,I3,5X4F15.4,I15))               VER70109
      WRITE(6,270)                                     VER70110
270  FORMAT(11H0///10X,90HELEMENT  NODE 1  NODE 2  NODE 3  ELEMENVER70111
    1T TYPE  AREA OR THICK.  MATERIAL TYPE,/)        VER70112
      DO 300 K=1,NELEM                                VER70113
      IF (I3(K).EQ.0) WRITE(6,280) K,I1(K),I2(K),I3(K),Z(K),NTYPE(K) VER70114
      IF (I3(K).NE.0) WRITE(6,290) K,I1(K),I2(K),I3(K),Z(K),NTYPE(K) VER70115
280  FORMAT( 6X,4I9,11X,3HBAR,F22.5,I14)           VER70116
290  FORMAT( 6X,4I9,11X,5HPLATE,F20.5,I14)          VER70117
300  CONTINUE                                         VER70118
C                                                     VER70119
C  INITIALIZATION                                    VER70120

```

```

C
310 XDIV=NDIV
GO TO(320,340,340),ILAW
320 CONTINUE
DO 330 I=1,MAT
F=FF(I)
F1=FF1(I)
F2=FF2(I)
CC=F1/F
G1=(7.0*E/3.0)**(1.0/E2)*F1**(1.0-1.0/E2)
CALL TBLF(I)
330 CONTINUE
340 CONTINUE
C
C **** DETERMINE BAND WIDTH ****
C
DO 350 K=1,NELEM
I4(K)=I3(K)
350 IF(I3(K).EQ.0) JX(K,3)=JX(K,1)
J=0
DO 380 N=1,NELEM
DO 380 I=1,3
DO 370 L=1,3
KK=IARS(JX(N,I)-JX(N,L))
IF(KK-J)370,370,360
360 J=KK
370 CONTINUE
380 CONTINUE
MBAND=2*J+3
IF(MBAND.GT.MAXBND) WRITE(6,390) MBAND
IF(MBAND.GT.MAXBND) GO TO 10
390 FORMAT(1H0)OX20H BAND WIDTH TOO LARGE5X6HMBAND=I4)
DO 400 I=1,NELEM
400 I3(I)=I4(I)
DO 410 J=1,N2
DO 410 J=1,MBAND
410 R(I,J)=0.
C
C CALCULATION OF STIFFNESS MATRIX
C
CALL STIFF
C
C **** REDUCE MATRIX ****
C
CALL SYMSOL(1)
C
C **** INCREMENT LOADS,ADD PLASTIC FORCES AND SOLVE FOR DISPLACEMENTS**
C
DO 420 I=1,NFLEM
SET(I)=0
SEF(I)=0
EFP(I)=0
EXPL(I)=0
EYP(I)=0
420 EXYP(I)=0
KN=KSTART-1
KU=KU
DO 430 I=1,N2
430 FP(I)=0
GO TO 490

```

```

VER70121
VER70122
VER70123
VER70124
VER70125
VER70126
VER70127
VER70128
VER70129
VER70130
VER70131
VER70132
VER70133
VER70134
VER70135
VER70136
VER70137
VER70138
VER70139
VER70140
VER70141
VER70142
VER70143
VER70144
VER70145
VER70146
VER70147
VER70148
VER70149
VER70150
VER70151
VER70152
VER70153
VER70154
VER70155
VER70156
VER70157
VER70158
VER70159
VER70160
VER70161
VER70162
VER70163
VER70164
VER70165
VER70166
VER70167
VER70168
VER70169
VER70170
VER70171
VER70172
VER70173
VER70174
VER70175
VER70176
VER70177
VER70178
VER70179
VER70180

```

```

440 WRITE (6,450)KU,(1,FE(2*I-1),FE(2*I),X(2*I-1),X(2*I),I=1,NNODE) VER70181
450 FORMAT(1H120X38HFORCES AND DISPLACEMENTS FOR INCREMENT,14//10X4HNOVER70182
10F5X7HX-FORCE8X7HY-FORCE9X8HX-DISPL.7X8HY-DISPL./(9X13,2F15.3,5X2FVER70183
215.4 )) VER70184
WRITE (6,460)XERR,KEL,IT VER70185
460 FORMAT(13HOMAX. ERROR =F8.5,5X14HIN ELEMENT NO.14,5X17HNO. OF ITERVER70186
IATIONS14) VER70187
470 IF(MOD(K0,NPRNT))490,480,490 VER70188
480 CALL OUTPT VER70189
IF(K0.EQ.KSTOP)GO TO 620 VER70190
GO TO 500 VER70191
490 IF(K0.EQ.KSTOP) CALL OUTPT VER70192
IF(K0.EQ.KSTOP)GO TO 620 VER70193
500 K0=K0+1ONE VER70194
KU=KU+1 VER70195
IF(K0-NDIV)510,510,620 VER70196
510 XK0=K0 VER70197
DO 520 I=1,N2 VER70198
520 FE(I)=XK0/XDIV*F(I) VER70199
DO 530 K=1,NELEM VER70200
530 SEF(K)=SFT(K) VER70201
IT=0 VER70202
540 DO 570 I=1,NNODE VER70203
IF(ICODE(I).EQ.0) GO TO 570 VER70204
CALL DCODE(ICODE,I,IRCS,IRCX,IRCY,IC,IX,IY,NRC) VER70205
IF(IRCS.NE.1) GO TO 550 VER70206
ALF=RC(IC,3) VER70207
FP(IX)=FP(IX)+ALF*FP(IY) VER70208
FP(IY)=0. VER70209
550 DO 560 N=1,2 VER70210
IF(JFIX(N).NE.1) GO TO 560 VER70211
IR=IX+N-1 VER70212
FP(IR)=0. VER70213
560 CONTINUE VER70214
570 CONTINUE VER70215
C VER70216
C **** SOLVE FOR DISPLACEMENTS **** VER70217
C VER70218
DO 580 I=1,N2 VER70219
580 X(I)=FE(I)+FP(I) VER70220
CALL SYMSOL(2) VER70221
C VER70222
C CALCULATE TOTAL STRAINS,STRESSES AND PLASTIC VER70223
C FORCES AND STRAINS FOR EACH ELEMENT VER70224
C VER70225
DO 590 I=1,N2 VER70226
590 FP(I)=0 VER70227
XERR=0.0 VER70228
KEL=0 VER70229
CALL STRAIN VER70230
C VER70231
C **** PICK LARGEST ERROR AND DETERMINE WHEN TO REITERATE **** VER70232
C VER70233
IT=IT+1 VER70234
IF(XERR-TOL)440,440,600 VER70235
600 IF(IT-NIT)540,610,610 VER70236
610 K0=NDIV VER70237
IUNLD=0 VER70238
GO TO 440 VER70239
620 IF(IUNLD.EQ.0) GO TO 10 VER70240

```

```

IUNLD=0
IUNF=-1
KSTOP=0
GO TO 440
700 WRITE (6,710)
710 FORMAT (/10X,13H JOB FINISHED)
STOP
END
SUBROUTINE FLEM(M)
COMMON/ADD/ FE(10),FE1(10),FE2(10),PRR(10)
COMMON F,CC,G1,E2,PR,EPR,X21,Y21,X31,Y31,X32,Y32,XERR,
1 N2,NELEM,KEL,ILAW,MAT,NBC,
2 R(900,60),RC(30,3),TAB(101,20),IFIX(2),
3 X(900),XCORD(450),Y(450),ICODE(450),
4 EP(900),F(900),
5 I1(800),I2(800),I3(800),NTYPE(800),Z(800),I4(800),
6 SEF(800),SET(800),EEP(800),EXPL(800),EYP(800),EXYP(800),
7 NNODE,MRAND
DIMENSION XX(450)
EQUIVALENCE (XCORD,XX)
J1=I1(M)
J2=I2(M)
J3=I3(M)
X21=XX(J2)-XX(J1)
Y21=Y(J2)-Y(J1)
IF(J3.EQ.0) GO TO 10
Y32=Y(J3)-Y(J2)
Y31=Y(J3)-Y(J1)
X32=XX(J3)-XX(J2)
X31=XX(J3)-XX(J1)
RETURN
10 Y32=SQRT(X21**2+Y21**2)
RETURN
END
C0C00
SUBROUTINE DCODE(ICODE,I,IRCS,IRCX,IRCY,IC,IX,IY,NBC)
DIMENSION ICODE(450)
IRCS=MOD(ICODE(I),10)
IRCX=MOD(ICODE(I),1000)/100
IRCY=MOD(ICODE(I),100)/10
IC=MOD(ICODE(I),100000)/1000
IX=2*I-1
IY=IX+1
IF(IC.EQ.0) IC=NBC
RETURN
END
C2222 PLASTIC STRAIN DETERMINATION
SUBROUTINE PNEW1 (EEPK,EFT,E,E1,E2)
J=1
XU=EFT
XL=0
10 EEPK=.5*(XL+XU)
20 Y=EEPK+E1/E*EEPK**(1.0/E2)-EFT
30 YP=1.0+E1/E/E2*EEPK**(1.0/E2-1.0)
J=J+1
IF(J-50)40,40,100
40 IF(Y)50,100,60
50 XL=EEPK
GO TO 70
60 XU=EEPK

```

VER70241
VER70242
VER70243
VER70244

VER70245
ELM 0001
ELM 0002
ELM 0003
ELM 0004

ELM 0010
ELM 0011
ELM 0012
ELM 0013
ELM 0014
ELM 0015
ELM 0016
ELM 0017
ELM 0018
ELM 0019
ELM 0020
ELM 0021
ELM 0022
ELM 0023
ELM 0024
ELM 0025
ELM 0026

DC000001
DC000002
DC000003
DC000004
DC000005
DC000006
DC000007
DC000008
DC000009
DC000010
DC000011
DC000012
PNEW0001
PNEW0002
PNEW0003
PNEW0004
PNEW0005
PNEW0006
PNEW0007
PNEW0008
PNEW0009
PNEW0010
PNEW0011
PNEW0012
PNEW0013
PNEW0014

```

70 XT=FEPK-Y/YP
   IF(XU-XT)10,10,80
80 IF(XT-XL)10,10,90
90 FEPK=XT
   DIFF=ABS(Y/YP/FEPK)
   IF(DIFF-.00001)100,100,20
100 RETURN
    END
CTABL   STRAIN-PLASTIC STRAIN TABLE
SUBROUTINE TABLE(K)
COMMON/ADD/ EE(10),EE1(10),EE2(10),PRR(10)
COMMON  E,CC,G1,F2,PR,EPR,X21,Y21,X31,Y31,X32,Y32,XERR,
1      N2,NELEM,KEL,ILAW,MAT,NRC,
2      R(900,60),RC(30,3),TAB(101,20),IFIX(2),
3      X(900),XCORD(450),Y(450),ICODE(450),
4      FP(900),F(900),
5      I1(800),I2(800),I3(800),NTYPE(800),Z(800),I4(800),
6      SEF(800),SET(800),EEP(800),EXPL(800),EYP(800),EXYP(800),
7      NNODE,MRAND
   I12=2*K
   I11=I12-1
   TAB(1,I11)=0.
   TAB(1,I12)=0.
   DO 20 I=1,101
   IF(I-1)20,20,10
10  TAB(1,I11)=FLOAT(I-1)*CC/5.
   EET=TAB(1,I11)
   CALL PNEW1(FEPK,EET,E,G1,F2)
   TAB(1,I12)=FEPK
20  CONTINUE
   RETURN
    END
SUBROUTINE STIFF
COMMON/ADD/ EE(10),EE1(10),EE2(10),PRR(10)
COMMON  E,CC,G1,E2,PR,EPR,X21,Y21,X31,Y31,X32,Y32,XERR,
1      N2,NELEM,KEL,ILAW,MAT,NRC,
2      R(900,60),RC(30,3),TAB(101,20),IFIX(2),
3      X(900),XCORD(450),Y(450),ICODE(450),
4      FP(900),F(900),
5      I1(800),I2(800),I3(800),NTYPE(800),Z(800),I4(800),
6      SEF(800),SET(800),EEP(800),EXPL(800),EYP(800),EXYP(800),
7      NNODE,MRAND
   DIMENSION FFP(2),INODE(3),LNODE(6),DSK(6,6)
   EQUIVALENCE (IFIX(1),IRCX),(IFIX(2),IRCY)
   EQUIVALENCE (INODE(1),J1),(INODE(2),J2),(INODE(3),J3)
   DO 80 M=1,NELEM
   J1=I1(M)
   J2=I2(M)
   J3=I3(M)
   CALL ELEM(M)
   NTY=NTYPE(M)
   E=FF(NTY)
   PR=PRR(NTY)
   IF(J3.EQ.0) GO TO 30
   IF(NTY.LE.MAT) GO TO 10
   GO TO 160
30
C
C  **** STIFFNESS MATRIX CALCULATIONS FOR TRIANGULAR ELEMENTS ****
C
10  IMAT=6

```

```

PNEW0015
PNEW0016
PNEW0017
PNEW0018
PNEW0019
PNEW0020
PNEW0021
PNEW0022
PLST0001
PLST0002
PLST0003
PLST0004
PLST0005
PLST0011
PLST0012
PLST0013
PLST0014
PLST0015
PLST0016
PLST0017
PLST0018
PLST0019
PLST0020
PLST0021
PLST0022
PLST0023
PLST0024
STIF0001
STIF0002
STIF0003
STIF0004
STIF0010
STIF0011
STIF0012
STIF0013
STIF0014
STIF0015
STIF0016
STIF0017
STIF0018
STIF0019
STIF0020
STIF0021
STIF0022
STIF0023
STIF0024
STIF0025
STIF0026
STIF0027
STIF0028

```



```

AF=E*7(M)
A123=X21*Y31-X31*Y21
A123=ABS(A123)
FT1=AF/(2.0*A123*(1.0-PR**2))
ET2=AF/(4.0*A123*(1.0+PR))
DSK(1,1)= FT1*Y32**2      +ET2*X32**2
DSK(2,1)=-FT1*PR*Y32*X32  -ET2*Y32*X32
DSK(2,2)= FT1*X32**2      +ET2*Y32**2
DSK(3,1)=-ET1*Y31*Y32     -ET2*X32*X31
DSK(3,2)= FT1*PR*Y31*X32  +ET2*Y32*X31
DSK(3,3)=FT1*Y31**2       +ET2*X31**2
DSK(4,1)= ET1*PR*Y32*X31  +ET2*Y31*X32
DSK(4,2)=-ET1*X31*X32     -ET2*Y31*Y32
DSK(4,3)=-FT1*PR*Y31*X31  -ET2*Y31*X31
DSK(4,4)= ET1*X31**2      +ET2*Y31**2
DSK(5,1)= ET1*Y21*Y32     +ET2*X32*X21
DSK(5,2)=-ET1*PR*Y21*X32  -ET2*Y32*X21
DSK(5,3)=-ET1*Y31*Y21     -ET2*X31*X21
DSK(5,4)= ET1*PR*Y21*X31  +ET2*Y31*X21
DSK(5,5)= ET1*Y21**2      +ET2*X21**2
DSK(6,1)=-ET1*PR*Y32*X21  -ET2*Y21*X32
DSK(6,2)= ET1*X32*X21     +ET2*Y21*Y32
DSK(6,3)= ET1*PR*Y31*X21  +ET2*Y21*X31
DSK(6,4)=-ET1*X31*X21     -ET2*Y21*Y31
DSK(6,5)=-ET1*PR*Y21*X21  -ET2*Y21*X21
DSK(6,6)= ET1*X21**2      +ET2*Y21**2
DO 20 I=1,JMAT
DO 20 J=1,JMAT
20 DSK(I,J)=DSK(J,I)
GO TO 50

C
C ***** STIFFNESS MATRIX CALCULATIONS FOR BARS *****
C
30 ET1=Z(M)*E/Y32**3
FFP(1)=X21
FFP(2)=Y21
DO 40 I=1,2
DO 40 J=1,2
DSK(I,J)=ET1*FFP(I)*FFP(J)
DSK(I+2,J)=-DSK(I,J)
DSK(I,J+2)=-DSK(I,J)
40 DSK(I+2,J+2)=DSK(I,J)
JMAT=4

C
C ***** INCORPORATION OF ELEMENT MATRICES INTO
C COMPLETE STIFFNESS MATRIX *****
C
50 JMAT2=JMAT/2
K=0
DO 60 I=1,JMAT2
DO 60 J=1,2
K=K+1
60 LNODE(K)=2*INODE(I)-2+J
DO 80 I=1,JMAT
KI=LNODE(I)
DO 80 J=1,JMAT
KJ=LNODE(J)
IF(KJ-KI)80,70,70
70 K=KJ-KI+1
R(KI,K)=R(KI,K)+DSK(I,J)

```

STIF0029
 STIF0030
 STIF0031
 STIF0032
 STIF0033
 STIF0034
 STIF0035
 STIF0036
 STIF0037
 STIF0038
 STIF0039
 STIF0040
 STIF0041
 STIF0042
 STIF0043
 STIF0044
 STIF0045
 STIF0046
 STIF0047
 STIF0048
 STIF0049
 STIF0050
 STIF0051
 STIF0052
 STIF0053
 STIF0054
 STIF0055
 STIF0056
 STIF0057
 STIF0058
 STIF0059
 STIF0060
 STIF0061
 STIF0062
 STIF0063
 STIF0064
 STIF0065
 STIF0066
 STIF0067
 STIF0068
 STIF0069
 STIF0070
 STIF0071
 STIF0072
 STIF0073
 STIF0074
 STIF0075
 STIF0076
 STIF0077
 STIF0078
 STIF0079
 STIF0080
 STIF0081
 STIF0082
 STIF0083
 STIF0084
 STIF0085
 STIF0086
 STIF0087
 STIF0088

```

      RD CONTINUE
C
C ***** DISPLACEMENT BOUNDARY CONDITIONS *****
C
      DO 150 I=1,NNODE
      IF(ICODE(I).EQ.0) GO TO 150
      CALL DCODE(ICODE,I,IRCS,IRCX,IRCY,IC,IX,IY,NRC)
      IF(IRCS.NE.1) GO TO 110
      ALF=RC(IC,3)
      R(IX,1)=R(IX,1)+ALF*(ALF*(R(IY,1)+1.)+2.*R(IX,2))
      R(IX,2)=-ALF
      R(IY,1)=1.
      F(IX)=ALF*F(IY)+F(IX)
      F(IY)=0
      KL=IX-MRAND+2
      KU=IX+MRAND-1
      IF(KL.LT.1) KL=1
      IF(KU.GT.N2) KU=N2
      DO 100 K=KL,KU
      IF(K.EQ.IX.OR.K.EQ.IY) GO TO 100
      IF(K.GT.IY) GO TO 90
      L=IX-K+1
      R(K,L)=R(K,L)+ALF*B(K,L+1)
      R(K,L+1)=0.
      GO TO 100
90    L=K-IX+1
      R(IX,L)=R(IX,L)+ALF*B(IY,L-1)
      R(IY,L-1)=0.
100   CONTINUE
110   DO 140 N=1,2
      IF(1FIX(N).NE.1) GO TO 140
      IR=IX+N-1
      ML=IR-MRAND+1
      MU=IR+MRAND-1
      IF(ML.LT.1) ML=1
      IF(MU.GT.N2) MU=N2
      DO 130 M=ML,MU
      L=IR-M+1
      IF(L.LE.1) GO TO 120
      F(M)=F(M)-R(M,L)*RC(IC,N)
      R(M,L)=0.
      GO TO 130
120   L=M-IR+1
      F(M)=F(M)-R(IR,L)*RC(IC,N)
      R(IR,L)=0.
130   CONTINUE
      R(IR,1)=1.
      F(IR)=RC(IC,N)
140   CONTINUE
150   CONTINUE
      RETURN
160   WRITE(6,170) M
170   FORMAT(1H010X32HINVALID ELEMENT CODE ELEMENT NO.14)
      STOP
      END
C
      SUBROUTINE SYMSOL(KKK)
      COMMON/ADD/ EE(10),EE1(10),EE2(10),PRR(10)
      COMMON F,CC,G1,F2,PR,FPR,X21,Y21,X31,Y31,X32,Y32,XERR,
1      N2,NFLEM,KEL,ILAW,MAT,NRC,

```

```

STIF0089
STIF0090
STIF0091
STIF0092
STIF0093
STIF0094
STIF0095
STIF0096
STIF0097
STIF0098
STIF0099
STIF0100
STIF0101
STIF0102
STIF0103
STIF0104
STIF0105
STIF0106
STIF0107
STIF0108
STIF0109
STIF0110
STIF0111
STIF0112
STIF0113
STIF0114
STIF0115
STIF0116
STIF0117
STIF0118
STIF0119
STIF0120
STIF0121
STIF0122
STIF0123
STIF0124
STIF0125
STIF0126
STIF0127
STIF0128
STIF0129
STIF0130
STIF0131
STIF0132
STIF0133
STIF0134
STIF0135
STIF0136
STIF0137
STIF0138
STIF0139
STIF0140
STIF0141
STIF0142
STIF0143
STIF0144
SYMS0001
SYMS0002
SYMS0003
SYMS0004

```

```

2      R(900,60),RC(30,3),TAB(101,20),IFIX(2),
3      X(900),XCORD(450),Y(450),ICODE(450),
4      FP(900),F(900),
5      I1(800),I2(800),I3(800),NTYPE(800),Z(800),I4(800),
6      SEF(800),SET(800),EEP(800),EXPL(800),EYP(800),EXYP(800),
7      NMODE,MRAND
C
      NM=N2
      MM=MRAND
      GO TO (10,60),KKK
C
      REDUCE MATRIX
C
10  DO 50 N=1,MM
      DO 40 L=2,MM
      C=R(N,L)/R(N,1)
      I=N+L-1
      IF(NN-1) 40,20,20
20  J=0
      DO 30 K=L,MM
      J=J+1
30  R(I,J)=R(I,J)-C*R(N,K)
40  R(N,L)=C
50  CONTINUE
      GO TO 130
C
      REDUCE VECTOR
C
60  DO 80 N=1,MM
      DO 70 L=2,MM
      I=N+L-1
      IF(NN-1) 80,70,70
70  X(I)=X(I)-R(N,L)*X(N)
80  X(N)=X(N)/R(N,1)
C
      BACK SUBSTITUTION
C
      N=NN
90  N=N-1
      IF(N) 100,130,100
100 DO 120 K=2,MM
      L=N+K-1
      IF(NN-L) 120,110,110
110 X(N)=X(N)-R(N,K)*X(L)
120 CONTINUE
      GO TO 90
C
130 RETURN
C
      END
      SUBROUTINE STRAIN
      COMMON/ADD/ EE(10),FE1(10),FE2(10),PRR(10)
      COMMON F,CC,G1,F2,PR,EPR,X21,Y21,X31,Y31,X32,Y32,XERR,
1      N2,NFLEM,KEL,ILAW,MAT,NRC,
2      R(900,60),RC(30,3),TAB(101,20),IFIX(2),
3      X(900),XCORD(450),Y(450),ICODE(450),
4      FP(900),F(900),
5      I1(800),I2(800),I3(800),NTYPE(800),Z(800),I4(800),
6      SEF(800),SET(800),EEP(800),EXPL(800),EYP(800),EXYP(800),
7      NMODE,MRAND
      STRN0001
      STRN0002
      STRN0003
      STRN0004
      STRN0010

```

```

DO 130 K=1,NFLFM
J1=2*I1(K)-1
J2=2*I1(K)
J3=2*I2(K)-1
J4=2*I2(K)
J5=2*I3(K)-1
J6=2*I3(K)
CALL FLEM(K)
NTY=NTYPE(K)
E=EF(NTY)
E1=EF1(NTY)
F2=FE2(NTY)
CC=F1/E
PR=PRR(NTY)
IF(ILAW.EQ.1) G1=(7.*E/3.)*(1./E2)*E1*(1.-1./E2)
IF(ILAW.GT.1) G1=E1
EPR=E/(1.0-PR*PR)
IF(I3(K).EQ.0) GO TO 60
C
C **** TRIANGULAR ELEMENT CALCULATIONS ****
C
10 A123=X21*Y31-X31*Y21
SN=A123/ABS(A123)
EXT=(-Y32*X(J1)+Y31*X(J3)-Y21*X(J5))/A123
EYT=(-X32*X(J2)-X31*X(J4)+X21*X(J6))/A123
EXYT=(X32*X(J1)-Y32*X(J2)-X31*X(J3)+Y31*X(J4)
+X21*X(J5)-Y21*X(J6))/A123
EXE=EXT-EXPL(K)
EYE=EYT-EYP(K)
EXYE=EXYT-EXYP(K)
SX=EPR*(FXE+PR*EYE)
SY=FPR*(FYE+PR*FXE)
SXY=E/(1.0+PR)*EXYE/2.0
SE=SQRT(SX**2-SX*SY+SY**2+3.0*SXY**2)
CRIT=ABS(SE)-SEF(K)
IF(CRIT)40,40,20
20 EET=SE/E+EEP(K)
CALL STRSTN(EET,EEP,K,SETK,NTY)
DEEP=EEP(K)-EEP(K)
30 EEP(K)=EEP(K)
SETK=SETK
EXPL(K)=DEEP/SE*(SX-SY/2.0)+EXPL(K)
EYP(K)=DEEP/SE*(SY-SX/2.0)+EYP(K)
EXYP(K)=3.0*DEEP/SE*SXY+EXYP(K)
ERR=E*DEEP/SE
ERR=ABS(ERR)
GO TO 50
40 FRR=0.0
50 CONTINUE
Q1=F*Z(K)/(1.0-PR**2)/2.0*SN
Q2=F*Z(K)/(1.0+PR)/4.0*SN
FXPT=EXPL(K)
FYPT=EYP(K)
EXYPT=EXYP(K)
FP(J1)=-Q1*Y32*EXPT-Q1*Y32*PR*FYPT+Q2*X32*EXYPT+FP(J1)
FP(J2)= Q1*X32*PR*EXPT+Q1*X32*FYPT-Q2*Y32*EXYPT+FP(J2)
FP(J3)= Q1*Y31*EXPT+Q1*Y31*PR*FYPT-Q2*X31*EXYPT+FP(J3)
FP(J4)=-Q1*X31*PR*EXPT-Q1*X31*FYPT+Q2*Y31*EXYPT+FP(J4)
FP(J5)=-Q1*Y21*EXPT-Q1*Y21*PR*FYPT+Q2*X21*EXYPT+FP(J5)
FP(J6)= Q1*X21*PR*EXPT+Q1*X21*FYPT-Q2*Y21*EXYPT+FP(J6)
STRN0011
STRN0012
STRN0013
STRN0014
STRN0015
STRN0016
STRN0017
STRN0018
STRN0019
STRN0020
STRN0021
STRN0022
STRN0023
STRN0024
STRN0025
STRN0026
STRN0027
STRN0028
STRN0029
STRN0030
STRN0031
STRN0032
STRN0033
STRN0034
STRN0035
STRN0036
STRN0037
STRN0038
STRN0039
STRN0040
STRN0041
STRN0042
STRN0043
STRN0044
STRN0045
STRN0046
STRN0047
STRN0048
STRN0049
STRN0050
STRN0051
STRN0052
STRN0053
STRN0054
STRN0055
STRN0056
STRN0057
STRN0058
STRN0059
STRN0060
STRN0061
STRN0062
STRN0063
STRN0064
STRN0065
STRN0066
STRN0067
STRN0068
STRN0069
STRN0070

```

```

      GO TO 110
C
C **** BAR CALCULATIONS ****
C
60 EET=(X21*(X(J3)-X(J1))+Y21*(X(J4)-X(J2)))/Y32**2
   STRN=ABS(EET-FXPL(K))
   SIGN=(EET-FXPL(K))/STRN
   SE=F*STRN
   CRIT=SE-SFF(K)
   EET=STRN+EEP(K)
   IF(CRIT)90,90,70
70 CONTINUE
   CALL STRSTN(EET,EEP,K,SETK,NTY)
   DEEP=EEP-K
80 EEP(K)=EEP
   SET(K)=SETK
   EXPL(K)=FXPL(K)+SIGN*DEEP
   FRR=E*DEEP/SE
   ERR=ABS(FRR)
   GO TO 100
90 ERR=0.0
100 CONTINUE
   EXPT=EXPL(K)
   Q1=E*Z(K)/Y32
   FP(J1)=FP(J1)-Q1*X21*EXPT
   FP(J2)=FP(J2)-Q1*Y21*EXPT
   FP(J3)=FP(J3)+Q1*X21*EXPT
   FP(J4)=FP(J4)+Q1*Y21*EXPT
110 IF(ERR-XERR)130,130,120
120 XERR=FRR
   KEL=K
130 CONTINUE
   RETURN
   END
   SUBROUTINE STRSTN(EET,EEP,K,SETK,NTY)
   COMMON/ADD/ FE(10),EE1(10),EE2(10),PRR(10)
   COMMON E,CC,G1,E2,PR,EPR,X21,Y21,X31,Y31,X32,Y32,XERR,
1       N2,NFLFM,KEL,ILAW,MAT,NHC,
2       R(900,60),RC(30,3),TAB(101,20),IFIX(2),
3       X(900),XCORD(450),Y(450),ICODF(450),
4       FP(900),F(900),
5       I1(800),I2(800),I3(800),NTYPE(800),Z(800),I4(800),
6       SEF(800),SET(800),EEP(800),EXPL(800),EYP(800),EXYP(800),
7       NMNDE,MRAND
   GO TO(10,50,60),ILAW
10 J=5.0*EET/CC+1.0
   NT2=2*NTY
   NT1=NT2-1
   IF(J-101)20,30,30
20 EEPK=TAB(J,NT2)+(TAB(J+1,NT2)-TAB(J,NT2))*(EET-TAB(J,NT1))/
1(TAB(J+1,NT1)-TAB(J,NT1))
   GO TO 40
30 CALL PNEW1(EEP,K,E,G1,F2)
40 SETK=G1*EEP**(.5/F2)
   RETURN
50 SETK=E*EET/(1.+(ABS(E*EET/G1))**F2)**(.5/E2)
   EEPK=EET-SETK/F
   RETURN
60 FC=G1/F
   IF(EET-FC)70,70,80

```

```

STRN0071
STRN0072
STRN0073
STRN0074
STRN0075
STRN0076
STRN0077
STRN0078
STRN0079
STRN0080
STRN0081
STRN0082
STRN0083
STRN0084
STRN0085
STRN0086
STRN0087
STRN0088
STRN0089
STRN0090
STRN0091
STRN0092
STRN0093
STRN0094
STRN0095
STRN0096
STRN0097
STRN0098
STRN0099
STRN0100
STRN0101
STRN0102
STRN0103
STRN0104
STRS0001
STRS0002
STRS0003
STRS0004
STRS0010
STRS0011
STRS0012
STRS0013
STRS0014
STRS0015
STRS0016
STRS0017
STRS0018
STRS0019
STRS0020
STRS0021
STRS0022
STRS0023
STRS0024
STRS0025
STRS0026

```

```

70 FFPK=0.
   SETK=F*FFT
   RETURN
80 FFPK=FET-FC
   SETK=G1+E2*EFPK
   RETURN
END
C12345      OUTPUT SUBROUTINE
SUBROUTINE OUTPT
COMMON/ADD/  EF(10),FE1(10),FE2(10),PRR(10)
COMMON      F,CC,G1,E2,PR,FPR,X21,Y21,X31,Y31,X32,Y32,XERR,
1          NN2,NELEM,KFL,I1,AW,MAT,NRG,
2          R(900,60),RC(30,3),TAB(101,20),IFIX(2),
3          XCORD(450),Y(450),ICNDE(450),
4          FP(900),F(900),
5          I1(800),I2(800),I3(800),NTYPE(800),Z(800),I4(800),
6          SEF(800),SET(800),EFP(800),EXPL(800),EYP(800),EXYP(800),
7          NNODE,MBAND
   L=0
   DO 70 K=1,NELEM
C      **** TRIANGULAR ELEMENT CALCULATIONS ****
C      NTY=NTYPE(K)
C      E=EE(NTY)
C      PR= PRR(NTY)
C      EPR=E/(1.-PR*PR)
C      IF(I3(K).EQ.0) GO TO 70
10  CALL ELEM(K)
   A123=X21*Y31-X31*Y21
   J1=2*I1(K)-1
   J2=2*I1(K)
   J3=2*I2(K)-1
   J4=2*I2(K)
   J5=2*I3(K)-1
   J6=2*I3(K)
   EXT=(-Y32*X(J1)+Y31*X(J3)-Y21*X(J5))/A123
   EYT=( X32*X(J2)-X31*X(J4)+X21*X(J6))/A123
   EXYT=(X32*X(J1)-Y32*X(J2)-X31*X(J3)+Y31*X(J4)
1     +X21*X(J5)-Y21*X(J6))/A123
   EXE=EXT-EXPL(K)
   FYF=EYT-FYP(K)
   EXYE=EXYT-FXYP(K)
   SX=EPR*(EXF+PR*EYF)
   SY=EPR*(EYE+PR*EXE)
   SXY=E/(1.0+PR)*EXYE/2.0
   PF2=SQRT((.5*(SX-SY))*2+SXY**2)
   PH1=.5*ATAN2((-2.0*SXY),(SX-SY))*57.29578
   PH2=.5*ATAN2((-EXYT),(EXT-EYT))*57.29578
   PS1=.5*(SX+SY)
   SIGE1=PS1+PF2
   SIGE2=PS1-PF2
   PST1=.5*(EXT+EYT)
   PET2=SQRT((.5*(EXT-EYT))*2+EXYT**2/4.0)
   STRE1=PST1+PET2
   STRE2=PST1-PET2
   PET2=2.0*PET2
   N1=I1(K)
   N2=I2(K)
   N3=I3(K)

```

```

STRS0027
STRS0028
STRS0029
STRS0030
STRS0031
STRS0032
STRS0033
OTPU0001
OTPU0002
OTPU0003
OTPU0004
OTPU0005
OTPU0011
OTPU0012
OTPU0013
OTPU0014
OTPU0015
OTPU0016
OTPU0017
OTPU0018
OTPU0019
OTPU0020
OTPU0021
OTPU0022
OTPU0023
OTPU0024
OTPU0025
OTPU0026
OTPU0027
OTPU0028
OTPU0029
OTPU0030
OTPU0031
OTPU0032
OTPU0033
OTPU0034
OTPU0035
OTPU0036
OTPU0037
OTPU0038
OTPU0039
OTPU0040
OTPU0041
OTPU0042
OTPU0043
OTPU0044
OTPU0045
OTPU0046
OTPU0047
OTPU0048
OTPU0049
OTPU0050
OTPU0051
OTPU0052
OTPU0053

```

```

XC=XCORR(N1)+(X21+X31)/3.0      0TPU0054
YC=Y(N1)+(Y21+Y31)/3.0      0TPU0055
EPE=2.*SORT((EXPL(K)**2+EXPL(K)*EYP(K)+EYP(K)**2+EXYP(K)**2/4.)/3. 0TPU0056
1)      0TPU0057
SF=SORT(SX**2-SX*SY+SY**2+3.*SXY**2)      0TPU0058
L=L+1      0TPU0059
IF(MOD(L-1,14))30,20,30      0TPU0060
20 WRITE (6,40)      0TPU0061
30 WRITE(6,50)K,XC,YC,SX,SY,SXY,SIGF1,SIGE2,PE2,PHI,PH2,EXT,EYT, EX 0TPU0062
1YT,STRF1,STRF2,PFT2      0TPU0063
40 FORMAT(9H)EL. NO./5X11HCOORDINATES2RX33HS T R E S S E S / S T R A 0TPU0064
11 N S /8H PHI7X1HX8X1HY6X9H TAU-XX6X9H TAU-YY6X9H TAU-X 0TPU0065
2Y8X7HMAXIMUMRX7HMINIMUM6X9HMAX SHEAR )      0TPU0066
50 FORMAT(1H017,0PF8.3,F9.3,1P6E15.4/1H 0PF7.2,F8.2,9X1P6E15.4) 0TPU0067
WRITE(6,60) SE,EPE      0TPU0068
60 FORMAT(1H 23H***** EFFECTIVE STRESS=E12.5,23H***** EFFECTIVE STRAI 0TPU0069
1M=E12.5)      0TPU0070
70 CONTINUE      0TPU0071
C      0TPU0072
C ***** BAR CALCULATIONS *****      0TPU0073
C      0TPU0074
J=0      0TPU0075
DO 120 K=1,NELEM      0TPU0076
NTY=NTYPE(K)      0TPU0077
E=EE( NTY)      0TPU0078
PR=PRR( NTY)      0TPU0079
J1=2*I1(K)-1      0TPU0080
J2=2*I1(K)      0TPU0081
J3=2*I2(K)-1      0TPU0082
J4=2*I2(K)      0TPU0083
IF(I3(K).NE.0) GO TO 120      0TPU0084
80 CALL ELEM(K)      0TPU0085
EET=(X21*(X(J3)-X(J1))+Y21*(X(J4)-X(J2)))/Y32**2      0TPU0086
SE=E*(EET-EXPL(K))      0TPU0087
SEMZK=SF*Z(K)      0TPU0088
K1=J1(K)      0TPU0089
K2=J2(K)      0TPU0090
IF(J)100,90,100      0TPU0091
90 WRITE (6,130)      0TPU0092
J=1      0TPU0093
100 CONTINUE      0TPU0094
110 WRITE(6,140)K,K1,K2,SE,EET,SEMZK      0TPU0095
120 CONTINUE      0TPU0096
130 FORMAT(9H)BAR NO. 6X10HNODE NOS. 8X7HSTRESS 8X7HSTRAIN ,4X, 0TPU0097
113HMEMBER FORCES)      0TPU0098
140 FORMAT(1H0 318,2E15.5,2X,E15.5)      0TPU0099
RETURN      0TPU0100
END      0TPU0101

```

EXAMPLE PROBLEM NO. 1 W16X40 'CANTILEVER BEAM' ULTIMATE LOAD.

BILINEAR LAW

MATERIAL----- 1
 MODULUS OF ELASTICITY----- 0.2900E 05
 SECANT YIELD STRESS----- 0.2600E 02
 SHAPE PARAMETER----- 0.0
 POISSON'S RATIO----- 0.3000
 ERROR TOLERANCE----- 0.0300

NO. OF NCDES ANODE = 21
 NO. OF ELEMENTS AELEM = 34
 NO. OF STEPS NDIV = 20
 NO. OF ITERATIONS/STEP NIT = 100

BOUNDARY CONDITION ARRAY

NCODE PT	CODE	X VALUE	CCODE	Y VALUE	CODE	SLIDING VALUE
1	1	0.0	1	0.0	0	0.0
2	1	0.0	1	0.0	0	0.0
3	1	0.0	1	0.0	0	0.0
4	1	0.0	1	0.0	0	0.0
5	1	0.0	1	0.0	0	0.0

NCODE PT	Y-COORD	Y-FORCE	Y-COORD	Y-FORCE	CODE
1	0.0	0.0	0.0	0.0	110
2	0.0	0.0	4.0000	0.0	110
3	0.0	0.0	8.0000	0.0	110
4	0.0	0.0	12.0000	0.0	110
5	0.0	0.0	16.0000	0.0	110
6	5.0000	0.0	0.0	0.0	0
7	5.0000	0.0	4.0000	0.0	0
8	5.0000	0.0	8.0000	0.0	0
9	5.0000	0.0	12.0000	0.0	0
10	5.0000	0.0	16.0000	0.0	0
11	10.0000	0.0	0.0	0.0	0
12	10.0000	0.0	4.0000	0.0	0
13	10.0000	0.0	8.0000	0.0	0
14	10.0000	0.0	12.0000	0.0	0
15	10.0000	0.0	16.0000	0.0	0
16	20.0000	0.0	0.0	0.0	0
17	20.0000	0.0	4.0000	0.0	0
18	20.0000	0.0	8.0000	0.0	0
19	20.0000	0.0	0.0	0.0	0
20	36.0000	0.0	8.0000	0.0	0
21	36.0000	0.0	16.0000	-80.0000	0

ELEMENT	NCODE 1	NCODE 2	NODE 3	ELEMENT TYPE	AREA OR THICK.	MATERIAL TYPE
1	1	6	0	BAR	0.32200E 01	1
2	1	6	2	PLATE	0.30700E 00	1
3	6	7	2	PLATE	0.30700E 00	1
4	2	7	3	PLATE	0.30700E 00	1

5	7	8	3	PLATE	0.30700E 00	1
6	3	8	9	PLATE	0.30700E 00	1
7	3	9	4	PLATE	0.30700E 00	1
8	4	9	10	PLATE	0.30700E 00	1
9	4	10	5	PLATE	0.30700E 00	1
10	5	10	0	BAR	0.32200E 01	1
11	6	11	0	BAR	0.32200E 01	1
12	6	11	7	PLATE	0.30700E 00	1
13	11	12	7	PLATE	0.30700E 00	1
14	7	12	13	PLATE	0.30700E 00	1
15	7	13	8	PLATE	0.30700E 00	1
16	8	13	9	PLATE	0.30700E 00	1
17	13	14	9	PLATE	0.30700E 00	1
18	9	14	15	PLATE	0.30700E 00	1
19	9	15	10	PLATE	0.30700E 00	1
20	10	15	0	BAR	0.32200E 01	1
21	11	16	0	BAR	0.32200E 01	1
22	11	16	12	PLATE	0.30700E 00	1
23	16	17	12	PLATE	0.30700E 00	1
24	12	17	13	PLATE	0.30700E 00	1
25	13	17	14	PLATE	0.30700E 00	1
26	17	18	14	PLATE	0.30700E 00	1
27	14	18	15	PLATE	0.30700E 00	1
28	15	18	0	BAR	0.32200E 01	1
29	16	19	0	BAR	0.32200E 01	1
30	16	19	17	PLATE	0.30700E 00	1
31	19	20	17	PLATE	0.30700E 00	1
32	17	20	21	PLATE	0.30700E 00	1
33	17	21	18	PLATE	0.30700E 00	1
34	18	21	0	BAR	0.32200E 01	1

FORCES AND DISPLACEMENTS FOR INCREMENT 19

NODE	X-FCRCE	Y-FCRCE	X-DISPL.	Y-DISPL.
1	0.0	0.0	0.0	0.0
2	0.0	0.0	0.0	0.0
3	0.0	0.0	0.0	0.0
4	0.0	0.0	0.0	0.0
5	0.0	0.0	0.0	0.0
6	0.0	0.0	-0.2947E-01	-0.3895E-01
7	0.0	0.0	-0.1416E-01	-0.3616E-01
8	0.0	0.0	-0.1959E-03	-0.3600E-01
9	0.0	0.0	0.1414E-01	-0.3585E-01
10	0.0	0.0	0.2958E-01	-0.3859E-01
11	0.0	0.0	-0.3525E-01	-0.6606E-01
12	0.0	0.0	-0.1741E-01	-0.6491E-01
13	0.0	0.0	-0.3339E-03	-0.6453E-01
14	0.0	0.0	0.1730E-01	-0.6469E-01
15	0.0	0.0	0.3584E-01	-0.6584E-01
16	0.0	0.0	-0.4316E-01	-0.1304E 00
17	0.0	0.0	-0.8716E-03	-0.1295E 00
18	0.0	0.0	0.4398E-01	-0.1307E 00
19	0.0	0.0	-0.4688E-01	-0.2400E 00
20	0.0	0.0	0.1002E-02	-0.2425E 00
21	0.0	-76.000	0.4809E-01	-0.2481E 00

MAX. ERROR = 0.03939

IN ELEMENT NO. 9

NO. OF ITERATIONS 100

EL. NO./ PHI	COORDINATES X Y	TAU-XX	TAU-YY	TAU-XY	STRESS S / S T R A I N S TAU-XX	TAU-YY	TAU-XY	MAXIMUM	MINIMUM	MAX SHEAR
2	1.667 1.333	-3.5012E-01	-1.7718E-01	-1.1326E-01	-1.7718E-01	-1.7718E-01	-1.1326E-01	-1.2116E-01	-4.0614E-01	1.4249E-01
63.68	63.56	-5.8934E-03	0.0	-7.7697E-03	0.0	0.0	-7.7697E-03	1.9372E-03	-7.8306E-03	9.7679E-03
*****	EFFECTIVE STRESS= 0.36114E 02*****			EFFECTIVE STRAIN= 0.67364E-02						
3	3.333 2.667	-3.2931E-01	-5.6319E-00	-1.2034E-01	-5.6319E-00	-5.6319E-00	-1.2034E-01	-4.5179E-00	-3.8045E-01	1.6763E-01
67.01	68.01	-2.8322E-03	6.5709E-04	-3.4052E-03	6.5709E-04	6.5709E-04	-3.4052E-03	1.3846E-03	-3.5197E-03	4.9044E-03
*****	EFFECTIVE STRESS= 0.35959E 02*****			EFFECTIVE STRAIN= 0.22554E-02						
4	1.667 5.333	-2.5433E-01	-1.2534E-01	-1.6417E-01	-1.2534E-01	-1.2534E-01	-1.6417E-01	-1.3452E-00	-3.4621E-01	1.7638E-01
55.72	55.65	-2.8322E-03	0.0	-7.2320E-03	0.0	0.0	-7.2320E-03	2.4673E-03	-5.2555E-03	7.7668E-03
*****	EFFECTIVE STRESS= 0.35568E 02*****			EFFECTIVE STRAIN= 0.40526E-02						
5	3.333 6.667	-3.6548E-01	4.2195E-01	-2.0745E-01	4.2195E-01	4.2195E-01	-2.0745E-01	2.0775E-01	-2.0723E-01	2.0749E-01
45.55	45.62	-3.5181E-05	4.0752E-05	-3.7081E-03	4.0752E-05	4.0752E-05	-3.7081E-03	1.8533E-03	-1.8537E-03	3.7692E-03
*****	EFFECTIVE STRESS= 0.35938E 02*****			EFFECTIVE STRAIN= 0.10974E-02						
6	3.333 9.333	-4.1507E-01	3.5718E-01	-2.0746E-01	3.5718E-01	3.5718E-01	-2.0746E-01	2.0721E-01	-2.0779E-01	2.0750E-01
45.53	45.60	-2.9181E-05	3.6465E-05	-3.6145E-03	3.6465E-05	3.6465E-05	-3.6145E-03	1.8055E-03	-1.8092E-03	3.6157E-03
*****	EFFECTIVE STRESS= 0.35938E 02*****			EFFECTIVE STRAIN= 0.10135E-02						
7	1.667 10.667	2.5604E-01	1.2608E-01	-1.0351E-01	1.2608E-01	1.2608E-01	-1.0351E-01	3.6731E-01	1.5110E-00	1.7555E-01
36.16	36.24	2.8284E-03	0.0	-7.1702E-03	0.0	0.0	-7.1702E-03	5.2682E-03	-2.4397E-03	7.7079E-03
*****	EFFECTIVE STRESS= 0.35969E 02*****			EFFECTIVE STRAIN= 0.40290E-02						
8	3.333 13.333	3.2352E-01	5.7601E-00	-1.1747E-01	5.7601E-00	5.7601E-00	-1.1747E-01	3.8204E-01	4.9084E-00	1.6648E-01
22.44	21.21	2.8284E-03	-6.8545E-04	-3.2101E-03	-6.8545E-04	-6.8545E-04	-3.2101E-03	3.4512E-03	-1.3082E-03	4.7594E-03
*****	EFFECTIVE STRESS= 0.36002E 02*****			EFFECTIVE STRAIN= 0.21856E-02						
9	1.667 14.667	3.5155E-01	1.7805E-01	-1.1218E-01	1.7805E-01	1.7805E-01	-1.1218E-01	4.0601E-01	1.2299E-01	1.4181E-01
26.14	26.08	5.9565E-03	0.0	-7.7180E-03	0.0	0.0	-7.7180E-03	7.8854E-03	-1.2888E-03	9.7742E-03
*****	EFFECTIVE STRESS= 0.36118E 02*****			EFFECTIVE STRAIN= 0.58088E-02						
12	6.667 1.333	-2.2759E-01	9.8885E-00	-1.2142E-01	9.8885E-00	9.8885E-00	-1.2142E-01	1.3607E-01	-2.4818E-01	2.0363E-01
71.69	65.70	-1.1650E-03	6.5709E-04	-1.5956E-03	6.5709E-04	6.5709E-04	-1.5956E-03	9.9215E-04	-1.4601E-03	2.4522E-03
*****	EFFECTIVE STRESS= 0.35855E 02*****			EFFECTIVE STRAIN= 0.40310E-03						
13	8.333 2.667	-1.9003E-01	2.8961E-00	-1.4294E-01	2.8961E-00	2.8961E-00	-1.4294E-01	1.0153E-01	-2.5260E-01	1.7707E-01
63.08	63.08	-6.5074E-04	2.8610E-04	-1.2816E-03	2.8610E-04	2.8610E-04	-1.2816E-03	6.1142E-04	-9.7606E-04	1.5875E-03
*****	EFFECTIVE STRESS= 0.31585E 02*****			EFFECTIVE STRAIN= 0.0						
14	8.333 5.333	-1.5809E-01	3.1233E-00	-1.6516E-01	3.1233E-00	3.1233E-00	-1.6516E-01	7.0373E-00	-2.9949E-01	1.8503E-01
59.40	58.40	-6.5074E-04	9.7215E-05	-1.4807E-03	9.7215E-05	9.7215E-05	-1.4807E-03	5.5269E-04	-1.1052E-03	1.6589E-03
*****	EFFECTIVE STRESS= 0.34038E 02*****			EFFECTIVE STRAIN= 0.0						
15	6.667 6.667	-3.5473E-01	1.0412E-00	-2.0770E-01	1.0412E-00	1.0412E-00	-2.0770E-01	2.1125E-01	-2.0439E-01	2.0782E-01
45.56	45.88	-2.7600E-05	4.0752E-05	-2.2142E-03	4.0752E-05	4.0752E-05	-2.2142E-03	1.1143E-03	-1.1012E-03	2.2155E-03
*****	EFFECTIVE STRESS= 0.35597E 02*****			EFFECTIVE STRAIN= 0.20345E-03						
16	6.667 9.333	-4.4408E-01	7.4152E-01	-2.0775E-01	7.4152E-01	7.4152E-01	-2.0775E-01	2.0532E-01	-2.0635E-01	2.0783E-01
45.82	45.87	-2.7600E-05	3.6465E-05	-2.1213E-03	3.6465E-05	3.6465E-05	-2.1213E-03	1.0655E-03	-1.0567E-03	2.1222E-03
*****	EFFECTIVE STRESS= 0.35568E 02*****			EFFECTIVE STRAIN= 0.14948E-03						
17	8.333 10.667	1.9766E-01	4.7604E-00	-1.5144E-01	4.7604E-00	4.7604E-00	-1.5144E-01	2.9164E-01	-4.6376E-00	1.6901E-01
31.82	31.82	6.3234E-04	-4.0323E-05	-1.3578E-03	-4.0323E-05	-4.0323E-05	-1.3578E-03	1.0536E-03	-4.6161E-04	1.5152E-03
*****	EFFECTIVE STRESS= 0.31738E 02*****			EFFECTIVE STRAIN= 0.0						

EL. NO./ PHI	COORDINATES X Y		TAU-XX	TAU-YY	STRESSES / STRAINS TAU-XY		MINIMUM	MAX SHEAR
18	8.333	13.333	1.7397E 01	-3.1367E 00	-1.2850E 01	2.3422E 01	-9.1615E CC	1.6292E 01
25.47	25.47	6.2234E-04	6.2234E-04	-2.8813E-04	-1.1341E-03	9.0243E-04	-5.5822E-04	1.4607E-03
***** EFFECTIVE STRESS= 0.29105E 02***** EFFECTIVE STRAIN= 0.0								
19	6.667	14.667	2.3383E 01	-9.5521E 00	-1.1453E 01	2.6574E 01	-1.2143E 01	2.0059E 01
17.41	19.37	1.1707E-03	1.1707E-03	-5.8545E-04	-1.4892E-03	1.4224E-03	-9.4725E-04	2.3797E-03
***** EFFECTIVE STRESS= 0.35424E 02***** EFFECTIVE STRAIN= 0.37715E-03								
22	13.332	1.333	-1.8594E 01	7.2148E-01	-1.7571E 01	1.1114E 01	-2.8986E 01	2.0050E 01
59.40	59.33	-7.8634E-04	-7.8634E-04	2.8610E-04	-1.9626E-03	8.6815E-04	-1.3684E-03	2.2365E-03
***** EFFECTIVE STRESS= 0.35860E 02***** EFFECTIVE STRAIN= 0.26261E-03								
23	16.667	4.070	-1.3563E 01	-7.5540E-01	-1.3555E 01	7.8319E 00	-2.2151E 01	1.4991E 01
57.64	57.64	-4.5989E-04	-4.5989E-04	1.1426E-04	-1.2152E-03	4.9921E-04	-8.4483E-04	1.3440E-03
***** EFFECTIVE STRESS= 0.26939E 02***** EFFECTIVE STRAIN= 0.0								
24	13.333	6.667	-5.3830E-01	2.2508E 00	-2.0731E 01	2.1634E 01	-1.9922E 01	2.0778E 01
46.52	46.54	-5.3771E-05	-5.3771E-05	9.7215E-05	-2.2237E-03	1.1361E-03	-1.0927E-03	2.2289E-03
***** EFFECTIVE STRESS= 0.35599E 02***** EFFECTIVE STRAIN= 0.21129E-03								
25	13.333	9.333	-1.9179E 00	-1.7205E 00	-2.0736E 01	1.8939E 01	-2.2577E 01	2.0758E 01
45.14	45.13	-5.2771E-05	-5.2771E-05	-4.0323E-05	-2.0045E-03	9.9521E-04	-1.0893E-03	2.0845E-03
***** EFFECTIVE STRESS= 0.36000E 02***** EFFECTIVE STRAIN= 0.12918E-03								
26	16.667	12.000	1.2105E 01	-7.6189E-01	-1.0388E 01	1.7890E 01	-6.5472E 00	1.7219E 01
29.11	29.11	4.2528E-04	4.2528E-04	-1.5145E-04	-9.3132E-04	6.8462E-04	-4.1083E-04	1.0955E-03
***** EFFECTIVE STRESS= 0.21910E 02***** EFFECTIVE STRAIN= 0.0								
27	13.333	14.667	1.5625E 01	-5.8045E-01	-1.6823E 01	2.9146E 01	-1.0101E 01	1.8623E 01
29.51	29.50	8.1488E-04	8.1488E-04	-2.8813E-04	-1.9507E-03	1.3406E-03	-8.1384E-04	2.1544E-03
***** EFFECTIVE STRESS= 0.35297E 02***** EFFECTIVE STRAIN= 0.23779E-03								
30	25.333	2.667	-6.3242E 00	1.4166E 00	-1.7454E 01	1.5425E 01	-2.0322E 01	1.7878E 01
51.25	51.25	-2.3273E-04	-2.3273E-04	1.1427E-04	-1.5649E-03	7.4221E-04	-8.6067E-04	1.6029E-03
***** EFFECTIVE STRESS= 0.21063E 02***** EFFECTIVE STRAIN= 0.0								
31	30.667	5.333	7.7779E-01	-8.7276E 00	-1.2011E 01	8.9421E 00	-1.6992E 01	1.2917E 01
34.21	34.21	1.1711E-04	1.1711E-04	-3.0900E-04	-1.0703E-03	4.8309E-04	-6.7468E-04	1.1581E-03
***** EFFECTIVE STRESS= 0.22723E 02***** EFFECTIVE STRAIN= 0.0								
32	30.667	10.667	-2.9917E 00	-2.1292E 01	-1.3118E 01	3.8519E 00	-2.8136E 01	1.5994E 01
27.55	27.55	1.1711E-04	1.1711E-04	-7.0328E-04	-1.1701E-03	4.2989E-04	-1.0101E-03	1.4339E-03
***** EFFECTIVE STRESS= 0.30247E 02***** EFFECTIVE STRAIN= 0.0								
33	25.333	13.333	6.7270E 00	-2.3752E 00	-1.9305E 01	2.2010E 01	-1.7659E 01	1.9835E 01
38.37	38.37	2.5654E-04	2.5654E-04	-1.5145E-04	-1.7308E-03	9.4166E-04	-8.3661E-04	1.7783E-03
***** EFFECTIVE STRESS= 0.34423E 02***** EFFECTIVE STRAIN= 0.0								
BAR NO.	NODE NOS.		STRESS	STRAIN	MEMBER FORCES			
1	1	5	-0.36000E 02	-0.58934E-02	-0.11592E 03			
10	5	10	0.36000E 02	0.59965E-02	0.11592E 03			
11	6	11	-0.23785E 02	-0.11650E-02	-0.10679E 03			
20	10	15	0.33950E 02	0.11707E-02	0.10932E 03			

21	11	16	-0.28604E 02	-0.78634E-03	-0.73428E 02
28	15	18	0.23632E 02	0.81488E-03	0.76094E 02
29	16	19	-0.67492E 01	-0.22273E-03	-0.21732E 02
34	18	21	0.74396E 01	0.25654E-03	0.23955E 02

JOB FINISHED

Example Problem

To illustrate the use of the program a simple example of a cantilever beam is worked out. The beam, a W16 x 40, is 36 inches long with a load at its cantilevered tip.

The properties of the cross-section are listed below: $d = 16.0"$;
 $t_w = 0.307$; $t_f = 0.503"$; $b_f = 7.0"$; $Z = 72.8 \text{ in}^3$; $S = 64.6 \text{ in}^3$.

For a yield stress of 36 ksi, the theoretical ultimate load can be calculated as follows: The plastic moment of the section = $M_p = F_y Z$. Equating it to the externally applied load: $M_p = P_u L$

$$P_u = F_y Z/L = 72.8k$$

Similarly, the load at first yield can be given by:

$$P_y = F_y S/L = 64.6 k$$

Solution by the Finite Element Method

To work out the example by the use of the finite element program, the three dimensional beam is idealized into a two dimensional plane stress problem, see Fig. A1-1a. Having established 21 nodes in the cartesian coordinates, the web is comprised of 26 triangular elements of thickness 0.307 in. and the flanges are simulated by 8 bar elements having a cross-sectional area of 3.22 sq. in.

The beam is fixed at the left end by specifying zero displacements in the x and y directions for nodes 1 through 5.

The Bilinear law was made use of with the material properties as follows:

$$\text{Modulus of Elasticity} = 29 \times 10^3 \text{ ksi}$$

$$\text{Yield Stress} = 36 \text{ ksi}$$

$$\text{Poisson's Ratio} = 0.3$$

$$\text{Plastic Modulus} = 0.0$$

**THIS BOOK
CONTAINS
NUMEROUS PAGES
WITH DIAGRAMS
THAT ARE CROOKED
COMPARED TO THE
REST OF THE
INFORMATION ON
THE PAGE.**

**THIS IS AS
RECEIVED FROM
CUSTOMER.**

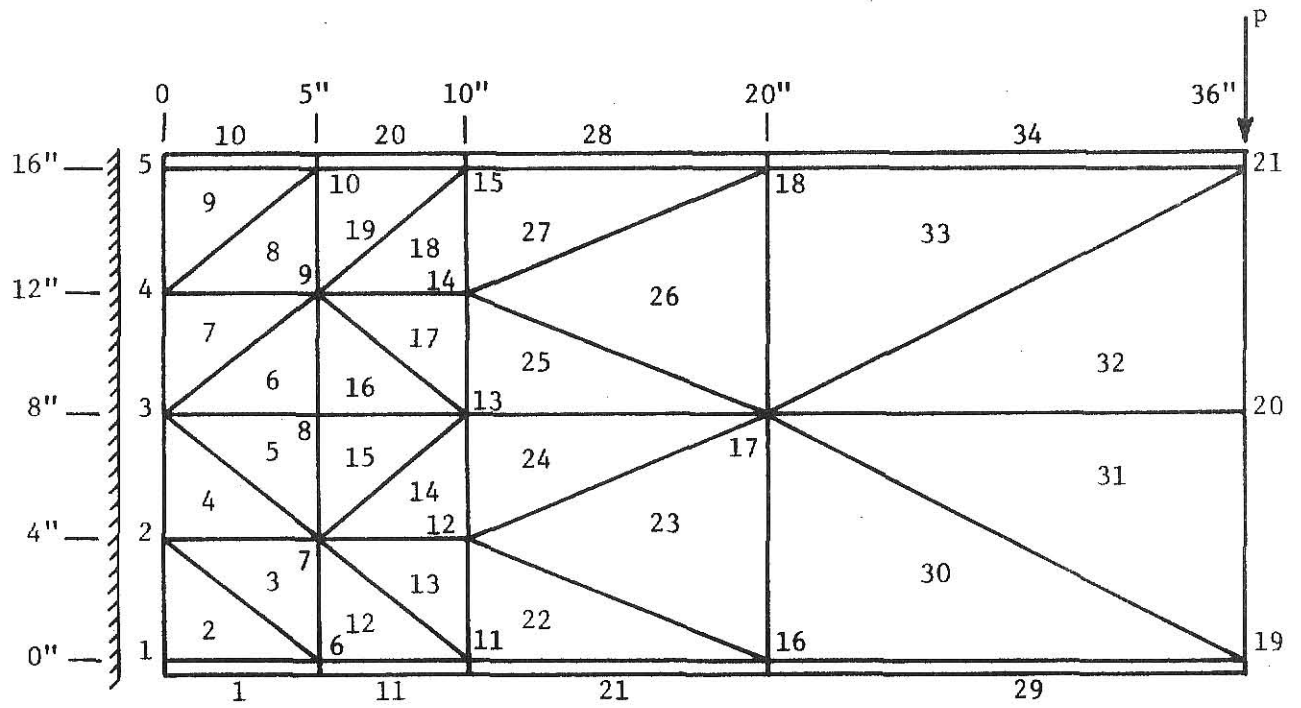


Fig. AI-Ia. Idealized Cantilever Beam.

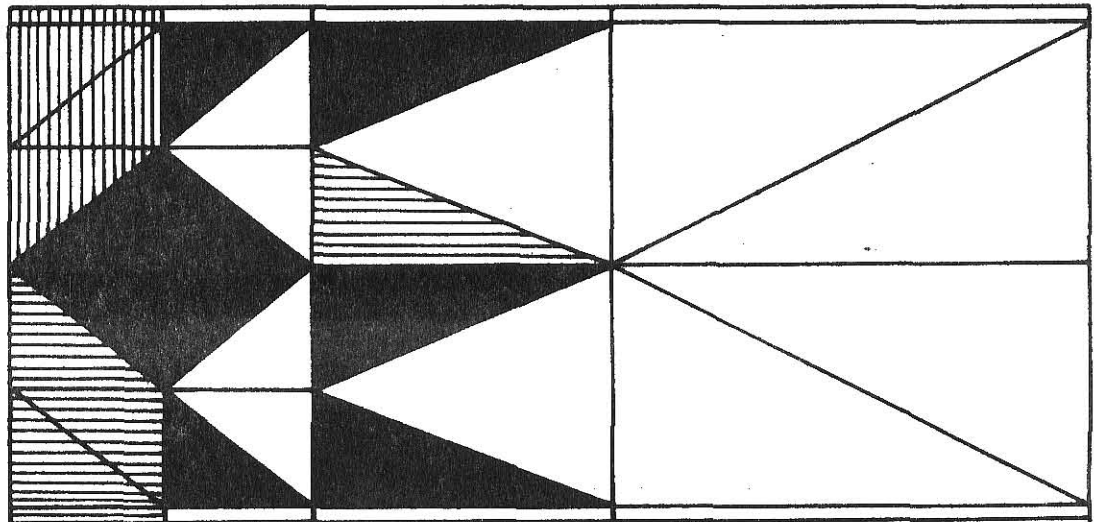


Fig. AI-Ib. Yield pattern at ultimate load (76 kips).

A total load of 80 kips was applied in 20 increments of 4 kips each. KSTART was specified as 15 and therefore the solution started with a load of 60 kips.

A maximum of 100 iterations per step and an error tolerance of 0.03 were specified. At increment number 19, that is a load of 76 kips, the error in element number 9 could not be reduced to less than 0.03 in 100 iterations and therefore, the solution was stopped at that increment. The load of 76 kips is considered as the ultimate load with an error of 0.03 in the effective plastic strain. A plot of the yielded elements at the ultimate load is shown in Fig. AI-Ib.

The choice of the maximum number of iterations per step and the error tolerance is left to the individual and depends on the accuracy desired and the computer time available. For the purpose of this project the above values were selected based on a few trial runs.

Trial Runs

Two sets of trial runs were made. One on Beam 1 and the other on Solid Beam 1. Table AI-III gives the details of these runs. The variables were, number of nodes at which the load was applied, error tolerance and the maximum number of iterations per step.

In the actual testing of the beam the load was applied through a plate 1" x 6" x 7". To simulate this condition a three point loading was tried in a few runs, with one half of the load applied at the center and one quarter of the load at the other two points. As can be observed in the tables, the three point loading had no significant effect on the maximum number of load increments reached, the idea of 3 point loading was therefore abandoned.

With the overall computer time available for the project as a limiting constraint, a maximum of 100 iterations per step and an error tolerance of 0.03 gave a reasonably good prediction of the ultimate load and were selected for the rest of the beams.

The execution time required to test a beam with the opening on the IBM 370 model 158 ranged from 7 to 9 minutes.

Run No.	No. of Nodes at which Load is Specified	No. of Increments at which Solution Stopped	Specified Error Tolerance	Specified Maximum No. of Iterations Per Step	Maximum Residual Error
Beam 1					
1	1	15	0.02	20	0.0244
2	1	16	0.03	25	0.0457
3	1	17	0.03	50	0.0514
4	3	17	0.03	50	0.0528
5	1	18	0.03	100	0.1057
6	1	18	0.10	25	0.1640
Solid Beam 1					
1	1	18	0.02	100	0.0708
2	3	18	0.02	100	0.0288
3	1	18	0.03	20	0.0756
4	3	18	0.03	20	0.0323
5	1	18	0.03	100	0.0710
6*	1	21	0.03	100	0.0503
7	3	20	0.10	100	0.1354

* with cover plates and stiffeners at supports

Table AI-III. Trial Runs on Beam 1 and Solid Beam 1.

APPENDIX II - REFERENCES

1. Salmon, M., Berke, L. and Sandhu, R., "An Application of the Finite Element Method to Elastic-Plastic Problems of Plane Stress," Illinois Institute of Technology Research Institute and the Air Force Flight Dynamics Laboratory, Project No. 1467, "Structural Analysis Methods," December 1968.
2. Kussman, R. L. and Cooper, P. B., "Ultimate Load Tests on Steel Beams with Reinforced Eccentric Web Openings," Research Project Report, Department of Civil Engineering, Kansas State University, August, 1975.
3. Muskhelishvili, N. I., "Some Basic Problems of the Mathematical Theory of Elasticity," 2nd Edition, P. Noorhoff Ltd., Groningen, The Netherlands, 1963.
4. Joseph, J. A. and Brock, J. S., "The Stresses Around a Small Opening in a Beam Subjected to Pure Bending," Journal of Applied Mechanics, Vol. 17, No. 4, 1950.
5. Timoshenko, S., "On Stresses in a Flat Plate with a Circular Hole," Journal of the Franklin Institute, Vol. 197, 1924.
6. Heller, S. R., Jr., "The Stresses Around a Small Hole in a Beam Subjected to Bending with Shear," Proceedings 1st National Congress of Applied Mechanics, ASME, N.Y., 1951.
7. Savin, G. N., "Stress Concentration Around Holes," International Series of Monographs in Aeronautics and Astronautics, Pergamon Press, 1961.
8. Heller, S. R., Jr., Brock, J. S. and Bart, R., "The Stresses Around a Rectangular Opening with Rounded Corners in a Uniformly Loaded Plate," Proc., 3rd U.S. National Congress of Applied Mechanics, 1958.
9. Heller, S. R., Jr., Brock, J. S. and Bart, R., "The Stress Around a Rectangular Opening with Rounded Corners in a Beam Subjected to Bending with Shear," Proc., 4th U.S. National Congress of Applied Mechanics, Berkeley, California, 1962.
10. Snell, R. R., "Reinforcing for a Rectangular Opening in a Plate," Journal of Structural Division, ASCE, Vol. 91, No. ST4, August 1965.
11. McCutcheon, J. O., So, W-C. and Gersovitz, B., "A Study of the Effects of Large Circular Openings in the Webs of Wide Flange Beams," McGill University, Applied Mechanics Series No. 2, November, 1963.
12. Segner, E. P., Jr., "An Investigation of the Requirements for Reinforcement around Large Rectangular Openings in the Webs of Wide Flange Beams Subject to Bending Moment and Shear," Research Report submitted to AISC, January 1963.

13. Segner, E. P., Jr., "Reinforcement Requirements for Girder Web Openings," Journal of the Structural Division, ASCE, Vol. 90, No. ST3, June 1964.
14. Bower, J. E., "Elastic Stresses Around Holes in Wide Flange Beams," Journal of the Structural Division, ASCE, Vol. 92, No. ST2, April 1966.
15. Bower, J. E., "Experimental Stresses in Wide Flange Beams with Holes," Journal of the Structural Division, ASCE, Vol. 92, No. ST5, Proc., Paper 4945, October 1966.
16. Redwood, R. G., "Experimental Stresses in Wide Flange Beams with Holes," Journal of the Structural Division, ASCE, Vol. 93, No. ST1, Discussion, February, 1967.
17. Redwood, R. G. and McCutcheon, J. O., "Experimental Tests of Wide Flange Beams with Large Unreinforced Web Openings," McGill University, Structural Mechanics Series No. 1, April, 1967.
18. Redwood, R. G. and McCutcheon, J. O., "Beam Tests with Unreinforced Web Openings," Journal of the Structural Division, ASCE, Vol. 94, No. ST1, Proc., Paper 5706, January 1968.
19. Bower, J. E., "Design of Beams with Web Openings," Journal of the Structural Division, ASCE, Vol. 94, No. ST3, Proc., Paper 5869, March 1968.
20. Redwood, R. G., "Plastic Behavior and Design of Beams with Web Openings," Proceedings of the Canadian Structural Engineering Conference, Canadian Institute of Steel Construction, Toronto, February, 1968.
21. Bower, J. E., "Ultimate Strength of Beams with Rectangular Holes," Journal of the Structural Division, ASCE, Vol. 94, No. ST6, Proc., Paper 5982, June 1968.
22. Cheng, Kho Shu, "Experimental Study of Beam with Web Opening," M.S. Thesis, Kansas State University, 1969.
23. Redwood, R. G., "Ultimate Strength Design of Beams with Multiple Openings," ASCE, Annual Meeting and National Meeting on Structural Engineering, Pittsburg, Pennsylvania, September 30 - October 4, 1968.
24. Delesque, R., "Stability of the Web Posts of Castellated Beams," Translated from Construction Metallique, No. 3, September, 1968.
25. Redwood, R. G., "The Strength of Steel Beams with Unreinforced Web Holes," Civil Engineering and Public Works Review, Vol. 64, No. 755, London, June, 1969.
26. Congdon, J. G., "Ultimate Strength of Beams with Reinforced Rectangular Openings," A Master's Thesis, McGill University, Montreal, Quebec, Canada, July, 1969.

27. Congdon, J. G. and Redwood, R. G., "Plastic Behavior of Beams with Reinforced Holes," Journal of the Structural Division, ASCE, Vol. 96, No. ST9, September, 1970.
28. Richard, M. W., "Ultimate Strength Analysis of Beams with Eccentric Rectangular Web Openings," A Master's Thesis, Department of Civil Engineering, Kansas State University, 1971.
29. Cooper, P. B. and Snell, R. R., "Test on Beams with Reinforced Web Openings," Journal of the Structural Division, ASCE, Vol. 98, No. ST3, March 1972.
30. Frost, R. W., "Behavior of Steel Beams with Eccentric Web Holes," Technical Report 46.019-400(1), Research Laboratory, United States Steel Corporation, February, 1973.
31. Turner, M. J., Clough, R. M., Martin, H. C. and Topp, L. J., "Stiffness and Deflection Analysis of Complex Structures," Journal of Aeronautical Science, 23, No. 9, 1956.
32. Clough, R. W., "The Finite Element in Plane Stress Analysis," Proceedings of the 2nd ASCE, Conference on Electronic Computation, Pittsburgh, Pa., September, 1960.
33. Zienkiewicz, O. C. and Cheng, Y. K., "The Finite Element Method in Structural and Continuum Mechanics," McGraw-Hill Publishing Company Limited, Berkshire, England, 1967.
34. "Manual of Steel Construction," 7th Edition, American Institute of Steel Construction, New York, 1970.
35. Connor, J. and Wills, G., "Computer Aided Teaching of the Finite Element Displacement Method," Research Report 69-23, Department of Civil Engineering, School of Engineering, Massachusetts Institute of Technology.
36. Wang, T. M., Snell, R. R. and Cooper, P. B., "Strength of Beams with Eccentric Reinforced Holes," Journal of the Structural Division, ASCE, Vol. 101, No. ST9, September, 1975.

APPENDIX III - NOTATIONS

A_{cp}	cross sectional area of cover plate
A_{eff}	effective flange area of idealized beam
A_{mod}	modified area of flange element with cover plates
A_{Reff}	effective reinforcement area of idealized beam
a	half the opening length
b_f	width of flange
d	overall depth of beam
d'	thickness of cover plate
F	nodal force vector
F^p	vector of plastic forces corresponding to plastic strains
h	half the opening depth
I	moment of inertia of actual beam
I_{cp}	moment of inertia of cover plates about the axis of beam
I_{eq}	moment of inertia of equivalent idealized beam
$I_{eq.mod.}$	moment of inertia of equivalent idealized beam at section with cover plates
I_{mod}	modified moment of inertia of beam at section with cover plates
i	size of load increment
K	stiffness matrix
M_1, M_2	primary bending moments
M_B^S	secondary bending moment in the bottom section at the opening
M_T^S	secondary bending moment in the top section at the opening
P_u^{exp}	experimental ultimate load corrected for strain hardening
P_u^{FE}	ultimate load obtained from finite element analysis
P_u^{Theo}	theoretical ultimate load

P_u^{true}	true ultimate load
P_u^{solid}	ultimate load of solid beam
r	radius of opening corners
t_f	thickness of flange
t_w	thickness of web
V	shear force at any section
V_B	vertical shear force in the bottom section at the opening
V_T	vertical shear force in the top section at the opening
X	distance between center of opening and centerline of beam
\bar{X}	element displacement vector
γ_{xy}^p	plastic angular strain
ϵ	total element strain vector
$\bar{\epsilon}^p$	effective plastic strain
ϵ_t	total strain
ϵ_x^p	plastic strain in x-direction
ϵ_y^p	plastic strain in y-direction
σ	element stress vector
$\bar{\sigma}$	effective stress
σ_x	normal stress in x-direction
σ_y	normal stress in y-direction
τ_{xy}	shear stress

Beam	1	2	5	6	7
X	24"	24"	25"	26"	26"
a	4.5"	4.5"	6"	8"	6"
h	3"	3"	3"	4"	4"
r	3/4"	3/4"	17/32"	1/2"	1/2"
Reinforcing bars	None	One Side	Both Sides	One Side	One Side
Cover Plates	None	PL $\frac{5}{16}$ x 4 x 24	PL $\frac{5}{16}$ x 4 x 31	None	None

Table 1. Test Variables.

Beam	Beam		Reinforcing bar	
	Average F_y (ksi)	Maximum Deviation from Average F_y (%)	Average F_y (ksi)	Maximum Deviation from Average F_y (%)
1	43.17	3.96	---	---
2	42.79	2.17	39.42	2.38
5	40.80	2.82	38.28	0.29
6	40.80	2.82	30.96	0.16
7	40.80	2.82	30.96	0.16

Table 2. Static Yield Stresses.

Beam	1	2	5	6	7
Beam Type	W16 x 45	W16 x 45	W16 x 40	W16 x 40	W16 x 40
Number of Nodes	302	302	296	341	341
Number of Elements	574	608	596	684	684
Web Thickness (in.)	0.346	0.346	0.307	0.307	0.307
Flange Area (in ²)	3.64	3.64	3.22	3.22	3.22
Modified Flange Area for Cover Plates (in ²)	---	4.96	4.52	---	---
Area of Reinforcement (in ²)	---	0.5	1.0	0.5	0.5
Area of each stiffener (in ²)	3.0	3.0	3.0	3.0	3.0

Table 3. Idealized Properties of Beams.

Beam	1	2	5	6 & 7
Beam Type	W16 x 45	W16 x 45	W16 x 40	W16 x 40
Number of Nodes	51	51	51	51
Number of Elements	98	102	102	102
Web Thickness (in.)	0.346	0.346	0.307	0.307
Flange Area (in ²)	3.64	3.64	3.22	3.22
Modified Flange Area for Cover Plates (in ²)	---	4.96	4.52	---
Area of each stiffener (in ²)	3.0	3.0	3.0	3.0

Table 4. Idealized Properties of Solid Beams.

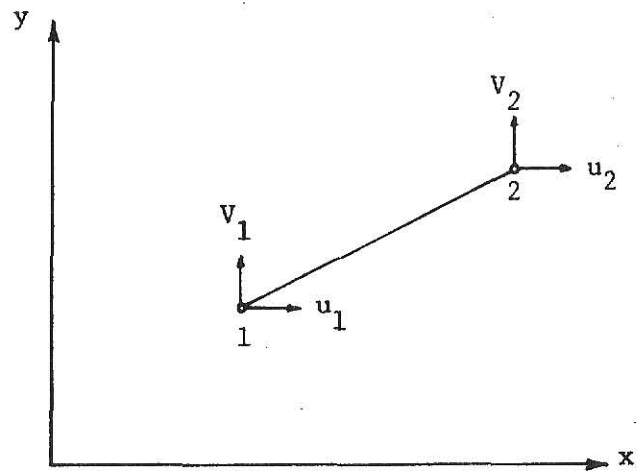
Beam	Increment Size (kips)	Increment Number at Start of Solution	Increment Number at First Yield	Increment Number at which Solution Stopped
Beams with Opening				
1	8	6	6	18
2	8	6	6	19
5	8	6	6	16
6	6	3	3	14
7	6	3	4	16
Solid Beams				
1	8	6	13	18
2	8	6	13	21
5	8	12	12	18
6&7	8	12	12	14

Table 5. Loading Details for Beams with Opening and Solid Beams.

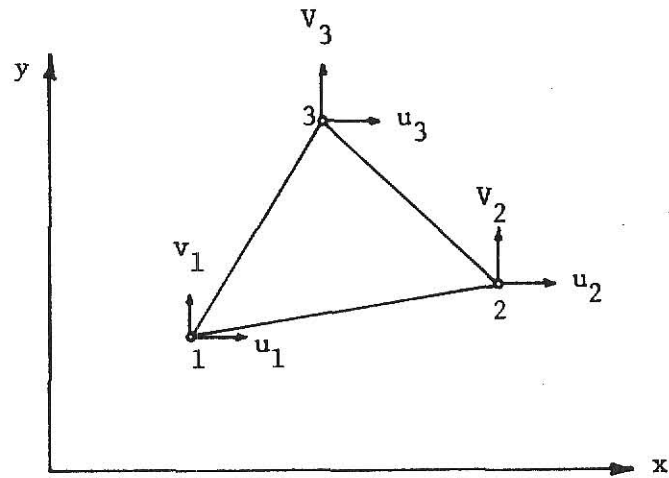
Beam	1	2	5	6	7
FE Load Increment (kips)	8	8	8	6	6
P_u^{FE} (kips)	144	152	128	84	96
$*P_u^{exp}$ (kips)	136	155	124	84	101
P_u^{FE}/P_u^{exp}	1.06	0.98	1.03	1.00	0.95
$*P_u^{Theo}$ (kips)	129	152	129	83	96
P_u^{FE}/P_u^{Theo}	1.12	1.00	0.99	1.01	1.00
P_u^{Solid} (kips)	144	168	144	112	112
P_u^{FE}/P_u^{Solid}	1.00	0.90	0.89	0.75	0.86

*These values are obtained from reference 2.

Table 6. Ultimate Loads.

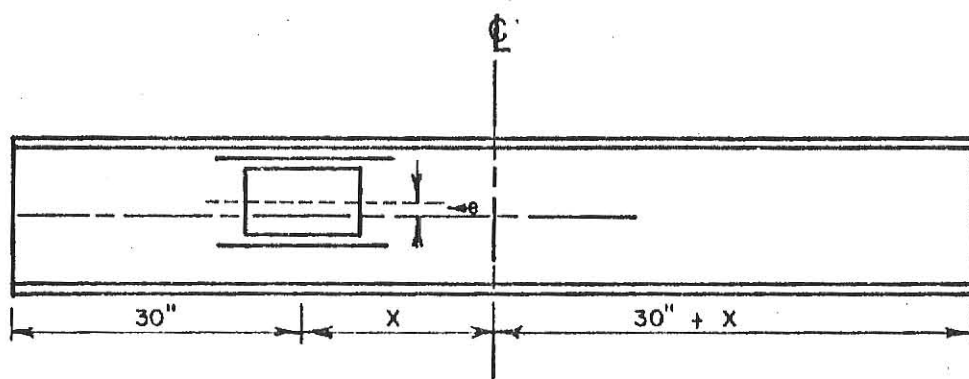


Bar Element

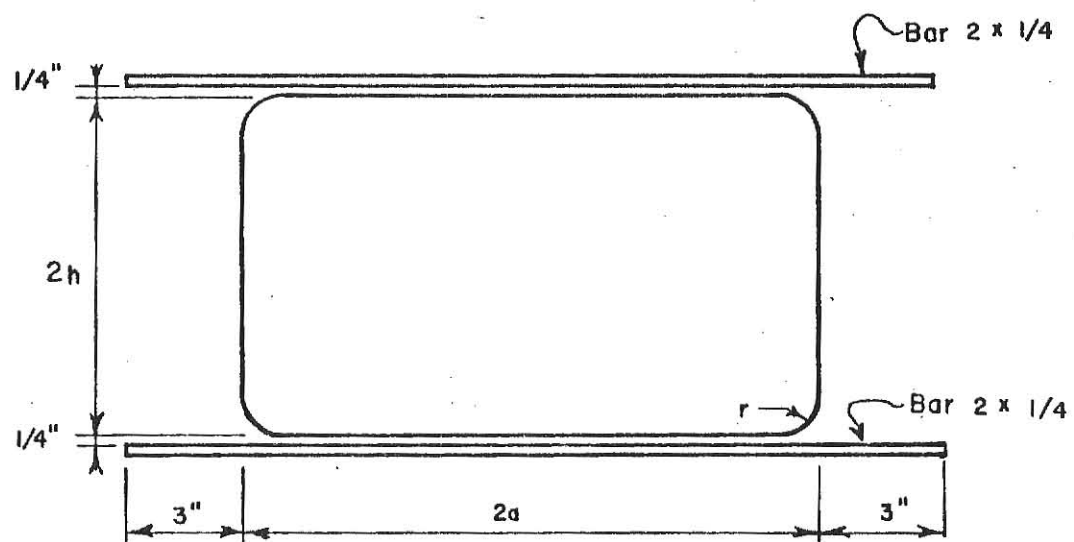


Triangular Plate Element

Figure 1. Bar and Plate Element.

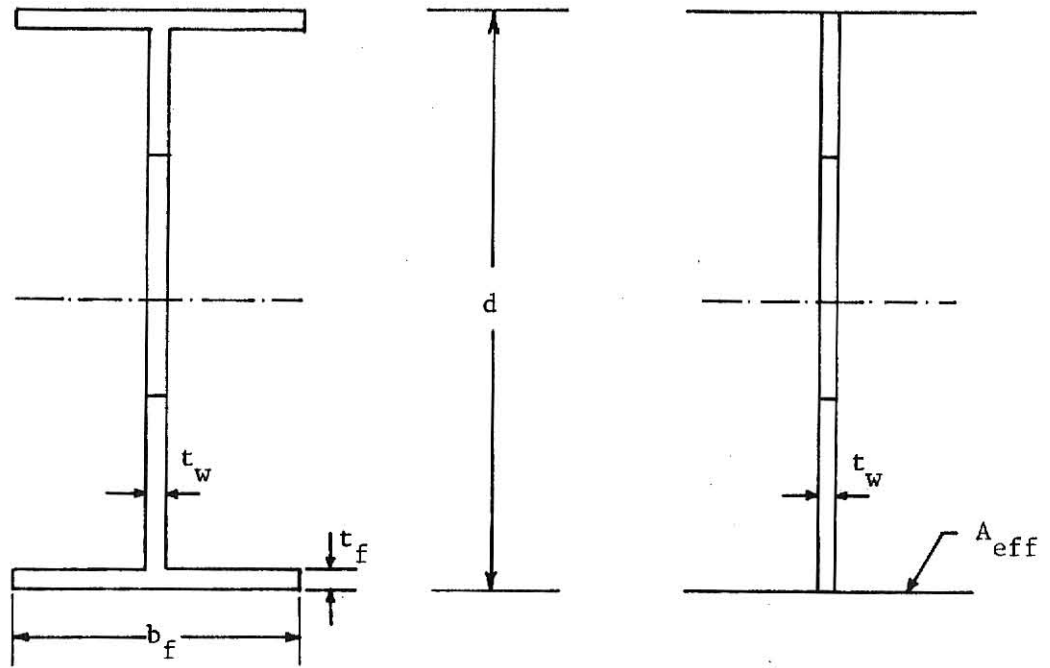


(a) Test Setup

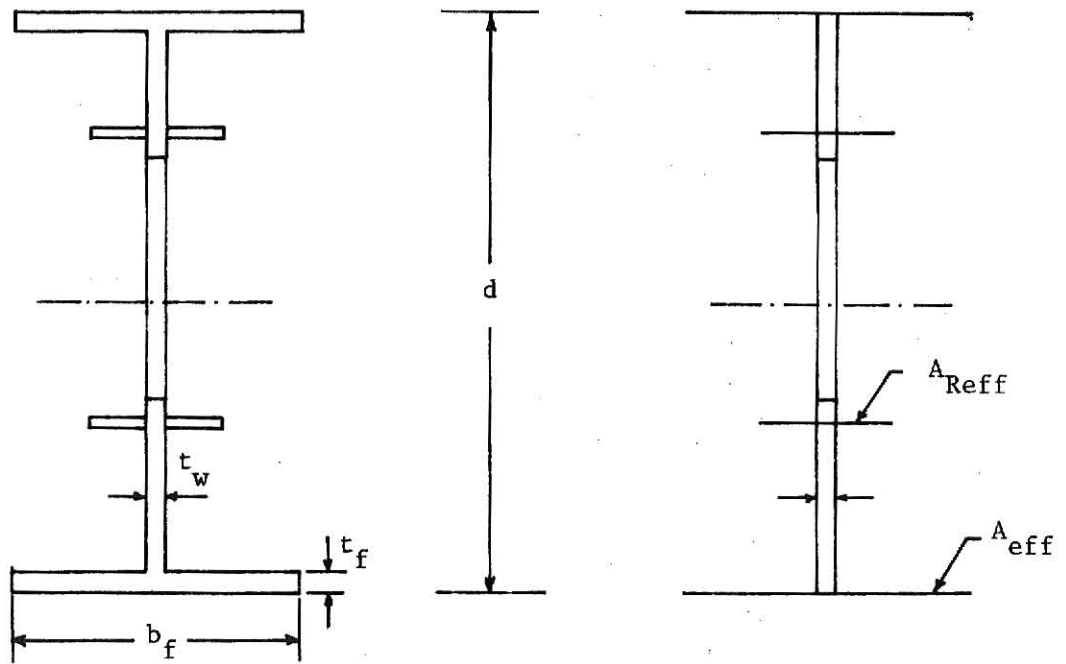


(b) Opening and Reinforcement Details

Figure 2. Test Setup and Reinforcement Details.



(a) Unreinforced



(b) Reinforced

Figure 3. Actual and Idealized Beam Sections.

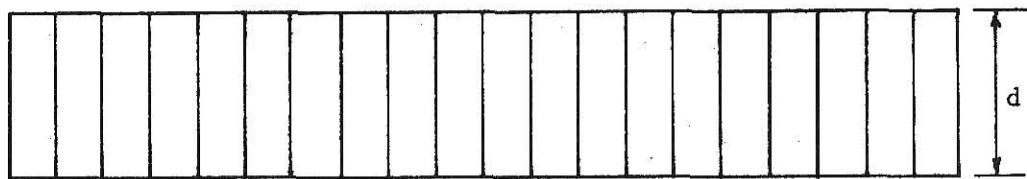
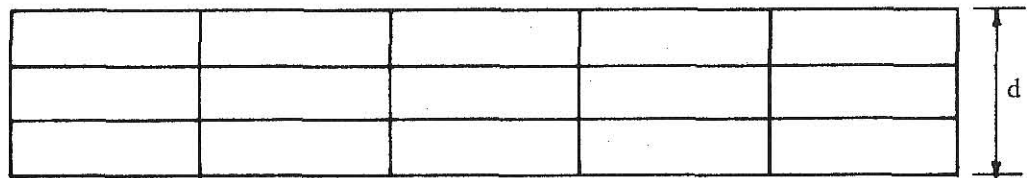
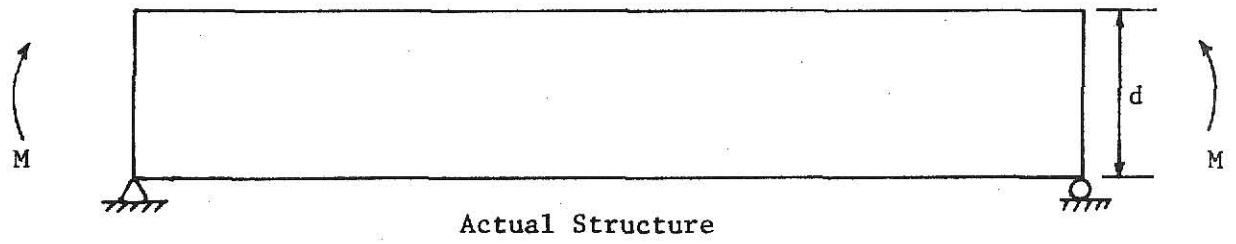


Figure 4. Discretization of a Deep Beam.

KEY TO FIGURES 5 THROUGH 26

Horizontal lines indicate compressive yielding

Vertical lines indicate tensile yielding

Solid shading indicates a combination of compressive and tensile yielding

In figures showing a full view of a beam, the portion near the opening has been omitted and is shown enlarged in the following figure.

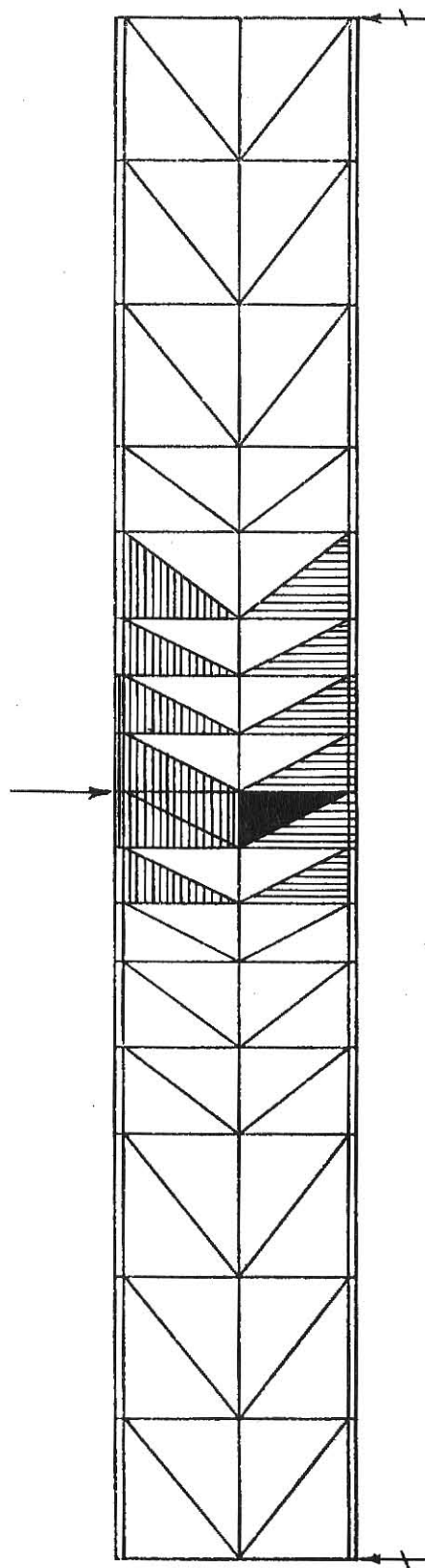


Figure 5. Yield Pattern for Solid Beam 1 at Ultimate Load (144^k).

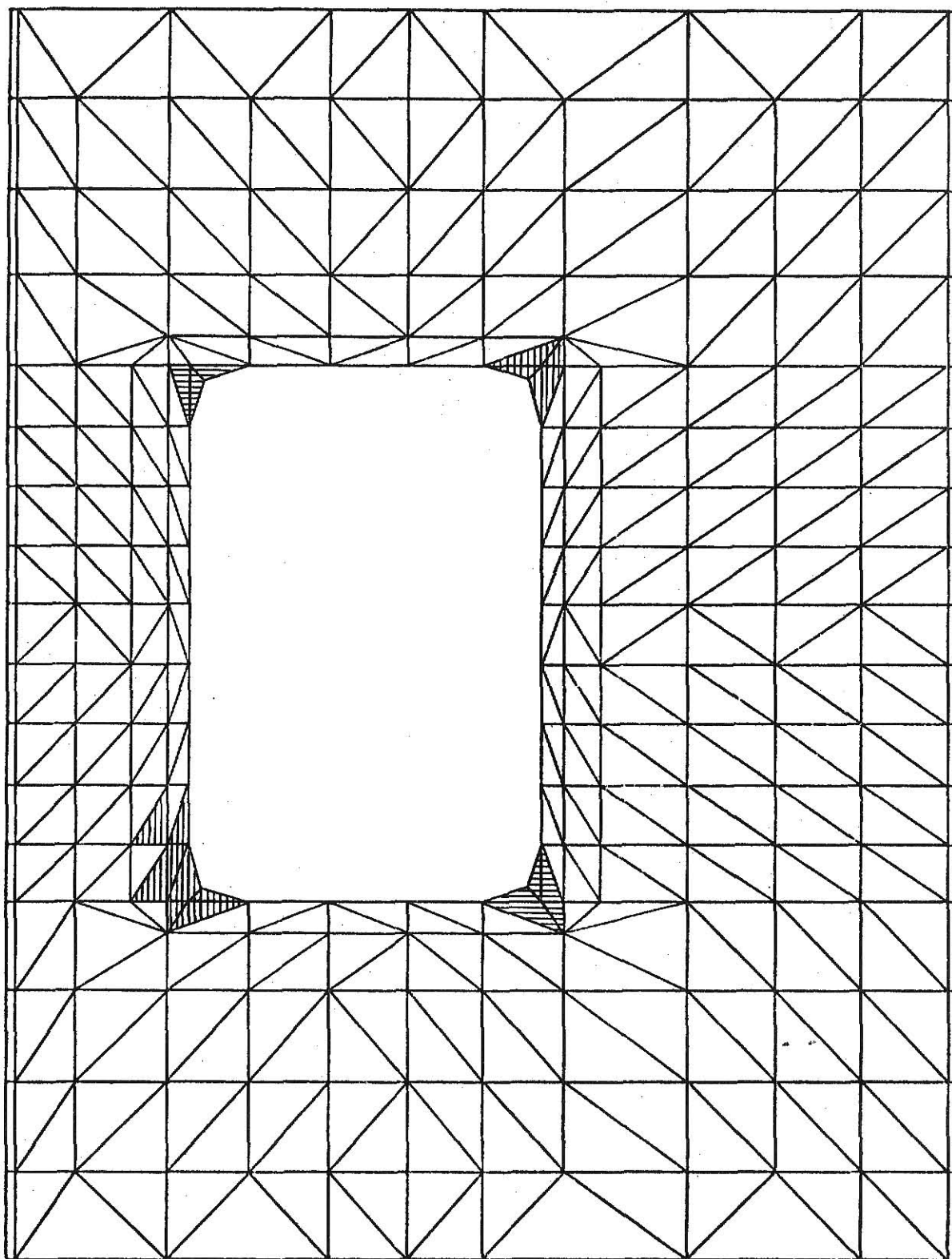


Figure 6. Yield Pattern in Vicinity of Opening for Beam 1 at 80^k .

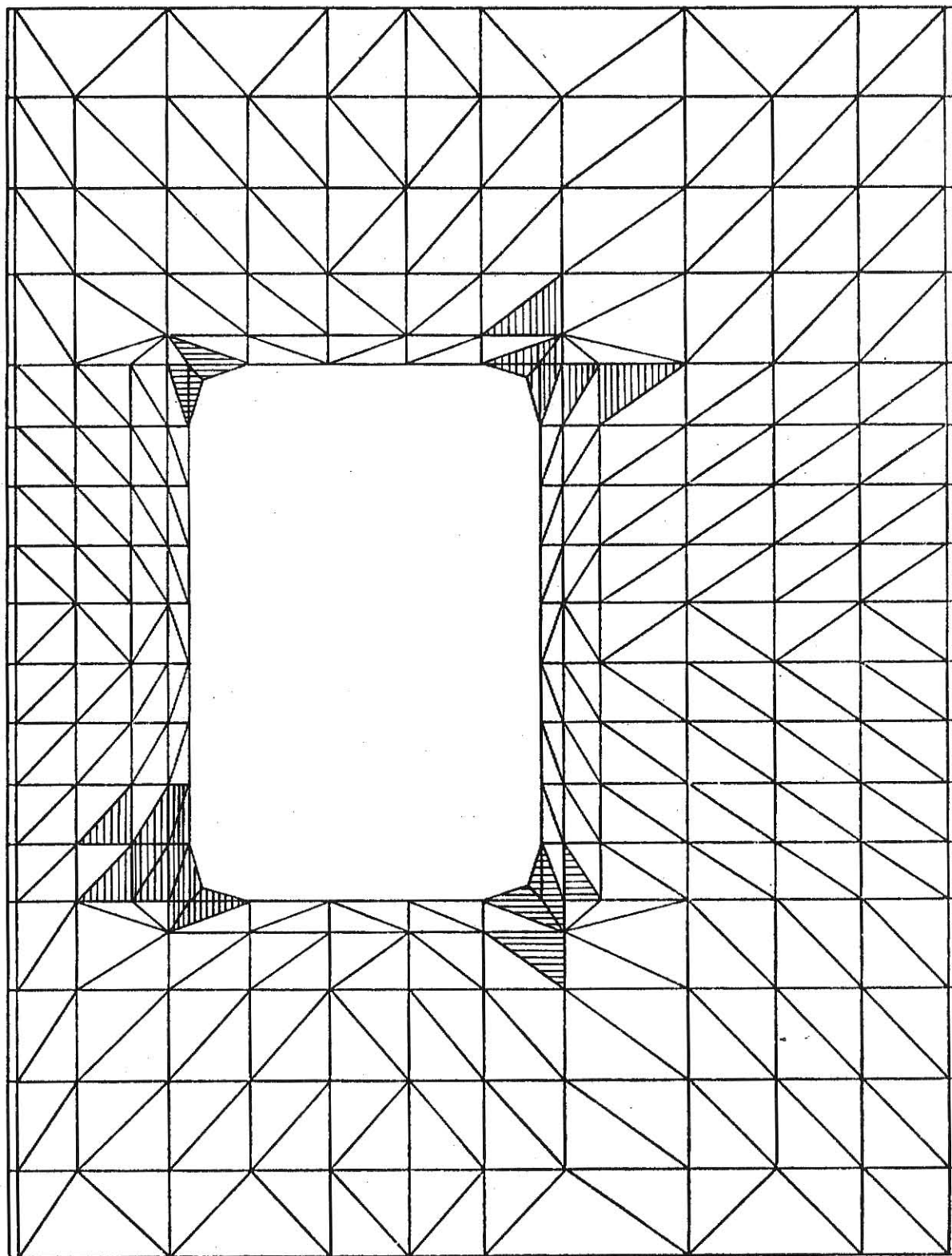


Figure 7. Yield Pattern in Vicinity of Opening for Beam 1 at 96^k .

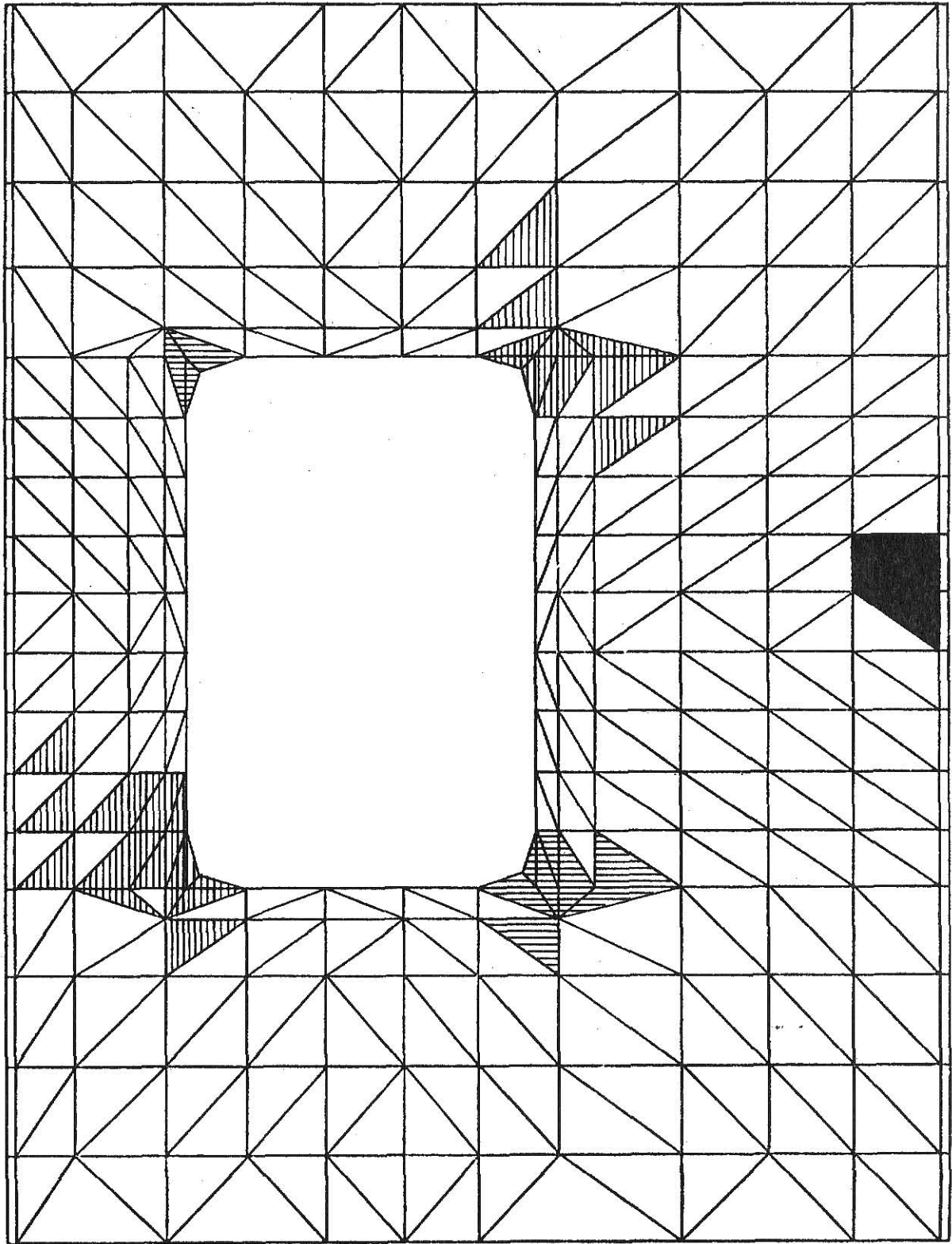


Figure 8. Yield Pattern in Vicinity of Opening for Beam 1 at 112° .

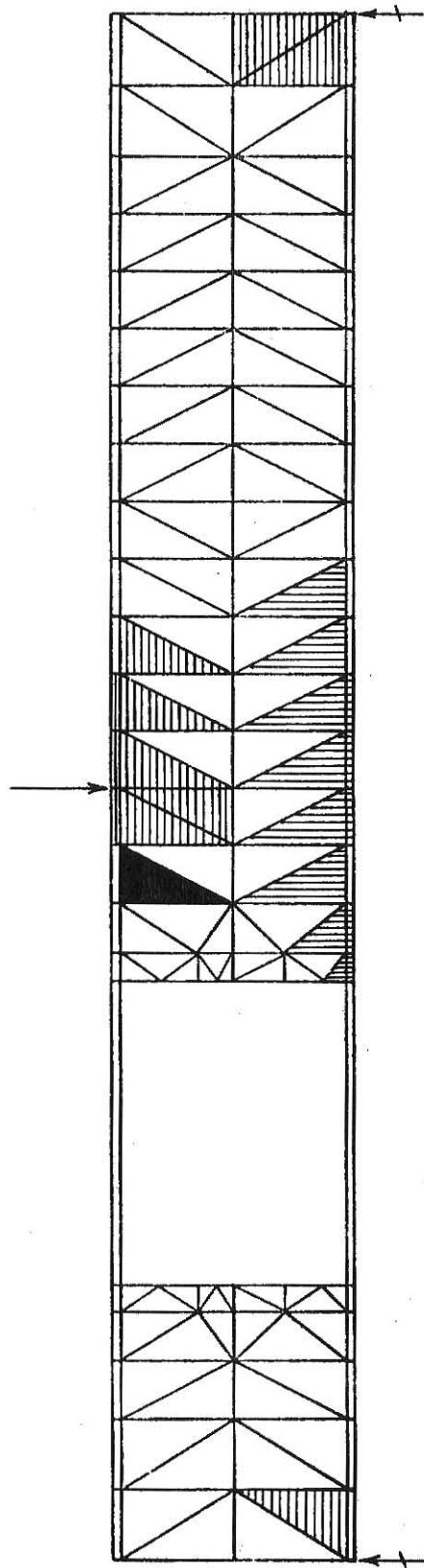


Figure 9. Yield Pattern for Beam 1 at Ultimate Load (144^k).

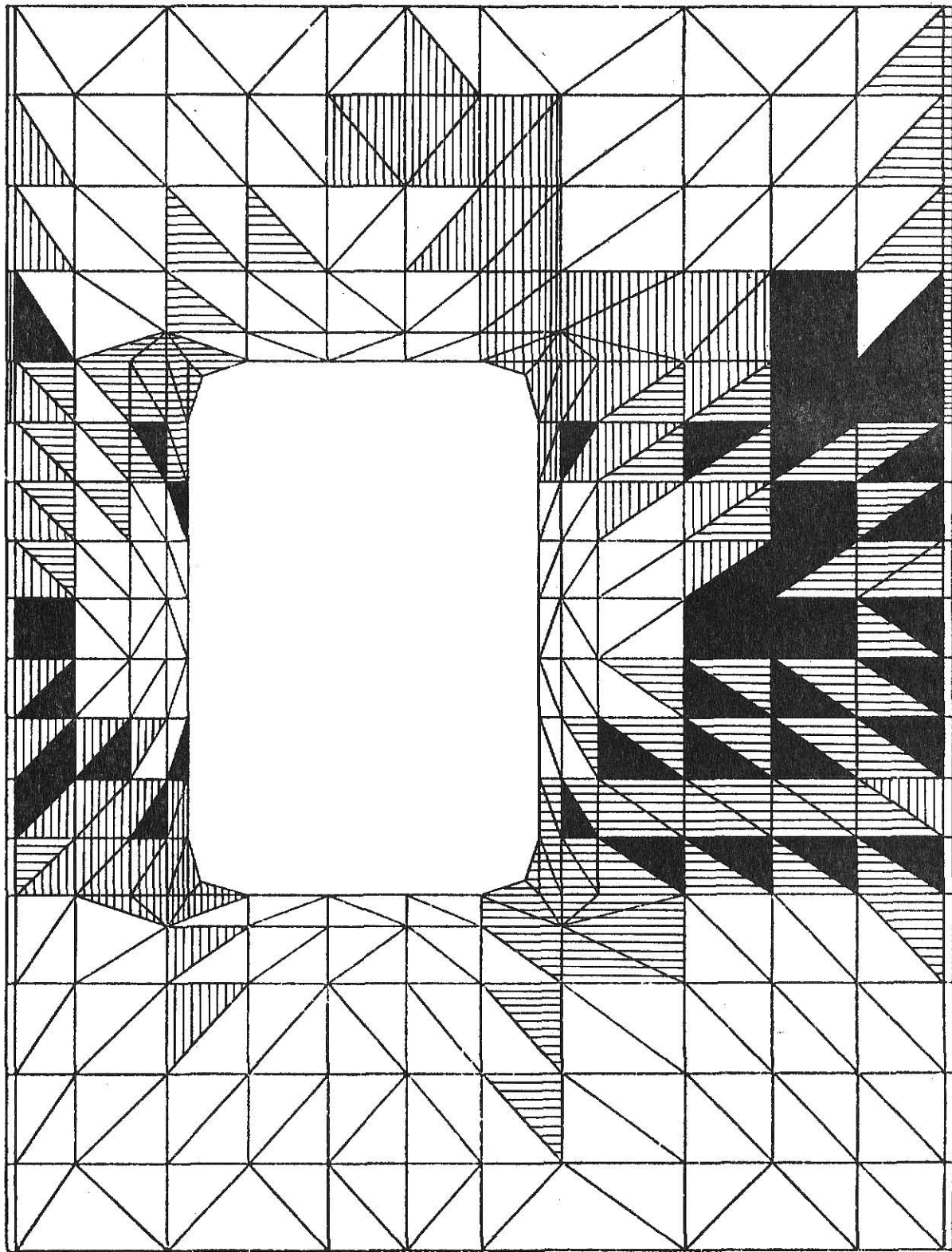


Figure 10. Yield Pattern in Vicinity of Opening for Beam 1 at Ultimate Load (144^k).

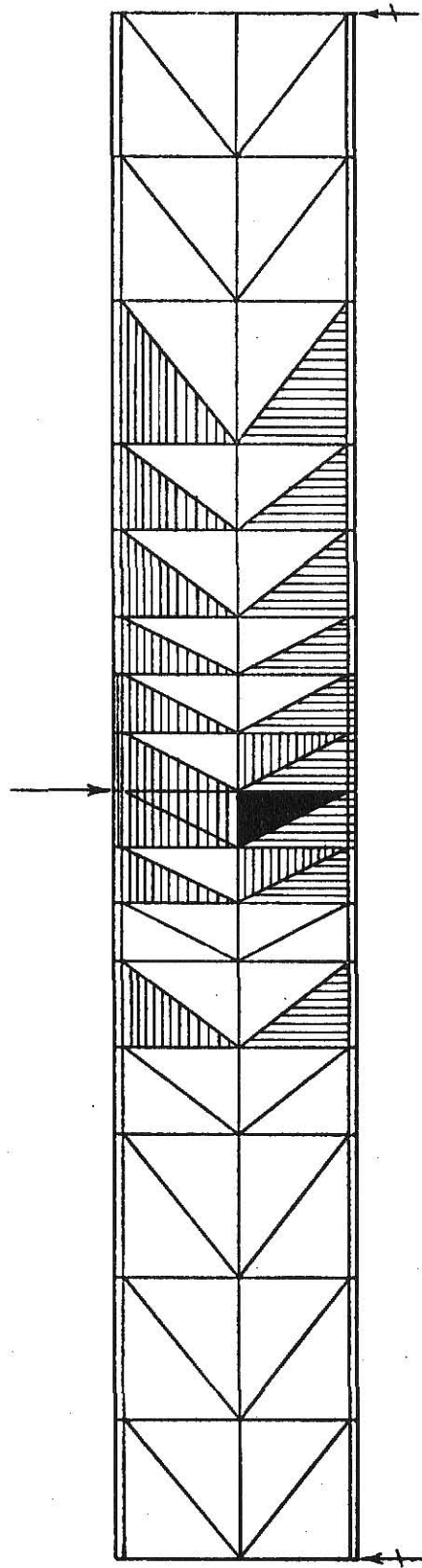


Figure 11. Yield Pattern for Solid Beam 2 at Ultimate Load (168^k).

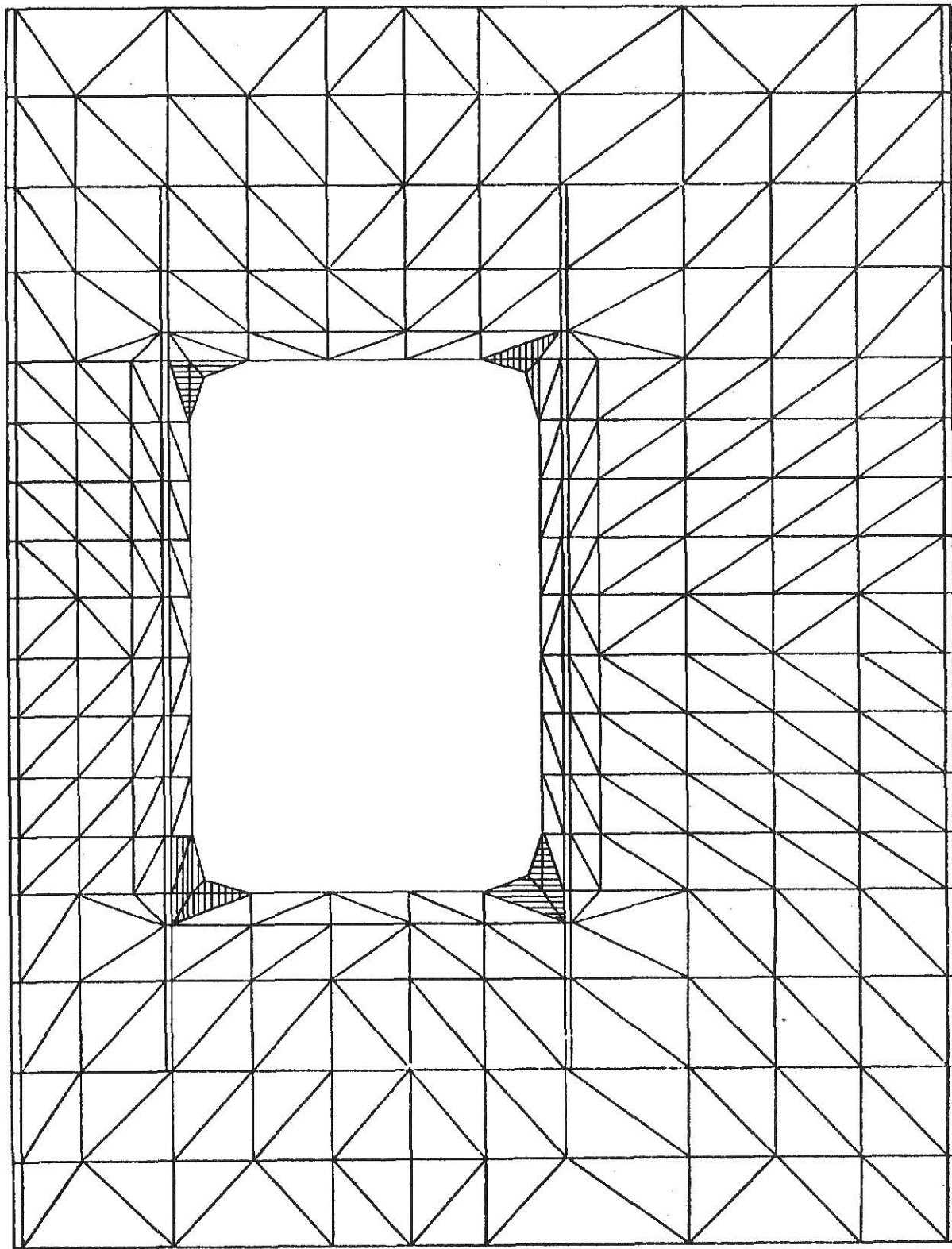


Figure 12. Yield Pattern in Vicinity of Opening for Beam 2 at 96^k .

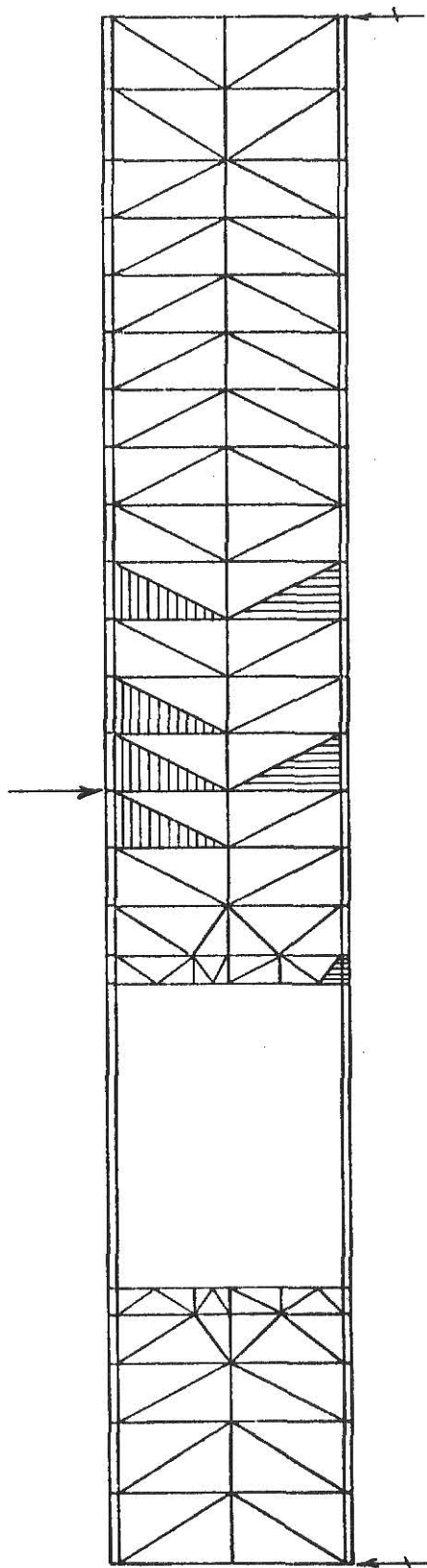


Figure 13. Yield Pattern for Beam 2 at 144^k .

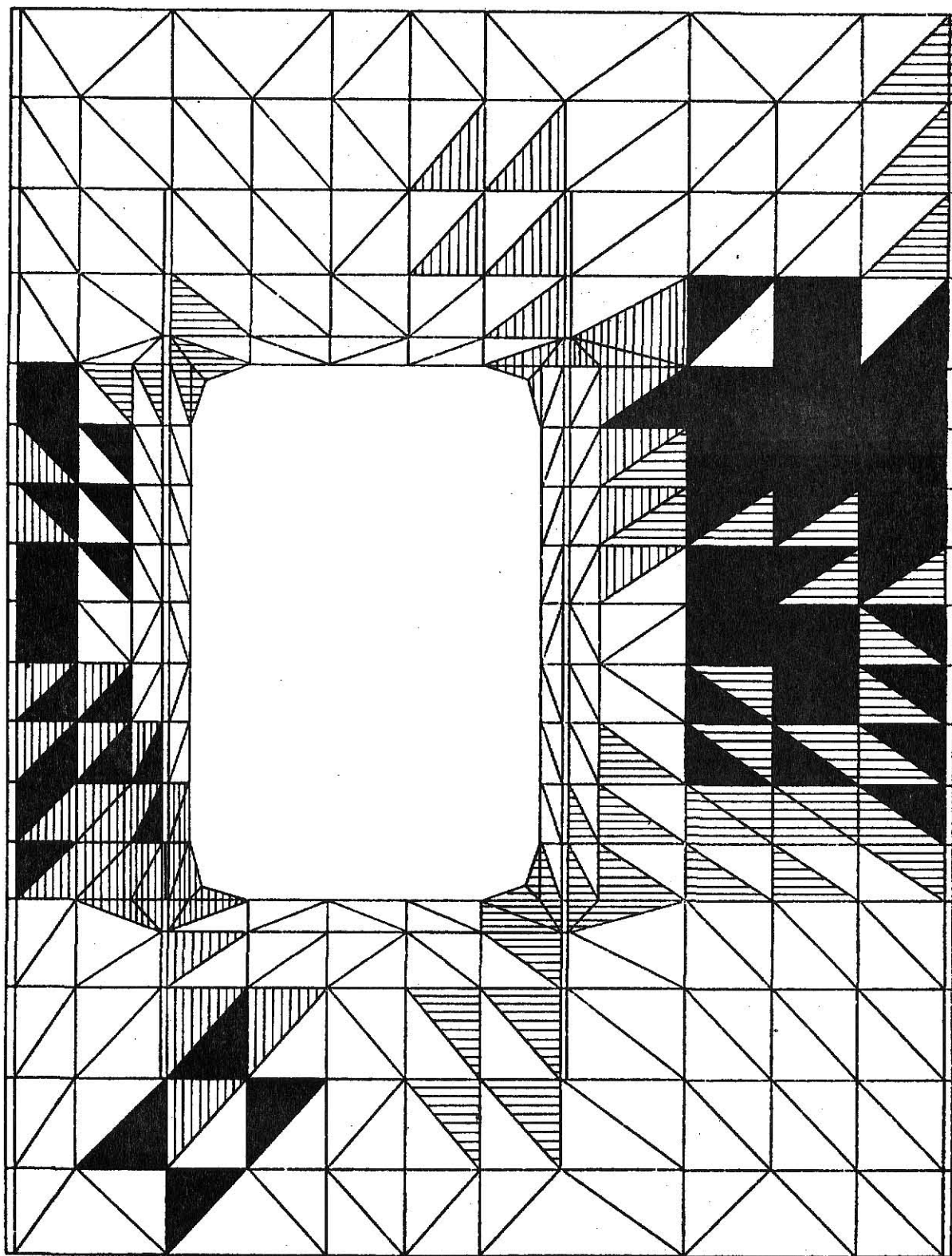


Figure 14. Yield Pattern in Vicinity of Opening for Beam 2 at 144^k .

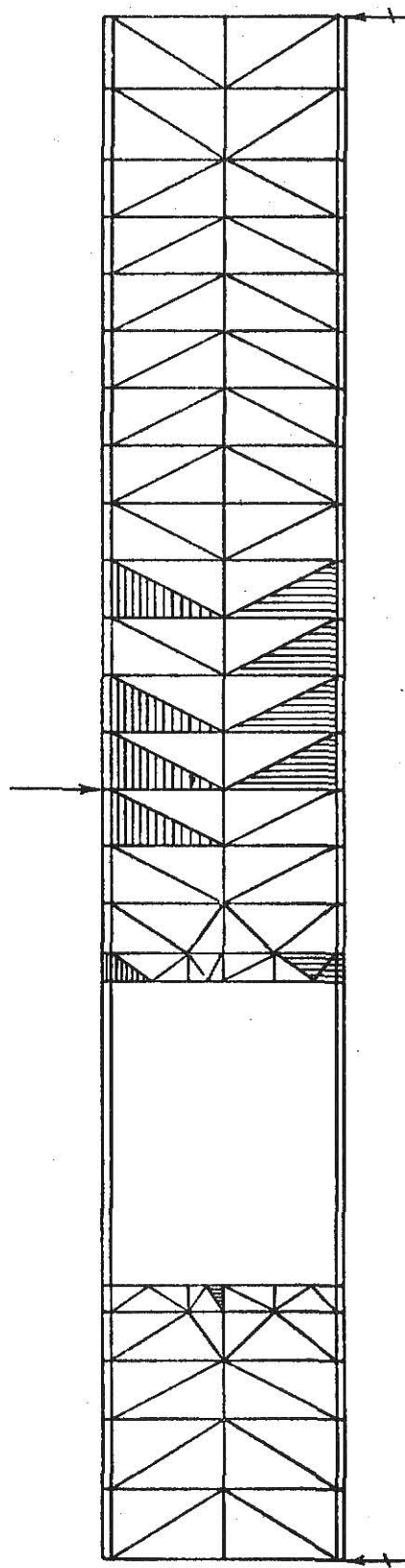


Figure 15. Yield Pattern for Beam 2 at Ultimate Load (152^k).

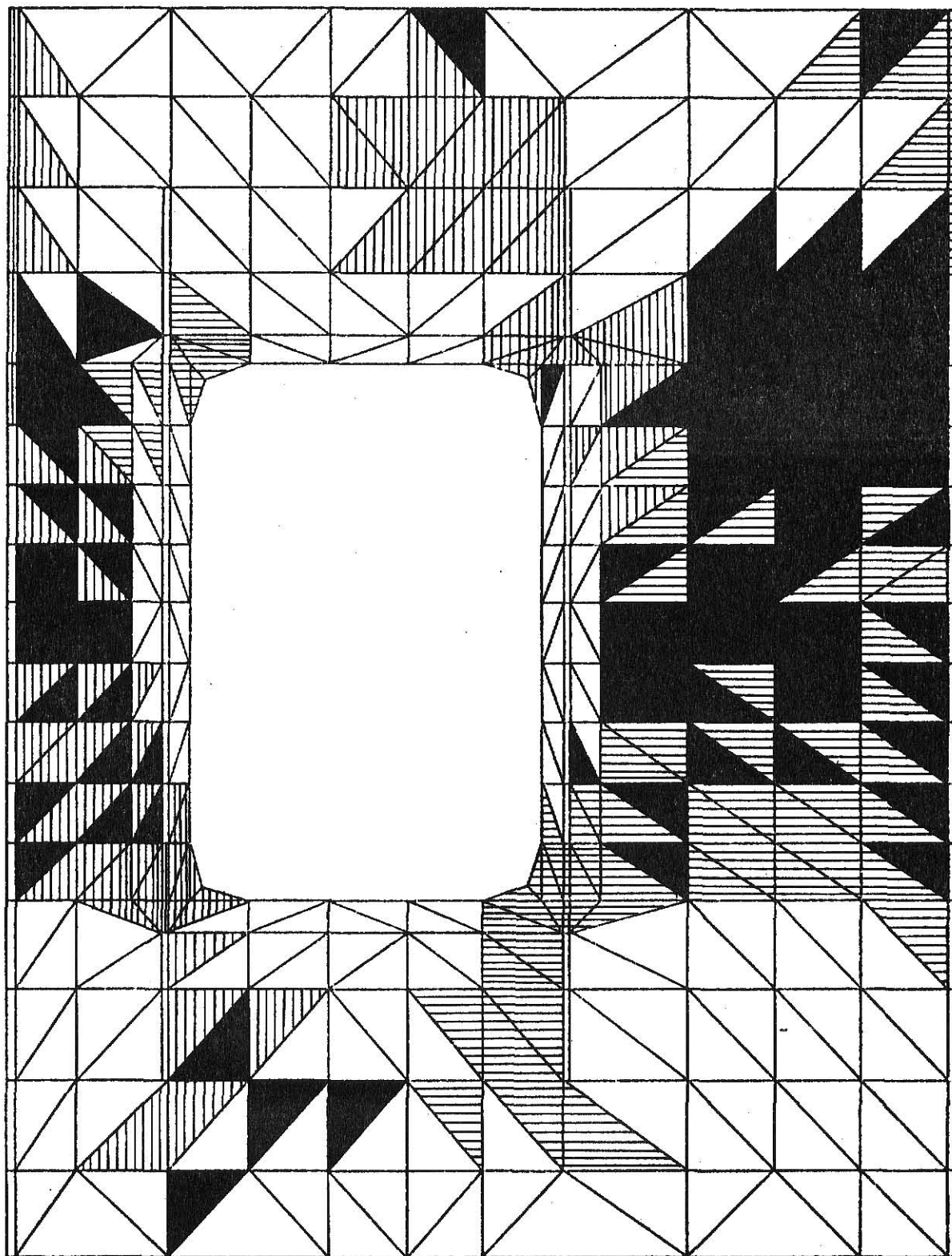


Figure 16. Yield Pattern in Vicinity of Opening for Beam 2 at Ultimate Load (152^k).

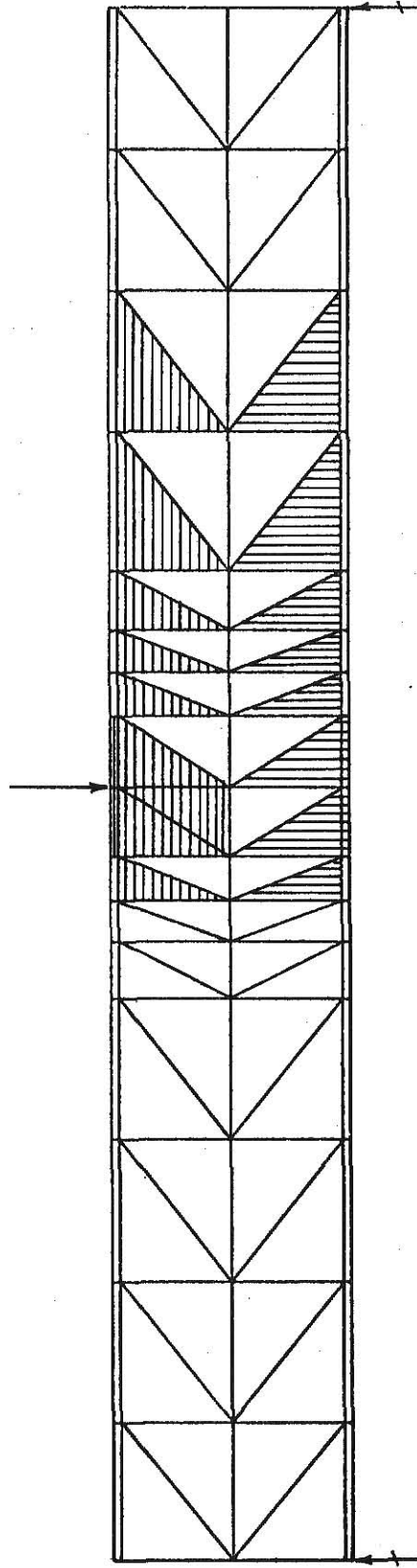


Figure 17. Yield Pattern for Solid Beam 5 at Ultimate Load (144^k).

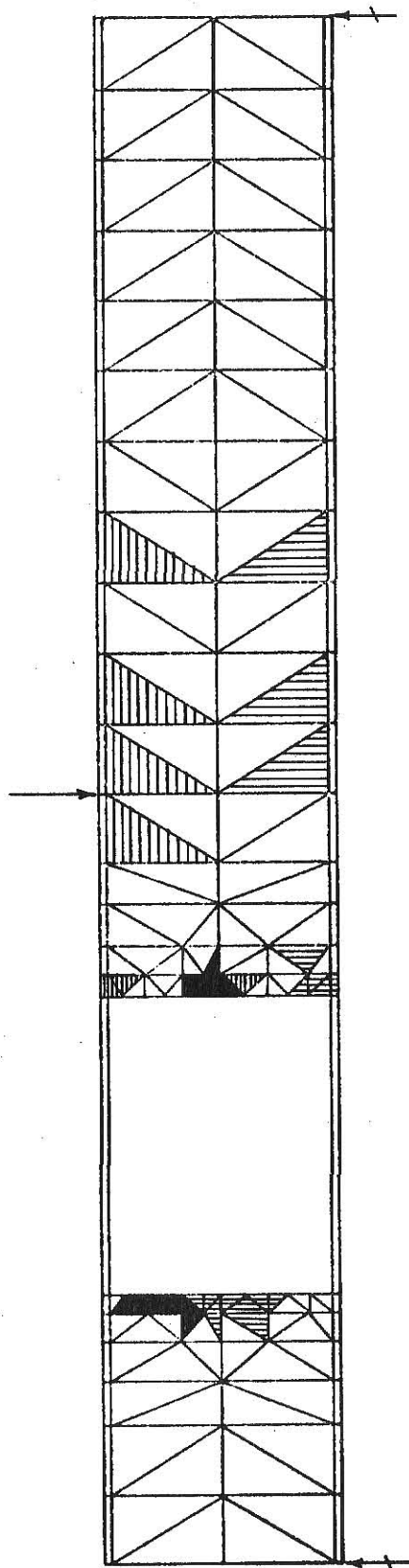


Figure 18. Yield Pattern for Beam 5 at Ultimate Load (128^k).

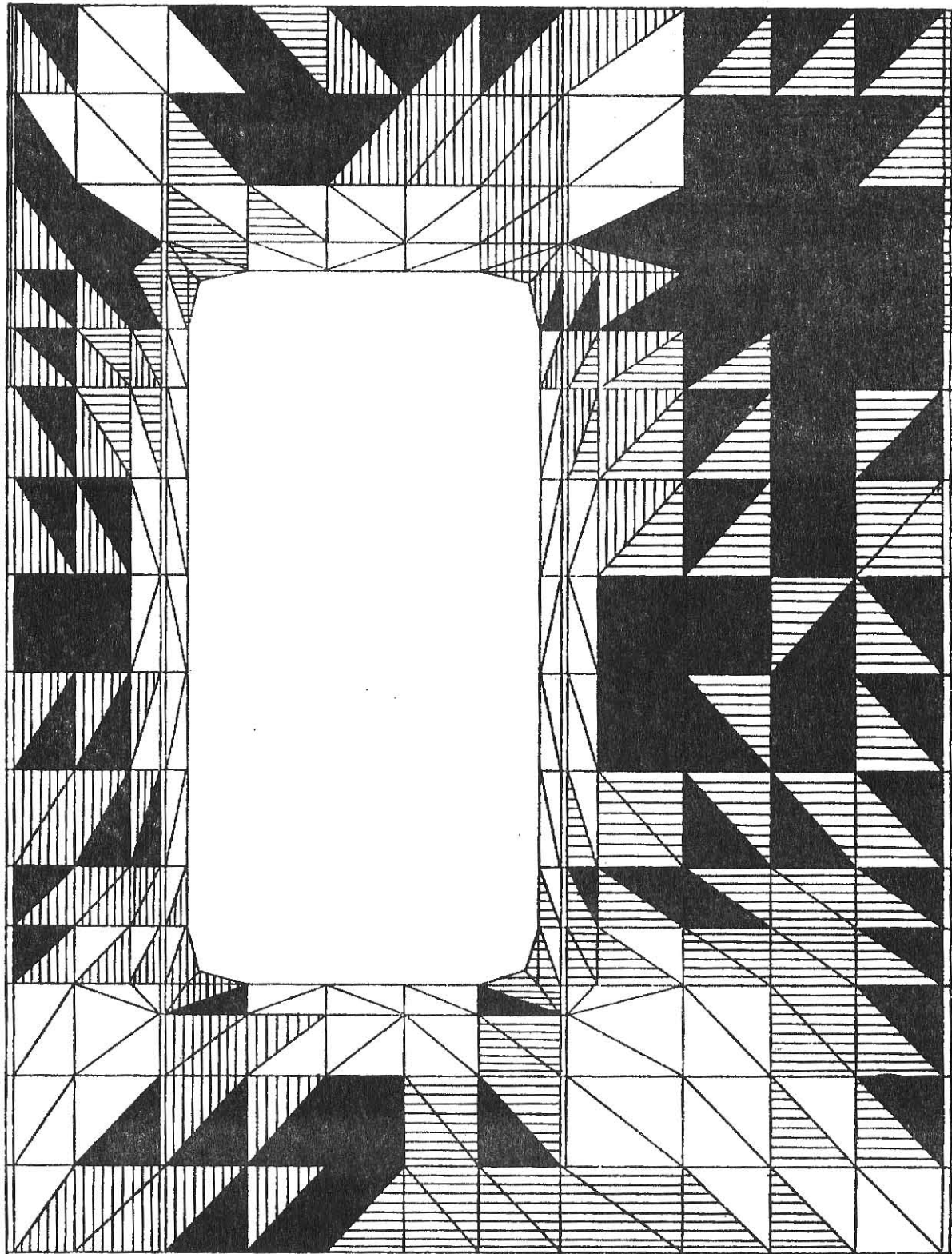


Figure 19. Yield Pattern in Vicinity of Opening for Beam 5 at Ultimate Load (128^k).

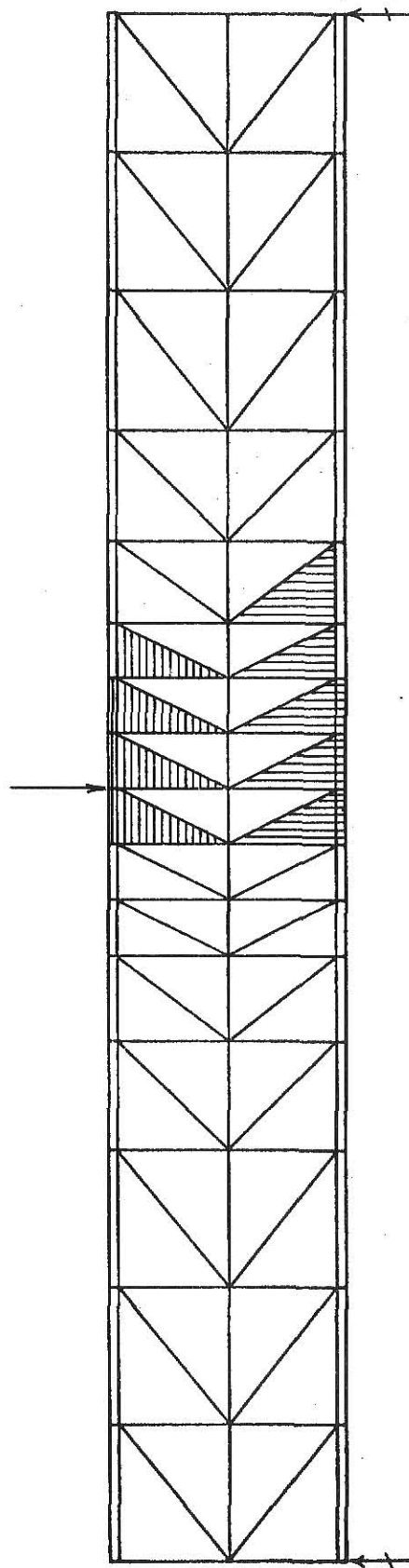


Figure 20. Yield Pattern for Solid Beam 6 and 7 at Ultimate Load (112^k).

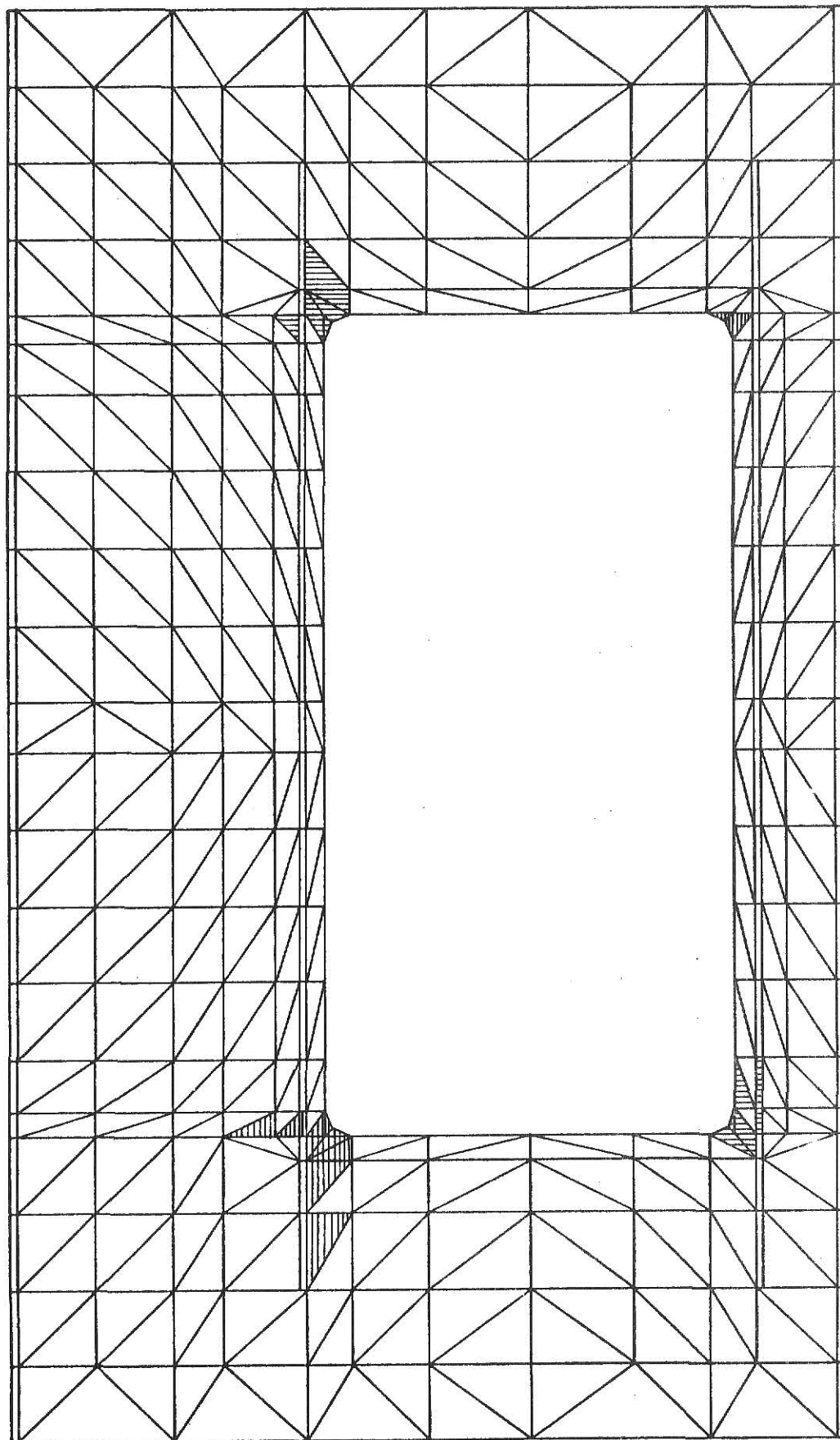


Figure 21. Yield Pattern in Vicinity of Opening for Beam 6 at 54^k .

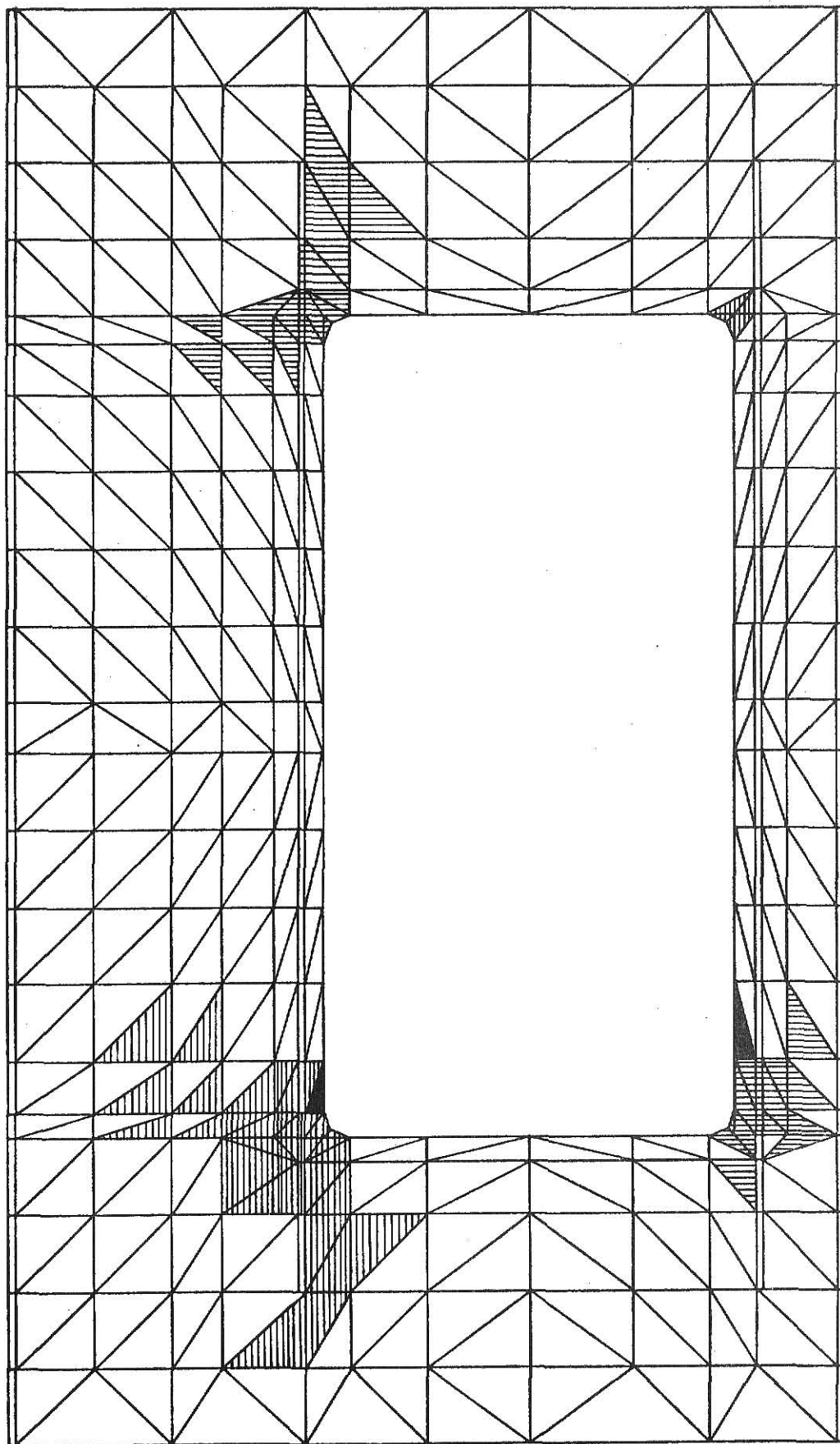


Figure 22. Yield Pattern in Vicinity of Opening for Beam 6 at 72^k .

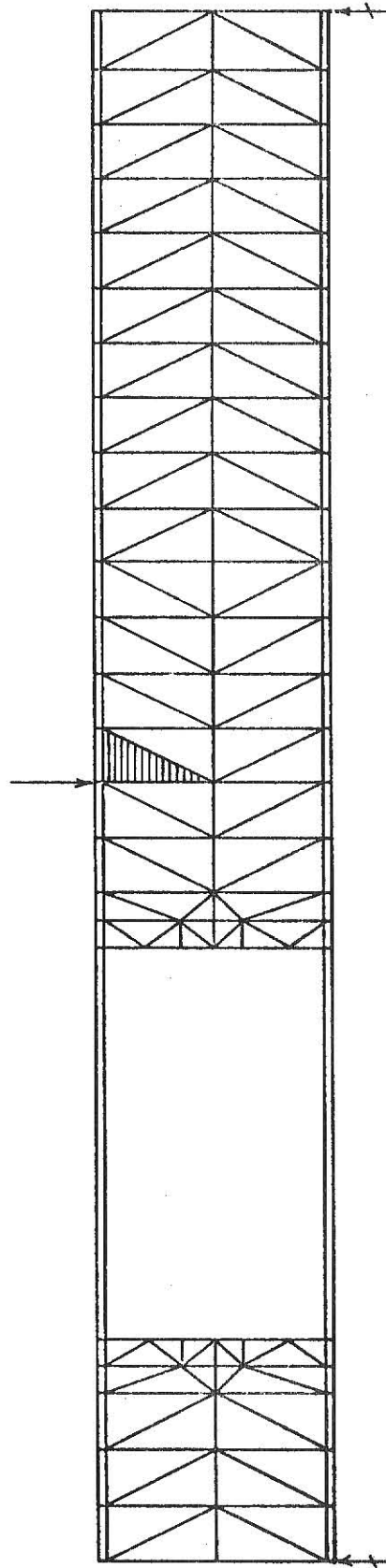


Figure 23. Yield Pattern for Beam 6 at Ultimate Load (84^k).

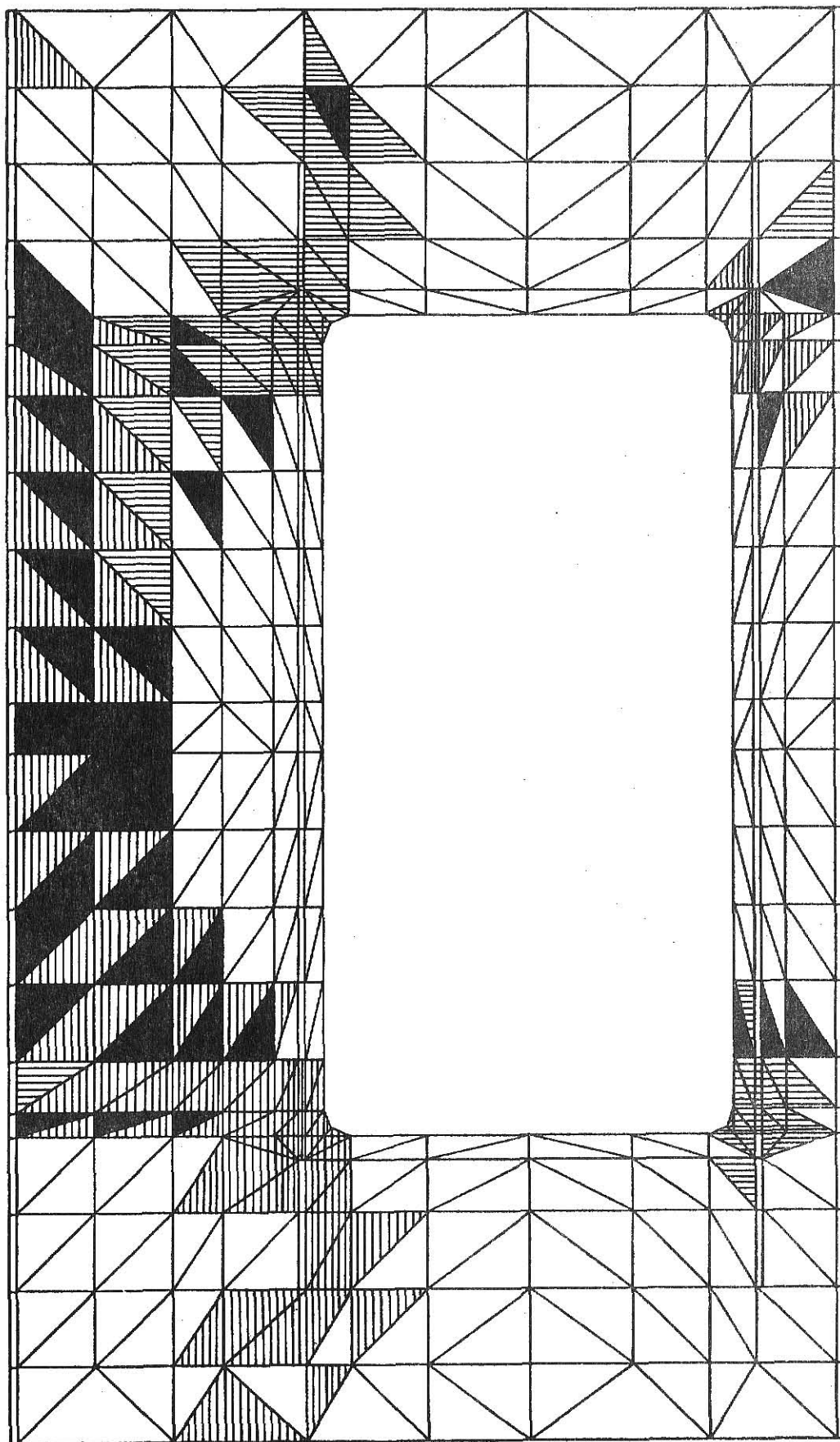


Figure 24. Yield Pattern in Vicinity of Opening for Beam 6 at Ultimate Load (84^k).

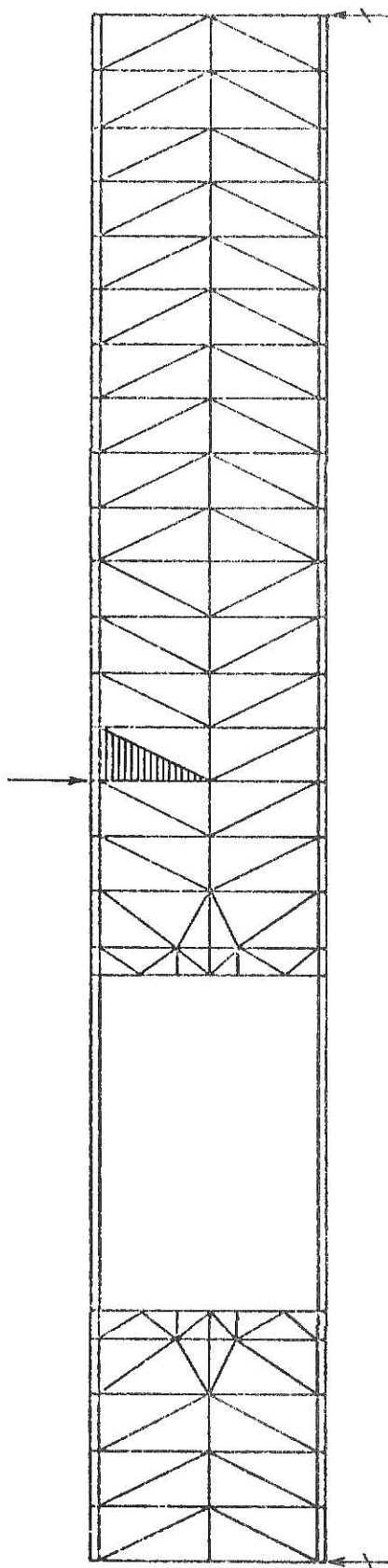


Figure 25. Yield Pattern for Beam 7 at Ultimate Load (96^k).

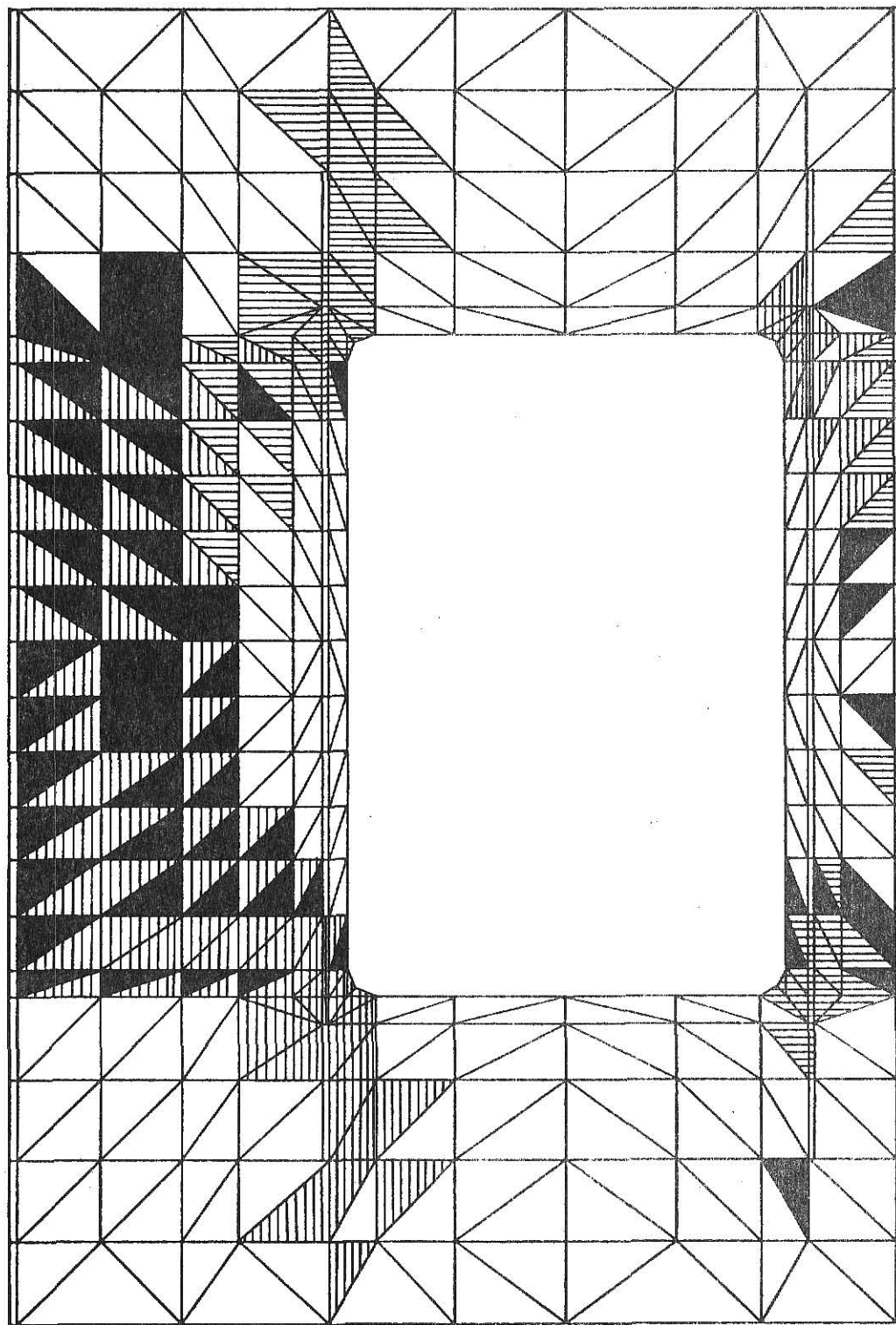
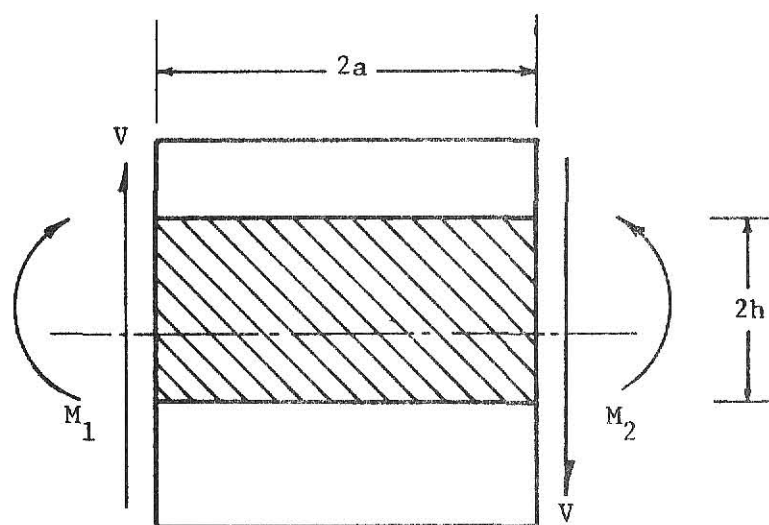


Figure 26. Yield Pattern in Vicinity of Opening for Beam 7 at Ultimate Load (96^k).



(a)



(b)

Figure 27. Secondary Moments.

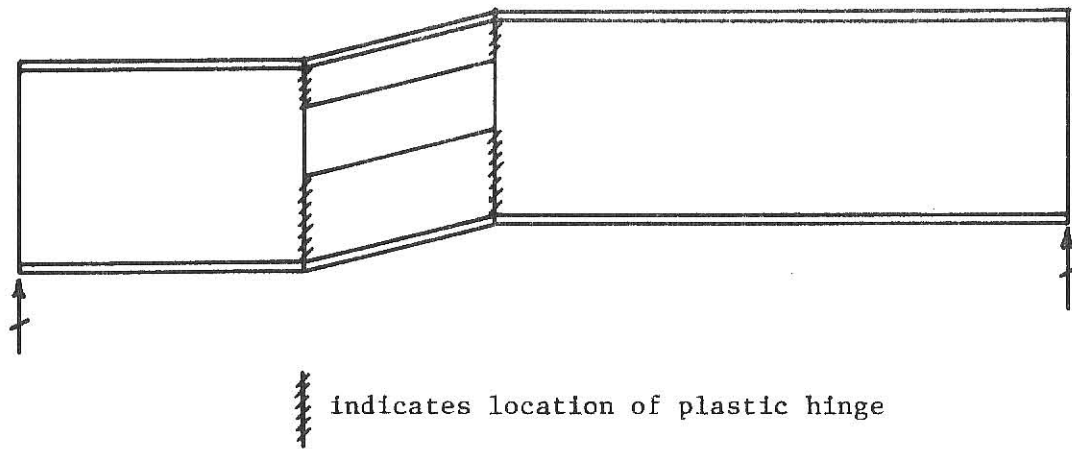


Figure 28. Four Hinged Mechanism at the Opening.

ULTIMATE LOAD CAPACITY OF STEEL BEAMS WITH WEB OPENINGS
BY THE FINITE ELEMENT METHOD

by

Aslam G. Porbandarwala

B. Tech., Indian Institute of Technology, Bombay, 1974

AN ABSTRACT OF A MASTER'S THESIS

submitted in partial fulfillment of the

requirements for the degree

MASTER OF SCIENCE

Department of Civil Engineering

KANSAS STATE UNIVERSITY
Manhattan, Kansas

1975

ABSTRACT

A finite element program was used to carry out ultimate load analyses on five A36 steel beams with varying sizes of rectangular web openings. Two of the beams were W16 x 45 shapes and three were W16 x 40 shapes. In all cases the opening had an eccentricity of 2 inches and the moment to shear ratio at the centerline of the opening was 30 inches. The openings in all but one beam were reinforced.

The ultimate loads based on the finite element analysis indicated good agreement with those obtained experimentally and with those obtained from an ultimate strength analysis. The yield patterns at various loads also agree closely with those observed in the experiments. It was confirmed that the failure at the opening is a four hinged mechanism as assumed in the theory, with a plastic hinge at each corner of the opening.